JULY 2018

M.Sc. in Mechanical Engineering

TUĞBERK HAKAN ÇETİN

UNIVERSITY OF GAZİANTEP

GRADUATE SCHOOL OF

NATURAL & APPLIED SCIENCES

PERFORMANCE ANALYSIS AND COMPARISON OF GAS LIQUEFACTION CYCLES

M. Sc. THESIS

IN

MECHANICAL ENGINEERING

BY

TUĞBERK HAKAN ÇETİN

JULY 2018

Performance Analysis and Comparison of Gas Liquefaction Cycles

M.Sc. Thesis

in

Mechanical Engineering

University of Gaziantep

Supervisor

Prof. Dr. Mehmet KANOĞLU

Co-Supervisor

Prof. Dr. Alp Er Ş. KONUKMAN

by

Tuğberk Hakan ÇETİN

July 2018

REPUBLIC OF TURKEY
UNIVERSITY OF GAZİANTEP
GRADUATE SCHOOL OF NATURAL & APPLIED SCIENCES
MECHANICAL ENGINEERING

Name of the thesis: Performance Analysis and Comparison of Gas Liquefaction Cycles

Name of the student: Tuğberk Hakan Çetin

Exam date: 26.07.2018

Approval of the Graduate School of Natural and Applied Sciences

Prof. Dr. A. Necmeddin YAZICI

Director

I certify that this thesis satisfies all the requirements as a thesis for the degree of Master of Science.

Prof. Dr. Sait SÖYLEMEZ

Head of Department

This is to certify that we have read this thesis and that in our consensus opinion it is fully adequate, in scope and quality, as a thesis for the degree of Master of Science.

Prof. Dr. Alp Er Ş. Konukman	Prof. Dr. Mehmet KANOĞLU
Co-Supervisor	Supervisor

Examining Committee Members	Signature
Prof. Dr. Mehmet KANOĞLU	……..
Assoc. Prof. Dr. Önder KAŞKA	..…….
Asst. Prof. Dr. Nehir TOKGÖZ	..……

I hereby declare that all information in this document has been obtained and presented in accordance with academic rules and ethical conduct. I also declare that, as required by these rules and conduct, I have fully cited and referenced all material and results that are not original to this work.

Tuğberk Hakan ÇETİN

ABSTRACT

PERFORMANCE ANALYSIS AND COMPARISON OF GAS LIQUEFACTION CYCLES

ÇETİN, Tuğberk Hakan
M.Sc. in Mechanical Engineering Department
Supervisor: Prof. Dr. Mehmet KANOĞLU
Co-Supervisor: Prof. Dr. Alp Er Ş. KONUKMAN
July 2018
102 pages

Gas liquefaction cycles are an important application of cryogenics and liquefied gases are used in variety of industries and processes. Gas liquefaction cycles are massive energy consumers. Therefore, their design and operation should be optimized thermodynamically and economically to minimize the energy consumption and cost. In this thesis, thermodynamic and economic assessment of commonly used gas liquefaction cycles including simple Linde-Hampson, precooled Linde-Hampson, Claude and Kapitza cycles were performed. The cycles were modeled in computer environment for various gases including air, nitrogen, oxygen, argon, fluorine, and methane. Thermodynamic performance parameters including liquid yield, liquefaction work, COP, and second law efficiency; and economic parameters including specific product cost and specific energy cost were calculated for all considered cycles and gases.

The fraction of the gas that was liquefied (i.e., liquid yield) is determined to be in the range of 0.07 - 0.20, 0.13 - 0.33, 0.22 - 0.26, and 0.09 - 0.1 for simple Linde-Hampson, precooled Linde-Hampson, Claude and Kapitza cycles, respectively. The second law efficiencies are determined to be 0.12 - 0.27, 0.22 - 0.45, 0.76 - 0.82 and 0.43 - 0.46 for the same cycles, respectively. Parametric studies are carried out to investigate effects of compressor inlet temperature, compressor outlet pressure, compressor isothermal efficiency, minimum temperature difference in heat exchanger, and turbine isentropic efficiency on the thermodynamic and economic performance parameters.

An economic comparison of the cycles indicates that Kapitza cycle has the highest specific product cost followed by simple Linde-Hampson cycle, precooled Linde-Hampson cycle, and Claude cycle. It also appears that for large scale applications, Claude and precooled Linde-Hampson cycles are most suitable options both thermodynamically and economically.

Key words: Cryogenics, gas liquefaction, thermodynamic analysis, economic analysis, Claude cycle, Linde-Hampson cycle

ÖZET

GAZ SIVILAŞTIRMA ÇEVRİMLERİNİN PERFORMANS ANALİZİ VE KARŞILAŞTIRILMASI

ÇETİN, Tuğberk Hakan
Yüksek Lisans Makine Mühendisliği
Danışmanlar: Prof. Dr. Mehmet Kanoglu
Prof. Dr. Alp Er Ş. Konukman
Temmuz 2018
102 sayfa

Gaz sıvılaştırma çevrimleri kriyojeninin önemli uygulama alanlarından biridir ve sıvılaştırılmış gazlar birçok endüstride ve proseste yaygınca kullanılmaktadırlar. Gaz sıvılaştırma çevrimleri yoğun enerji tüketmektedirler. Enerji tüketimi ve maliyeti minimize etmek için bu sistemler termodinamik ve ekonomik olarak optimize edilmelidir. Bu tezde, yaygın olarak kullanılan basit Linde-Hampson, ön soğutmalı Linde-Hampson, Claude ve Kapitza gaz sıvılaştırma çevrimlerinin termodinamik ve ekonomik değerlendirilmesi yapılmıştır. Değerlendirilmeye alınan çevrimler bilgisayar ortamında yaygın olarak kullanılan gazlar olan hava, azot, oksijen, argon, florin ve metan için modellenmiştir. Sistemin sıvılaşan gaz oranı, sıvılaştırma işi, –performans katsayısı ve ikinci kanun verimliliği gibi termodinamik performans parametreleri ve spesifik ürün maliyeti ve spesifik enerji maliyeti gibi ekonomik parametreleri her bir çevrim ve gaz için hesaplanmıştır.

Sıvılaşan gaz oranlarının basit Linde-Hampson, ön-soğutmalı Linde-Hampson, Claude ve Kapitza çevrimi için sırasıyla, 0.07-0.20, 0.13-0.33, 0.22-0.26 ve 0.09-0.1 olarak değiştiği gözlemlenmiştir. İkinci kanun verimliliklerinin ise basit Linde-Hampson, ön-soğutmalı Linde-Hampson, Claude ve Kapitza çevrimleri için, çalışan kriyojene bağlı olarak sırasıyla, 0.12-0.27, 0.22-0.45, 0.76-0.82 ve 0.43-0.46 aralıklarında değiştiği gözlemlenmiştir. Kompresör giriş sıcaklığı, kompresör çıkış basıncı, kompresör izotermal verimi, ısı değiştiricilerdeki minimum sıcaklık farkı, türbin izentropik verimi gibi parametreler ile sistemin termodinamik ve ekonomik performansını incelemek üzere parametrik çalışmalar yapılmıştır.

Yapılan ekonomik karşılaştırmanın sonucunda, Kapitza çevriminin en fazla spesifik ürün maliyetine sahip olduğu ve onu sırasıyla basit Linde-Hampson, ön-soğutmalı Linde-Hampson ve Claude çevrimlerinin takip ettiği gözlemlenmiştir. Ayrıca büyük ölçekli sistemler için Claude ve ön-soğutmalı Linde-Hampson çevriminin termodinamik ve ekonomik açıdan en uygun çevrimler olduğu gözlemlenmiştir.

Anahtar Kelimeler: Kriyojeni, gaz sıvılaştırma çevrimleri, termodinamik analiz, ekonomik analiz, Claude çevrimi, Linde-Hampson çevrimi

To My Beloved Family

ACKNOWLEDGEMENTS

First and foremost, I would like to thank God the almighty for being my strength and guide for finishing this study. Without Him, nothing including this thesis is ever possible.

I would like to express my most sincere gratitude to my supervisor Prof. Dr. Mehmet Kanoglu for providing me valuable support and crucial guidance for both in academic life and daily life. I'm honored to have a chance to study with him. His humbleness, honesty together with his outstanding useful academical capacity will always inspire me.

Also, I would like to thank my co-supervisor Prof. Dr. Alp Er Konukman for his constructive criticism throughout this study.

I would like to thank Assistant Professor Dr. Ceyhun Yılmaz for his guidance and crucial support throughout my undergraduate years to this study.

I would like to thank my colleagues from Gebze Technical University who share same office with me, Fethiye Coşkun, Gökçe Akgün, Neslihan Yanıkömer, İlke Algül and my dear friend Musa Dallaroğlu for their supports.

Most of all, I would like to thank my parents who raised me and provide endless support and my beloved Büşra. She has been my strength and perspective throughout.

TABLE OF CONTENT

Page

LIST OF TABLES

Page

LIST OF FIGURES

Page

LIST OF SYMBOLS

A: Area (m^2)

a: Plate thickness (m)

CC: Capital cost ($)

C: Purchased Equipment Cost ($)

C_e: Electricity Cost ($/kW-hr)

COP: Coefficient of Performance

h: Specific enthalpy-heat transfer coefficient (kJ/kg) -(W/m^2 K)

H: Annual Operating Hours (hours/year)

i: Annual Tax rate (%)

k: Thermal Conductivity (kW/m-K)

LMTD: Log-mean Temperature Difference (K, °C)

$\dot{m}$: Mass Flow rate (kg/s)

n: Expected Economic Life-number of compression stages (year)

O&M: Operation and Maintenance

P: Pressure (kPa)

PFHX: Plate-Fin Heat Exchanger

Q: Heat Transfer (kW)

q: Heat Transfer per unit mass (kJ/kg)

r: Mass Fraction Diverted to the Expander ($\dot{m}_e / \dot{m}$)

s: Specific Entropy (kJ/kg-K)

T: Temperature (K, °C)

U: Annual Cost-Overall Heat Transfer Coefficient ($/year) -($kW/m^2$-K)

V: Volume of Product (gallon)

W: Work (kW-HP)

w: Specific Work (kJ/kg)

w_{liq}: Specific Liquefaction Work (kJ/kg)

w_{rev}: Reversible Work (kJ/kg)

y: Liquid Yield ($\dot{m}_f / \dot{m}$)

Greek Letters

Δ: Difference

η: Efficiency

ε: Effectiveness

Subscripts, indices

0: Death State-Surface Efficiency

II: Second Law1, 2,3.: States of the cycle

c: Cold Stream

comp: Compressor

exp: Expander

f: Liquid state

g: Gas state

h: Hot stream

hx: Heat Exchanger

i: i'th element

CHAPTER 1

INTRODUCTION AND LITERATURE SURVEY

1.1 Introduction

Cryogenics is the branch of science and engineering which deals with low temperatures. Many of the modern science and engineering applications involve the field of cryogenics such as superconductivity, rocket engines, and gas liquefaction, etc. Cryogenic temperatures can be arbitrarily defined as below −150°C (123 K). All of the so called permanent gases such as helium, nitrogen and hydrogen have the boiling point below the −150°C[1]. In Table 1.1, boiling temperatures and critical points of commonly used substances for cryogenic applications are given.

Table 1.1 Boiling temperatures and critical pressure and temperatures of commonly used gases

Substance	Critical Temperature T (°C)	Critical Pressure P (atm)	Boiling Temperature T (°C)
Air	−140.6	37.86	−194.4
Nitrogen	−147	33.96	−195.9
Oxygen	−118.6	50.43	−183.1
Argon	−122.5	48.63	−186
Methane	−82.59	45.99	−161.6
Fluorine	−128.7	52.4	−188.2
Hydrogen	−240	12.96	−252.8
Helium	−268	2.275	−268.9

To liquefy any substance, temperature of the fluid must be below of its critical point. As can be seen from Table 1.1 critical points of commonly used gases are much below the ambient temperatures. By using conventional refrigeration cycles,

we cannot obtain these low temperatures. Instead, more complex cycles must be used. There are three common methods to obtain mechanical refrigeration effect. These are liquid expansion in Joule-Thompson (J-T) valve, gas expansion in J-T valve and expansion in expander[2].

An example of the liquid expansion cycles is the household refrigerator. The refrigerant enters the J-T valve in liquid phase and its temperature drops. As a result, the cooling effect is produced. By using liquid expansion cycles, a minimum temperature around −100°C can be obtained but this is not enough to liquefy permanent gases. For this purpose, two or more cycles combined in cascade configuration is used to produce enough refrigeration effect to liquefy gases. Cascade liquefaction cycles are commonly used in liquefaction of natural gas in which propane, ethane, and methane are used as refrigerant. In some cycles, mixed refrigerant which is a mixture of nitrogen, methane, and propane are used[3].

Gas expansion cycle is a common cycle used in the liquefaction of gases. Linde and precooled Linde-Hampson cycles are examples of gas expansion cycles. In this cycle, inlet stream to the J-T (Joule-Thompson) valve is in gas phase. With this cycle, small amounts of liquid can be produced. Both liquid and gas expansion cycles utilize the Joule-Thompson effect to produce temperature drop.

Cycles which utilize expansion in an expansion engine are examples of Brayton gas refrigeration cycles. An expansion engine is not capable of producing enough liquefaction effect alone and thus it is mostly combined with J-T valve. Claude and Kapitza cycles are examples of these combined cycles[4].

1.2 Joule-Thompson Effect

As mentioned earlier, there are two possible ways to obtain required temperature drop for refrigeration and liquefaction: isenthalpic expansion in a valve and isentropic expansion in an expansion engine, or combination of these. Isenthalpic expansion is directly related to Joule-Thompson effect.

In Figure 1.1, schematic representation of a J-T valve is given. When a fluid passes through a well-insulated porous medium or a valve, pressure of the fluid decreases significantly. The change of the kinetic energy and potential energy can be neglected during this process. Then, the relation for the first law can be written as

$$h_i = h_e \tag{1.1}$$

Figure 1.1 Schematic representation of an expansion valve

The process for which the enthalpy values of the inlet and outlet stages are the same is called as throttling. In this process, with the pressure drop, there are three possible scenarios regarding temperature. Temperature of the fluid at exit stage of the valve may be higher or lower than the inlet temperature, or it remains constant. Joule and Thompson experimentally investigated this phenomena and described a coefficient which identifies the behavior of gases at the exit of an isenthalpic expansion process[5]. Joule-Thompson coefficient is defined as

$$\mu_{JT} = (\frac{\partial T}{\partial P})_h \tag{1.2}$$

In Figure 1.2, temperature-pressure diagram of the nitrogen is given with constant enthalpy lines. The J-T coefficient is actually the slope of the curves. The purple lines indicate zero slop where J-T coefficient is zero. This line also called as inversion line. No temperature change occur in this case and gas behavior is ideal. On the left side of the inversion line, the slope and J-T coefficient is positive, and temperature drop occurs during the expansion process. On the right side of the inversion line, the slope and the J-T coefficient is negative, and temperature increases during the expansion process.

For liquefaction cycles, J-T valve is important component. In order to obtain liquefaction effect, the J-T coefficient must be positive.

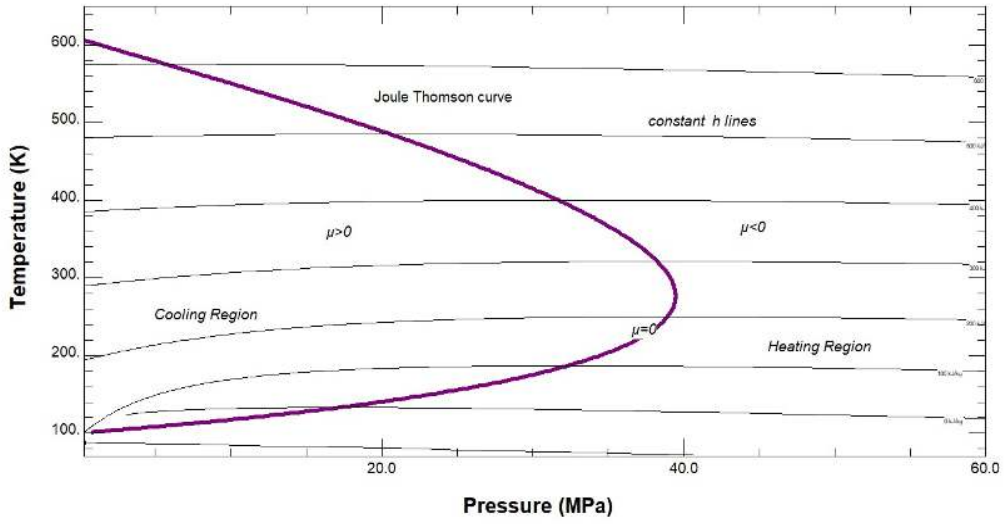

Figure 1.2 Temperature-Pressure diagram for nitrogen

1.3 Scope of Thesis

The liquefied gases are used by the variety of industries. Liquid air is not produced commercially but in air separation plants, air is separated into liquid nitrogen, liquid oxygen and argon. Liquid nitrogen is used in food industry, aerospace industry, etc. Liquid oxygen is mainly used in steel industry for carbon removing from steels and also used in rocket engines with liquid fluorine and liquid hydrogen[4]. On the other

hand, liquefied natural gas production is the one of the well-established area of cryogenics where 339.7 million tons per annum liquefaction capacity was reached in 2017 [6]. Also, using liquid hydrogen as an energy carrier and liquid air energy storage systems are promising applications.

Cryogenic processes are highly energy intensive. In Figure 1.3, the Carnot efficiency above and below the death state, where death state assumed as 300 K, is given. As can be seen from Figure 1.3, above the ambient temperature, some of the heat can converted into useful work. For a refrigerator working between 150 K and 300 K, heat rejected from low temperature source is less than work input. At the cryogenic limit 150 K, same amount of work is done as the amount of heat rejected from low temperature source. Below the cryogenic limit, more work is required than heat rejected from low temperature source, e.g. At 77.55 K (boiling point of nitrogen) almost 3 times more work required than cooling effect produced[7]. Due to these reasons, liquefaction cycles suffer from low efficiency.

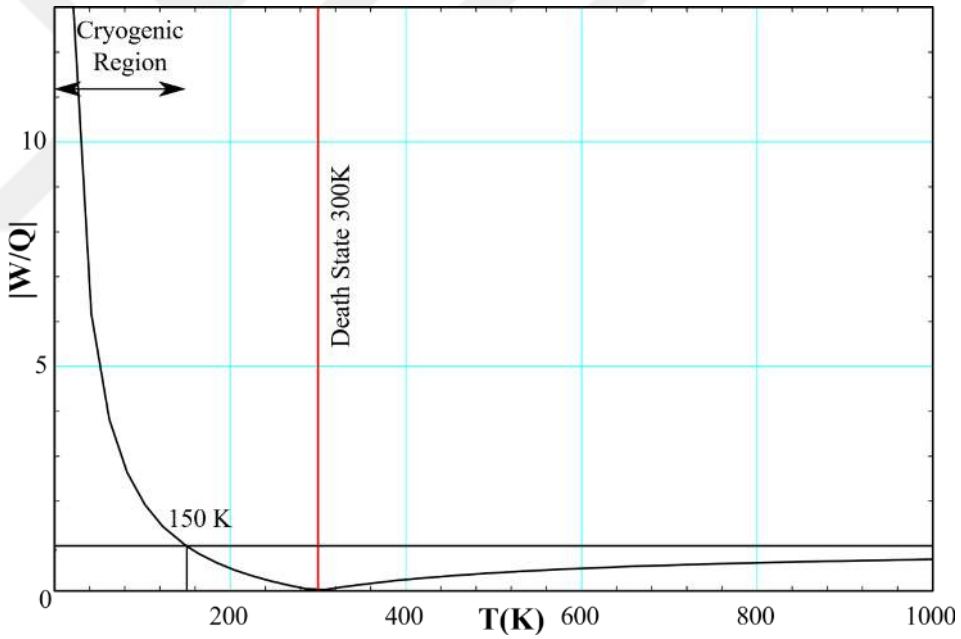

Figure 1.3 Variation of Carnot efficiency with temperature

In this thesis, commonly used liquefaction cycles, simple Linde-Hampson, precooled Linde-Hampson, Claude, and Kapitza cycles are modelled in computer environment using Engineering Equation Solver (EES)[8] and Unisim Design Suite[9] softwares. Economic analysis is also carried out to determine specific product cost and specific energy cost. Also, parametric studies are performed to determine effect of operation parameters such as compressor outlet pressure, compressor inlet temperature, minimum temperature difference in heat exchangers on the thermodynamic performance parameters such as liquid yield, liquefaction

work, COP, and second law efficiency as well as economic performance indicators such as specific product cost and specific energy cost.

1.4 Literature Survey

There are some useful books that covers thermodynamic analysis of gas liquefaction cycles[3,4,10]. These books cover fundamentals of gas liquefaction cycles from all aspects.

Kanoglu *et al.*[11], investigated effects of liquefaction temperature on the system performance and defined second law efficiency for liquefaction cycles with the help of Carnot refrigerators.

Maytal [12] studied effect of finite size recuperator performance on the efficiency of Linde-Hampson liquefiers. It was aimed to maximize production rates of the system for nitrogen and argon.

Syed *et al.* [13] carried out economic analysis of three hydrogen liquefaction cycles and found out that cost of the liquid hydrogen is mostly effected by energy cost.

Thomas *et al*. [14,15] investigated roles of expanders and heat exchangers in helium liquefaction cycles. They evaluated the effects of isentropic efficiency, mass flow rates of the expander and minimum temperature difference of heat exchangers on the exergetic performance of the cycles.

Cammatara *et al.*[16] carried out optimization of a liquefaction plant by using genetic algorithm. They determined optimum operation conditions including expander inlet temperature, the overall cycle efficiency, and liquid yield.

Nandi and Sarangi [17] studied hydrogen liquefaction cycles. They considered Linde-Hampson hydrogen liquefier, Claude hydrogen liquefier and helium-hydrogen condensing cycle and found out optimum operating conditions for all considered cycles.

Cardella *et al.*[18,19, 20] carried out optimization study for large scale hydrogen liquefaction plants. They discussed the current problems about high capital cost of hydrogen liquefaction plants and draw a road map for economically viable large-scale liquid hydrogen production.

Kanoglu [21] carried out exergy analysis of cascade operation of an LNG cycle. The governing equations for exergy destructions and exergy efficiencies for the components and overall cycle were evaluated.

Castle [22] summarized recent developments and promising future trends for air separation units. He discussed technical limitations and future advancements for both cryogenic and other air separation units.

Atrey [23] carried out thermodynamic analysis of Collins helium liquefier and pointed out the trade-off between optimum J-T valve temperature and expander inlet temperature.

Hassan *et al.*[24], carried out modelling and simulation study of main LNG heat exchanger. They created a physical model for main cryogenic heat exchanger and determined optimum configurations.

Chang *et al.*[25] studied effect of multi-stream heat exchangers on the performance of LNG liquefiers. They investigated effect of minimum temperature approach and UA on the figure of merit.

Guizzi *et al.*[26] performed thermodynamic analysis of liquid air energy storage systems. They developed a model using simple Linde-Hampson cycle with additional cold recovery system and calculated overall efficiency of the system.

Correa and Gundersen [27] proposed second law efficiency definitions for low temperature applications. They carried out a study on single-stage mixed refrigerant process and investigated applicability of several second law efficiency definitions in the literature to this process.

Krasae-in *et al.*[28] summarized the development of large-scale hydrogen liquefaction systems from 1898 to 2009.

Yılmaz *et al.*[29] proposed various hydrogen production and liquefaction systems using geothermal energy. They carried out thermodynamic and economic analysis of the proposed systems.

Krasae-in *et al.*[30] proposed novel hydrogen liquefaction system for small-scale applications. They carried out exergy analysis for this proposed system.

Ameel *et al.*[31] proposed a conceptual design of combined Linde-Hampson and Rankine cycles for liquid air energy storage applications.

Thomas *et al.*[32] investigated design of helium liquefiers using the second law of thermodynamics. They investigated effect of component performances on the system's overall performance and second law efficiency.

Chang [33] conducted thermodynamics analysis of natural gas liquefaction cycles. He investigated simple Linde-Hampson based cycles, reversed Brayton based cycles and combination of those cycles with mixed refrigerant and pure refrigerant used in precooling stages.

Li *et al.*[34]proposed an optimal design methodology for gas liquefaction cycles. They developed an algorithm based on genetic algorithm to maximize second law efficiency for cryo-expander based liquefaction configurations.

Nguyen *et al.* [35] carried out optimization study of three small scale LNG systems and compared them from efficiency and power consumption point of view.

The literature survey indicates that there are many studies for the investigation of gas liquefaction cycles considering both the first and second laws of thermodynamics. In this thesis, we intend to carry out a comprehensive analysis of common gas liquefaction cycles with various gases considering both the laws of thermodynamics and fundamental cost principles. We compare the performance of the cycles based on thermodynamic and economic analyses.

CHAPTER 2

THERMODYNAMIC ANALYSIS OF GAS LIQUEFACTION CYCLES

2.1 Introduction

In this chapter, ideal liquefaction cycle will be investigated first. Commonly used liquefaction cycles, Linde-Hampson, Pre-cooled Linde-Hampson, Claude, and Kapitza cycles are analyzed. First and second law analysis for each cycle are carried out and performance parameters such as liquid yield, liquefaction work, second law efficiencies are calculated for various working fluids.

Heat flows in the direction of increasing entropy, in other words, from high temperatures to low temperatures. With the help of refrigeration cycles, heat can be absorbed from a low temperature source and eventually transferred to a high temperature source. In a refrigeration cycle, working fluid, referred as refrigerant, continuously flow in a cycle. In contrast of refrigeration cycles, gas liquefaction systems operate on open cycles. Liquefied portion of the gas leaves the cycle as the product. Schematic representation of refrigeration and gas liquefaction cycles are given in Fig. 2.1.

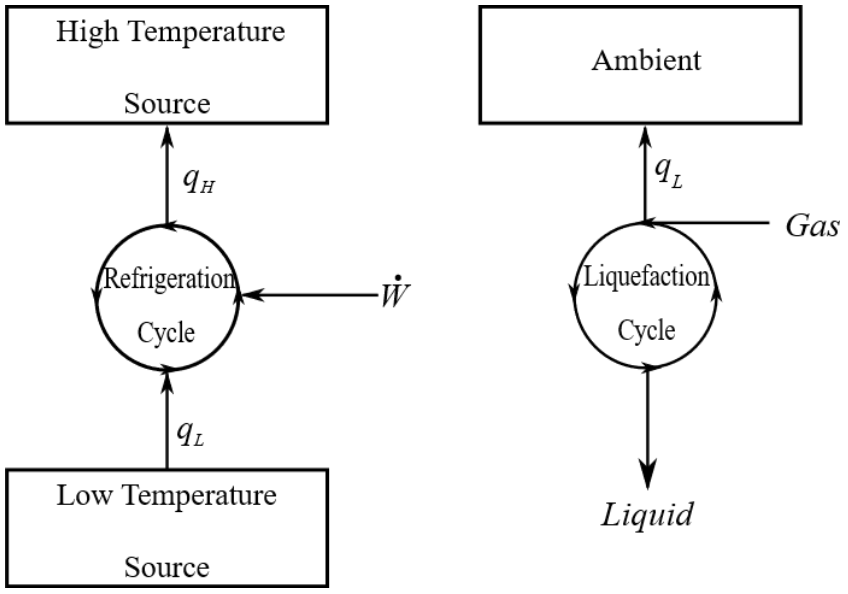

Figure 2.1 Schematic representation of refrigeration and liquefaction cycle

Gas liquefaction cycles are an important application of cryogenics. In this chapter, thermodynamic analysis of gas liquefaction cycles is performed. The cycles considered in this chapter are Simple Linde-Hampson cycle, Precooled Linde-Hampson cycle, Claude cycle and Kapitza cycle. The first and second law analysis are carried out for each cycle and their components. Before starting the analysis of gas liquefaction cycles, we start analysis with ideal refrigeration and gas liquefaction cycles.

2.2 Ideal Refrigeration and Gas Liquefaction Cycles

On his masterpiece study [35] Sadi Carnot describe thermodynamically perfect cycle which is called by his name Carnot cycle which composed of 4 reversible processes. Since all processes are reversible, Carnot cycle can operate as a heat engine or refrigerator. Carnot refrigerator is the most efficient refrigeration cycle operating between two thermal reservoirs. Schematic representation and *T-s* diagram of the Carnot cycle are given in Figures 2.2 and 2.3.

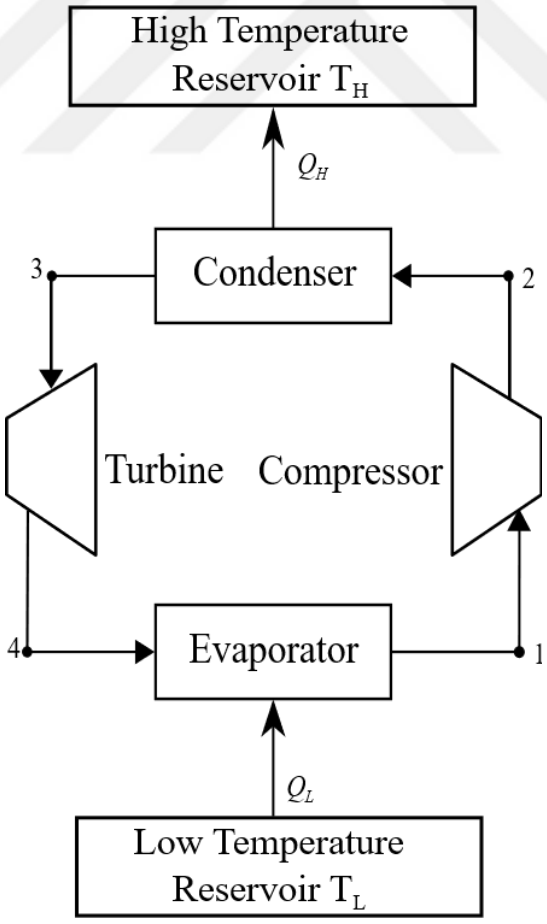

Figure 2.2 Schematic representation of Carnot Refrigerator

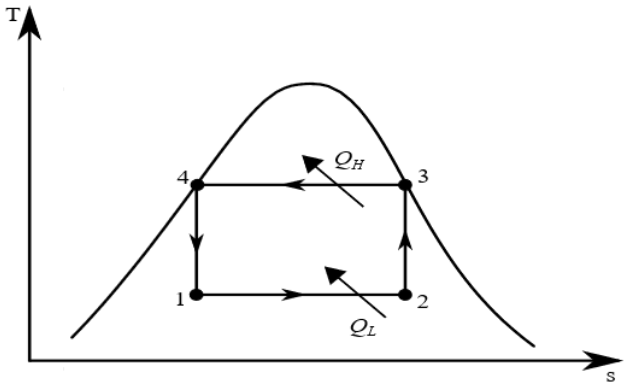

Figure 2.3 Temperature-entropy diagram of Carnot Refrigerator

Performance of any engineering system can be described as "Desired Output/Required Input" [36].The coefficient of performance of any refrigeration cycle can be expressed as

$$COP = \frac{\dot{Q}_L}{\dot{W}_{comp}} = \frac{\dot{Q}_L}{\dot{Q}_H - \dot{Q}_L} \tag{2.1}$$

For Carnot refrigerator, the performance of the cycle depends only on the temperatures of high and low temperature reservoirs. The coefficient of performance of the Carnot refrigerator can be expressed as

$$COP_C = \frac{T_L}{T_H - T_L} = \frac{1}{T_H / T_L - 1} \tag{2.2}$$

Eq. (2.2) is developed for Carnot refrigerator where heat rejection and addition processes are isothermal. This is not practical for gas coolers or liquefaction cycles where heat is absorbed in varying temperatures. It is more convenient to utilize the reversed Brayton cycle as the ideal cycle. Schematic representation and *T-s* diagram of the reversed Brayton cycle for gas cooling are given in Fig 2.4 and Fig 2.5, respectively.

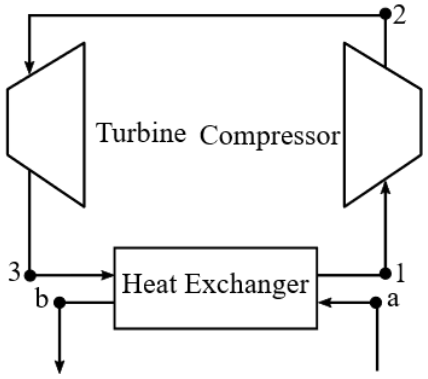

Figure 2.4 Schematic representation of ideal reversed Brayton cycle for gas cooling

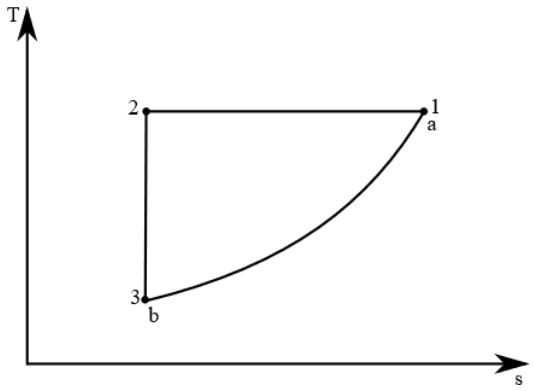

Figure 2.5 Temperature-entropy diagram of ideal reversed Brayton cycle for gas cooling

The coefficient of performance for ideal reversed Brayton cycle for gas cooling can be expressed as

$$COP = \frac{(h_1 - h_3)}{T(s_2 - s_1) - (\mathrm{h}_1 - \mathrm{h}_3)} \tag{2.3}$$

Ideal liquefaction cycle utilizes isothermal compression followed by isentropic expansion process. The schematic representation and *T-s* diagram of the cycles are shown in Fig. 2.6 and 2.7, respectively.

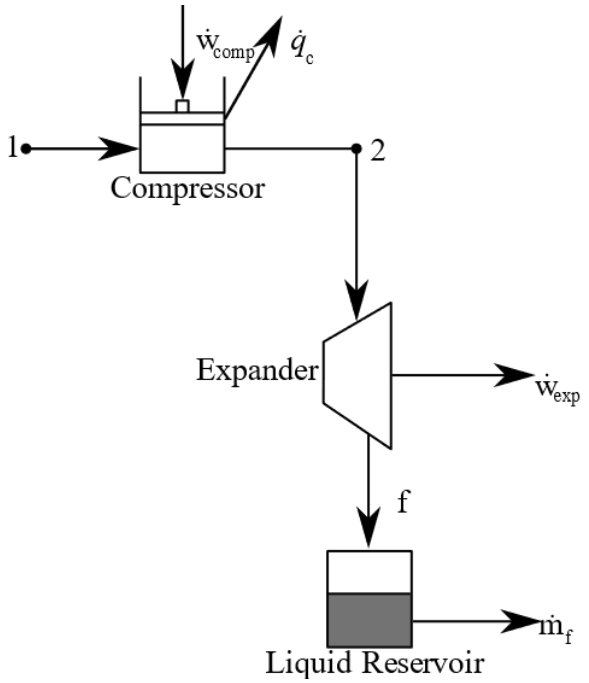

Figure 2.6 Schematic representation of ideal gas liquefaction cycle

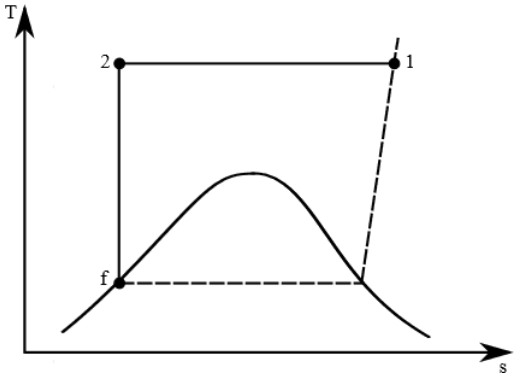

Figure 2.7 Temperature-entropy diagram of the ideal gas liquefaction cycle

Applying general energy and entropy balances for the ideal gas liquefaction cycle yields the reversible work for gas liquefaction systems

$$h_1 + \dot{w}_{comp} = \dot{w}_{exp} + h_f + \dot{q}_c \tag{2.4}$$

$$\dot{q}_c = T_0(s_1 - s_f) \tag{2.5}$$

$$w_{rev} = h_f - h_1 - T_0(s_f - s_1) \tag{2.6}$$

Since the state *f* is the saturated liquid at the pressure of state 1, Eq. (2.6) shows that the minimum work requirement to liquefy a gas depends only on the type of fluid and temperature and pressure of state 1[10]. In Table 2.1, the minimum work requirements for commonly used liquefied gases are given at 25°C and 101.325 kPa.

Table 2.1 Minimum work requirement for liquefaction of commonly used gases

Gas	Minimum work requirement for liquefaction w_{rev} (kJ/kg)	Reversible coefficient of performance COP_{rev}
Air	732.6	0.5794
Nitrogen	761.6	0.5663
Oxygen	629.1	0.6429
Argon	472.3	0.5703
Methane	1080	0.8425
Fluorine	564.2	0.6088
Hydrogen	11982	0.3281
Helium	6788	0.2289

The ideal liquefaction cycle provides the minimum work to liquefy a gas. But the ideal cycle is not practical due to extremely high pressure requirements [37]. Besides its impracticality, ideal gas liquefaction cycle is used to define the second law efficiency, which is a comparison between the ideal and actual performance.

$$\eta_{II} = \frac{w_{rev}}{w_{actual}} \tag{2.8}$$

Eq. (2.8) may be represented in terms of the coefficient of performance of ideal and actual systems[11]

$$\eta_{II} = \frac{COP_{actual}}{COP_{rev}} \tag{2.9}$$

In the following sections, thermodynamic analysis of the cycles, simple Linde-Hampson, precooled Linde-Hampson, Claude and Kapitza are presented. The cycles are simulated under the following assumptions:

- Cycles operate under steady state conditions
- Compressors are isothermal.
- The isentropic efficiency of the expanders is 100%
- There is no heat leakage in the cycles.
- There is no frictional pressure drop in the heat exchangers and pipes.

2.3 Simple Linde Hampson Cycle

The simple Linde-Hampson cycle has the simplest set-up among all other liquefaction cycles but suffer from low second law efficiencies. Simple Linde-Hampson cycle consist of one isothermal compressor, one heat exchanger and one expansion valve. Schematic representation and *T-s* diagram of the Simple Linde-Hampson cycle are given in Fig. 2.8 and 2.9, respectively.

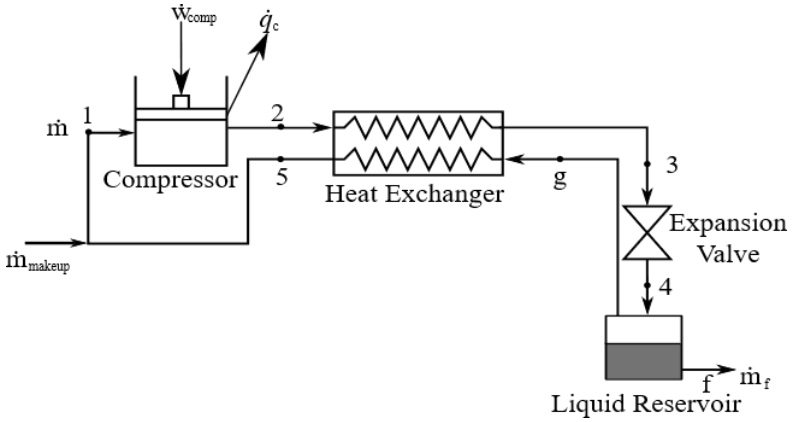

Figure 2.8 Schematic representation of Simple Linde Hampson Cycle

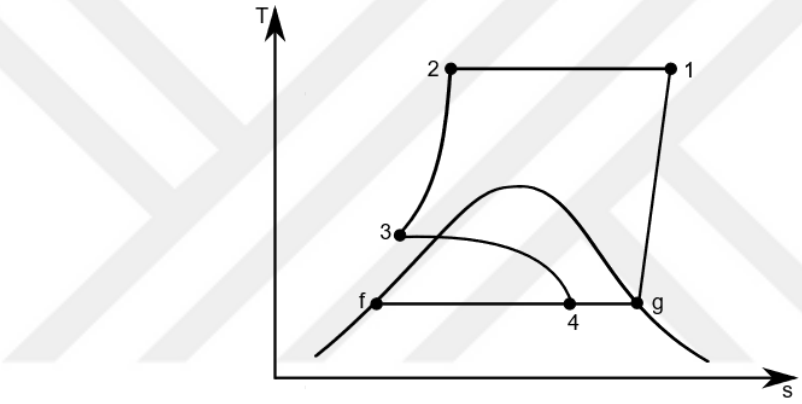

Figure 2.9 Temperature-entropy diagram of Simple Linde Hampson cycle

Gas at atmospheric conditions (101.325 kPa and 25°C) is compressed to high pressures in isothermal compressor, cooled in heat exchanger with the uncondensed portion of gas from previous cycle, and expand in Joule-Thompson valve. Liquefied portion of gas leave the cycle and uncondensed portion of gas mixed with makeup gas.

The refrigeration effect produced per unit mass of liquefaction can be determined from the heat rejected from makeup gas in order to turn into a liquid at state *f*. Assuming an ideal operation in the heat exchanger, the refrigeration effect per unit mass of the liquefied gas can be expressed as

$$q_L = h_1 - h_f \tag{2.10}$$

The refrigeration effect per unit mass of gas in the cycle may be expressed as

$$q_L = h_1 - h_2 \tag{2.11}$$

The cold box of any liquefaction system can be defined as where the main liquefaction process happens. In the simple Linde-Hampson cycle, the cold box

consists of heat exchanger, J-T valve and liquid reservoir. General energy balance on the cold box gives

$$\dot{m}h_2 = (\dot{m} - \dot{m}_f)h_1 + \dot{m}_f h_f \tag{2.12}$$

Rearranging Eq. (2.12) gives the mass fraction of the liquefied gas in the cycle:

$$y = \frac{h_1 - h_2}{h_1 - h_f} \tag{2.13}$$

The parameter y can be written as the liquefied mass fraction of the gas:

$$y = \frac{\dot{m}_f}{\dot{m}} \tag{2.14}$$

Energy balance on the heat exchanger gives

$$h_2 - h_3 = (1 - y)(h_5 - h_g) \tag{2.15}$$

The isenthalpic expansion in J-T valve yields

$$h_3 = h_4 \tag{2.16}$$

The quality of the mixture at state 4 can be written as in terms of fraction of liquid yield:

$$x_4 = 1 - y \tag{2.17}$$

An energy balance on isothermal compressor gives the compression work per unit mass of gas in the cycle:

$$w_{actual} = h_2 - h_1 - T_1(s_2 - s_1) \tag{2.18}$$

If we divide the liquefaction work to the liquid yield, we obtain the work consumed in the cycle in order to produce a unit mass liquefied gas:

$$w_{liq} = \frac{w_{net}}{y} \tag{2.19}$$

Eqs. (2.8) and (2.9) can be used to calculate the coefficient of performance and the second law of efficiency.

For thermodynamic analysis, gas at 25°C and 101.325 kPa is compressed to 20 MPa in an isothermal compressor. The minimum temperature difference in the heat exchanger is assumed as 0°Cat the hot end. Performance results for each fluid are given in Table 2.2.

Table 2.2 Performance data of simple Linde-Hampson cycle for various gases

	Air	Nitrogen	Oxygen	Argon	Methane	Fluorine
Liquid Fraction y	0.0829	0.0761	0.1082	0.1163	0.2004	0.0773
Refrigeration effect q_L (kJ/kg per gas)	35.22	32.82	43.74	31.69	182.4	26.56
Refrigeration effect q_L (kJ/kg per liquid)	424.4	431.3	404.4	272.5	909.9	343.5
Compressor work w_{comp} (kJ/kg per gas)	451.2	469.7	403.1	323.2	774.8	342
Liquefaction work w_{liq} (kJ/kg per liquid)	5442	6172	3727	2778	3866	4423
COP	0.0779	0.06988	0.1085	0.09809	0.2354	0.07767
Second law efficiency η_{II}	0.1345	0.1234	0.1688	0.1700	0.2794	0.1276

For the simple Linde-Hampson cycle, 8.2% of gas mass of the air liquefies. This value is 7.6%, 10%, 11%, 20%, and 7% for nitrogen, oxygen, argon, methane and fluorine, respectively. The cycle consumes 452 kJ per unit mass of gas entering the system and consumes 5449 kJ to produce 1 kg of liquefied product for air.

The simple Linde-Hampson cycle has low values of COP and second law efficiency. The COP value for nitrogen gas is 0.069. This means, to produce 1 kJ refrigeration effect, simple Linde-Hampson cycle should consume 14.4 kJ work. For the ideal gas liquefaction cycle this value is 1.78 for nitrogen gas. The second law efficiency of the simple Linde-Hampson cycle for nitrogen is 0.12.

Table 2.2 shows that the work requirement for producing 1 kg liquefied gas is very high for simple Linde-Hampson cycle. The high liquefaction work also effects COP and second law efficiency of the cycle. To improve the performance of the cycle, some modification may be made on cycle. Precooled Linde-Hampson cycle and Dual pressure Linde cycle are two of such modifications. In this study, Precooled Linde-Hampson cycle will be analyzed.

In Figures 2.10 to 2.12, performance indicators such as liquid yield, COP and second law efficiency are studied for various gases for simple Linde-Hampson cycle. Methane has the highest liquid yield followed by argon and highest COP and second law efficiency. They are followed by oxygen and argon, respectively. The differences in these values are due to different thermo-physical properties of the gases. This trend is also applicable to other cycles.

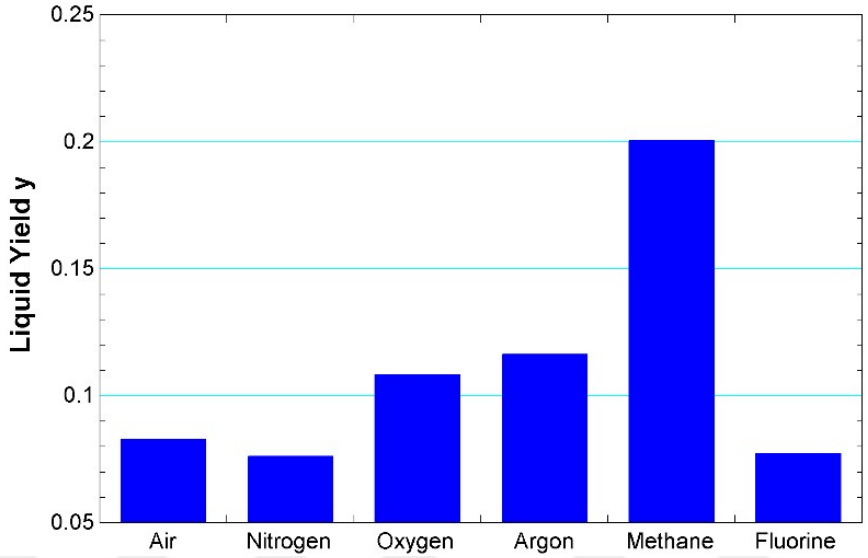

Figure 2.10 Liquid yield of the simple Linde-Hampson cycle for various gases

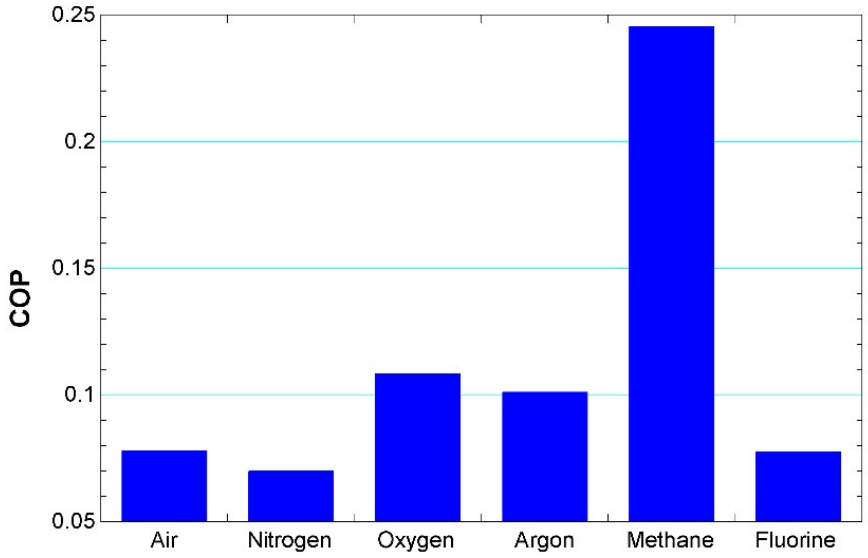

Figure 2.11 Coefficient of performance of the simple Linde-Hampson cycle for various gases

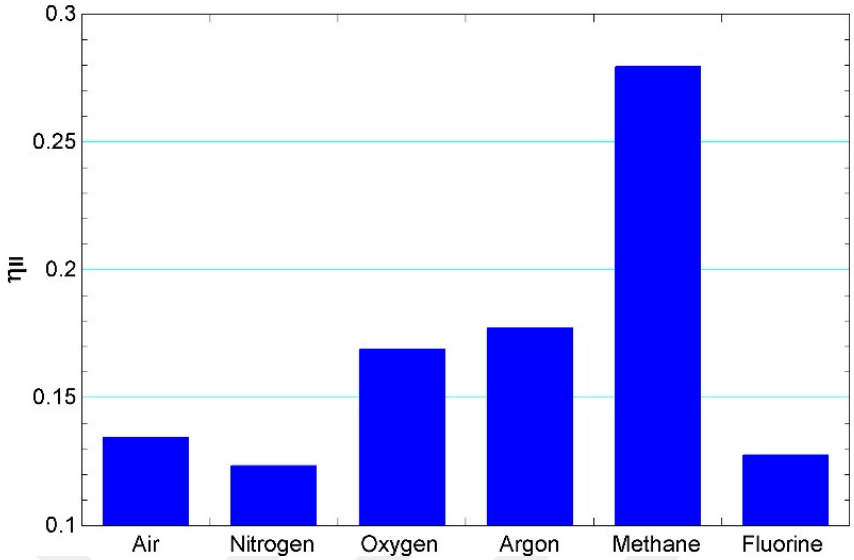

Figure 2.12 Second law efficiency of the simple Linde-Hampson cycle for various gases

2.4 Precooled Linde-Hampson Cycle

The second law efficiency of the simple Linde-Hampson cycle is very low. In order to increase the efficiency of the cycle, precooling can be applied to decrease the temperature at the inlet state of the Joule-Thompson valve. Precooled Linde-Hampson cycle is the one of the modifications of the simple Linde-Hampson cycle which utilize auxiliary refrigeration cycle for precooling. The schematic representation and *T-s* diagram of the precooled Linde-Hampson cycle are given in Figures 2.13 and 2.14, respectively.

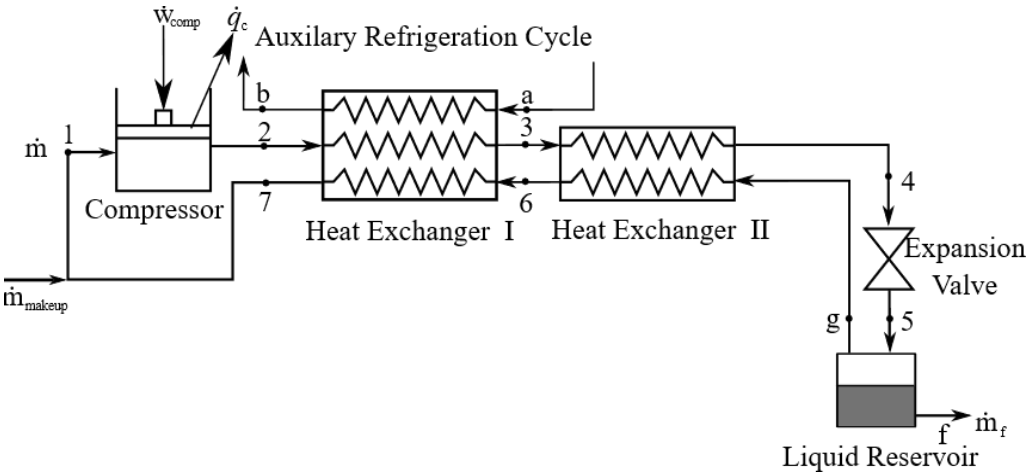

Figure 2.13 Schematic representation of precooled Linde-Hampson cycle

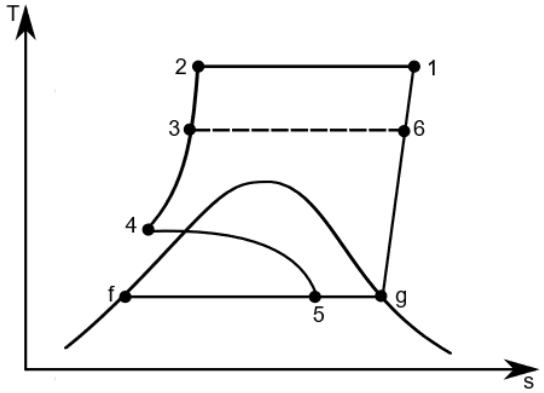

Figure 2.14 Temperature-entropy diagram of precooled Linde-Hampson cycle

As seen in Figure 2.10, the temperatures at state 3 and state 6 are the same for a 100% effective heat exchanger. There is also a second law limitation of this temperature. The temperature at state 3 and 6 cannot be lower than the boiling point of auxilary refrigerant[10].

With the ideal configuration, maximum yield can be obtained from the precooled Linde Hampson cycle. Applying energy balance to the second heat exchanger, J-T valve and liquid reservoir gives the maximum liquid yield for precooled Linde Hampson cycle:

$$y_{max} = \frac{h_6 - h_3}{h_6 - h_f} \tag{2.20}$$

Auxiliary refrigerant flow rate ratio to provide maximum liquid yield can be expressed determined from

$$z = \frac{\dot{m}_{aux}}{\dot{m}} \tag{2.21}$$

Work requirement for precooled Linde Hampson cycle with isothermal main compressor and isentropic auxilary compressor can be determined from

$$w_{actual} = h_2 - h_1 - T_1(s_2 - s_1) + (h_{2aux} - h_{1aux}) \tag{2.22}$$

In Eq. (2.22), h_{1aux} and h_{2aux} represent the inlet and outlet states the compressor in the auxiliary refrigeration cycle.

For thermodynamic analysis, gas at 25°C and 101.325 kPa is compressed to the 20 MPa in isothermal compressor and then precooled with auxiliary refrigeration cycle using R-134a as a working fluid in a three-way heat exchanger. After precooling, the cooling of gas continues with uncondensed portion of gas from the previous cycle. The gas expands freely in expansion valve. Results of the analysis are given in Table 2.3.

Table 2.3 Performance data of precooled Linde-Hampson cycle for various gases

	Air	Nitrogen	Oxygen	Argon	Methane	Fluorine
Liquid Fraction y	0.1424	0.1321	0.1837	0.2032	0.336	0.1364
Refrigeration Effect q_L (kJ/kg gas)	60.4	56.97	74.28	55.37	305.72	46.85
Refrigeration Effect q_L (kJ/kg liquid)	424.4	431.3	404.4	272.5	909.9	343.5
Compressor work w_{comp} (kJ/kg gas)	456.3	473.5	408.5	327	798.3	345.4
Liquefaction work w_{liq} (kJ/kg liquid)	3203	3585	2223	1609	2376	2533
COP	0.1325	0.1203	0.1819	0.1693	0.383	0.1356
Second Law Efficiency η_{II}	0.2288	0.2126	0.2831	0.2935	0.4549	0.2229

For each unit of gas mass entering the system, 14% of the gas is liquefied for air. Also, 456 kJ work is consumed per kg of gas and 3203 kJ is consumed per kg of liquid.

In Table 2.3, performance parameters of precooled Linde-Hampson cycle for various gases are given. Comparing the results with simple Linde-Hampson cycle, adding an auxiliary refrigeration cycle to the simple Linde-Hampson cycle significantly increases the refrigeration effect produced. As a result, the liquid yield also increases. Due to the auxiliary refrigeration cycle, compressor work per unit gas mass increases but the liquefaction work per unit liquid mass decreases due to relatively high liquid yield. The performance of the Linde-Hampson cycle can be further increased by adding an expander to provide additional refrigeration effect.

2.5 Claude Cycle

Most of the available work in the liquefaction cycles is destroyed in the isenthalpic expansion process. Claude cycle utilizes both isenthalpic and isentropic expansion processes in order to increase refrigeration effect. The schematic representation and *T-s* diagram of the Claude cycle are given in Figures 2.15 and 2.16 respectively.

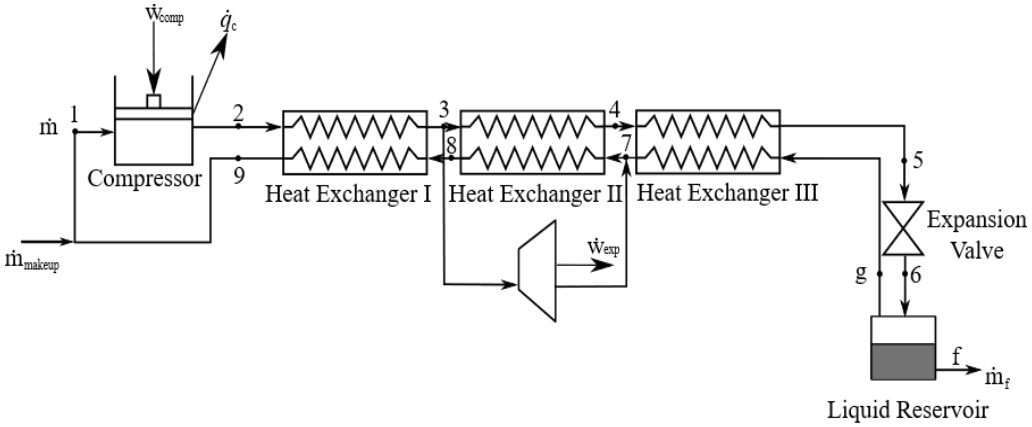

Figure 2.15 Schematic representation of Claude cycle

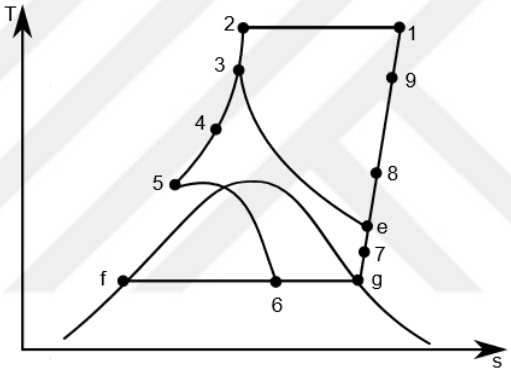

Figure 2.16 Temperature-entropy diagram of Claude cycle

In Claude cycle, gas is compressed to a pressure of 4 to 6 MPa in the compressor and then passed through the first heat exchanger. About 60-80 percent of the gas is diverted into the expander where gas is expanded isentropicly in order to produce work. This diverted stream returns to the cycle at state 7. The stream to be liquefied is cooled in the second and third heat exchangers and expand at constant enthalpy in the expansion valve. The expansion valve is still needed in Claude cycle due to the very high cost of the expander which would operate in the two phase region at cryogenic temperatures[38].

For Claude cycle, the refrigeration effect per unit mass of the liquefied gas can be expressed as

$$q_L = h_1 - h_f \tag{2.23}$$

The refrigeration effect per unit mass of the gas can be written as

$$q_L = h_1 - h_2 + r(h_3 - h_e) \tag{2.24}$$

The parameter *r* in eq. (2.25) represent the fraction of mass diverted to the expander and can be expressed as

$$r = \frac{\dot{m}_e}{\dot{m}} \tag{2.25}$$

Liquid yield for Claude cycle is given by

$$y = \frac{h_1 - h_2}{h_1 - h_f} + r\frac{h_3 - h_e}{h_1 - h_f} \tag{2.26}$$

In Eq. (2.26), the left side of the equation is the liquid yield expression of the simple Linde cycle. Right side of the equation is the refrigeration effect produced by the expansion process.

Energy balances on heat exchangers I, II, and III are given by

$$h_2 - (1-y)h_8 = h_3 - (1-y)h_9 \tag{2.27}$$

$$(1-r)\,\mathrm{h}_3 + (1-y)h_7 = (1-\mathrm{r})\,\mathrm{h}_4 + (1-y)\,\mathrm{h}_8 \tag{2.28}$$

$$(1-r)\,\mathrm{h}_4 + (1-y-r)h_g = (1-\mathrm{r})\,\mathrm{h}_5 + (1-y-r)\,\mathrm{h}_{co,HXIII} \tag{2.29}$$

where subscript co indicates the cold outlet.

The gas expanded in the expander is mixed with the cold outlet of the heat exchanger III. Energy balance of this mixing process can be written as

$$(1-y)h_7 = r(h_e) + (1-y-r)h_{\mathrm{co},HXIII} \tag{2.30}$$

The liquid yield also can be written in this manner:

$$y = (1-r)(1-\mathrm{x}_6) \tag{2.31}$$

Net work input to the cycle can be expressed as

$$w_{net} = h_2 - h_1 - T_0(s_2 - s_1) - r(h_3 - h_e) \tag{2.32}$$

For thermodynamic analysis, gas at atmospheric conditions (25°C and 101.325 kPa) is compressed to 4 MPa. The expander flow rate ratio is taken as 0.7. In Table 2.4 performance parameters for various gases are given.

Table 2.4 Performance data of the Claude cycle for various gases

	Air	Nitrogen	Oxygen	Argon	Methane	Fluorine
Liquid Fraction y	0.2506	0.2485	0.2415	0.2675	0.2650	0.2293
Refrigeration Effect q_L (kJ/kg per gas)	106.35	107.17	97.66	72.89	242.12	78.76
Refrigeration Effect q_L (kJ/kg per liquid)	424.4	431.3	404.4	272.5	909.9	343.5
Compressor Work w_{comp} (kJ/kg per gas)	312.8	324.2	281.9	226.1	555.7	238.6
Expander Work w_{exp} (kJ/kg per gas)	90.43	95.31	85.9	63.14	194.3	69.58
Liquefaction work w_{liq} (kJ/kg per liquid)	887.3	921.1	811.59	609.19	1358	737.15
COP	0.4783	0.4682	0.4982	0.4473	0.67	0.465
Second Law Efficiency η_{II}	0.8257	0.8268	0.7751	0.7752	0.7952	0.7653

Around 24% of the gas mass entering the system is liquefied for air, nitrogen and oxygen. To produce 1 kg liquid mass, the cycle consumes 887, 921 and 819 kJ for air, nitrogen and oxygen, respectively. The COP value of the Claude cycle for methane gas is 0.67. This means that, to produce 1 kJ refrigeration effect, Claude cycle must consume 1.49 kJ energy. When compared with other cycles, Claude cycle have the highest COP and second law efficiency values.

Table 2.4 shows that adding expander significantly increases the refrigeration effect produced per unit gas mass. Thus, the liquid yield increases as well as the second law efficiency and the COP. Also, the net work consumption decreases due to work produced by the expander. Adding isentropic expansion improves the performance of the cycle in two ways. Firs, adding expander to the system significantly increases the refrigeration effect produced,and thus more liquid yield is obtained. Second, the power produced by the expander is used in compressor, thus liquefaction work s reduced.

In Figure 2.17, heat duties of the heat exchangers in the Claude cycle for air liquefaction system are given. As can be seen from the figure, heat duty of the last heat exchanger is quite small compared to the first two. Sometimes third heat exchanger can be eliminated, reducing the Claude cycle to the Kapitza cycle.

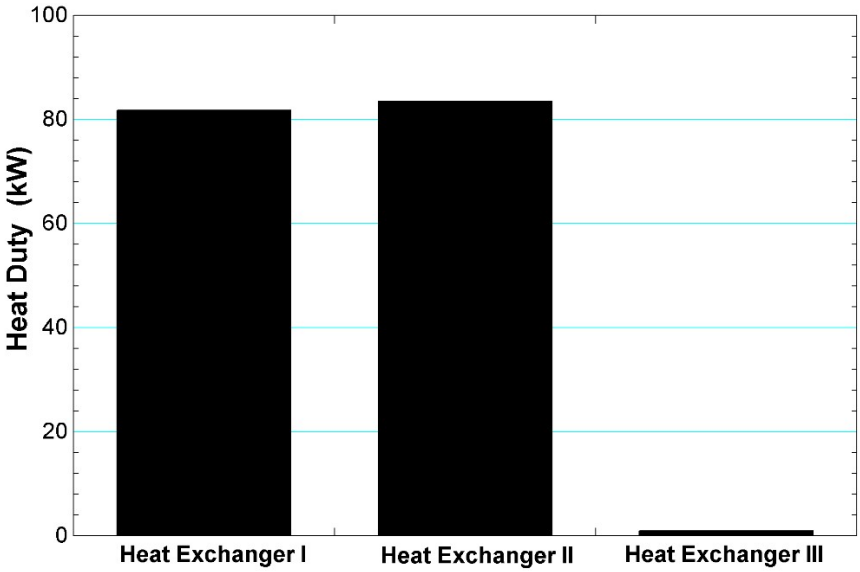

Figure 2.17 Heat duties of the heat exchangers in the Claude cycle for air

2.6 Kapitza Cycle

Kapitza cycle is a modification of the Claude cycle where the third heat exchanger of the cycle is eliminated due to low heat duty. Kapitza cycle's cold box consists of two heat exchangers, one expander and one expansion valve. Kapitza cycle usually operates at relatively low pressures, around 700 kPa. This is the biggest advantage of the Kapitza cycle compared with other cycles. Schematic representation and T-s diagram of the cycle is given by Figures 2.18 and 2.19, respectively.

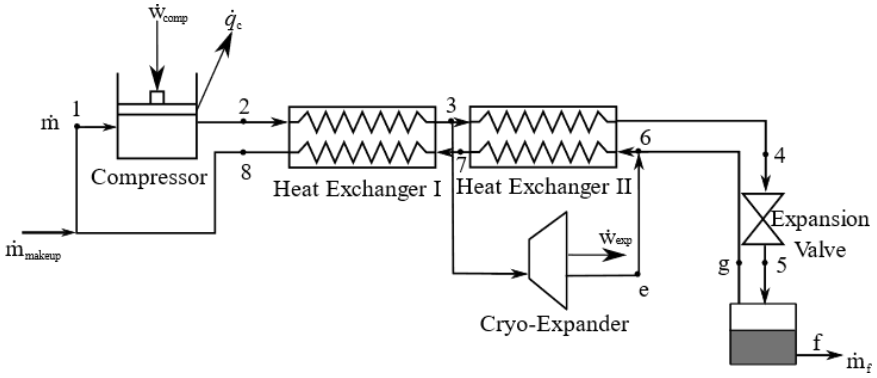

Figure 2.18 Schematic representation of Kapitza cycle

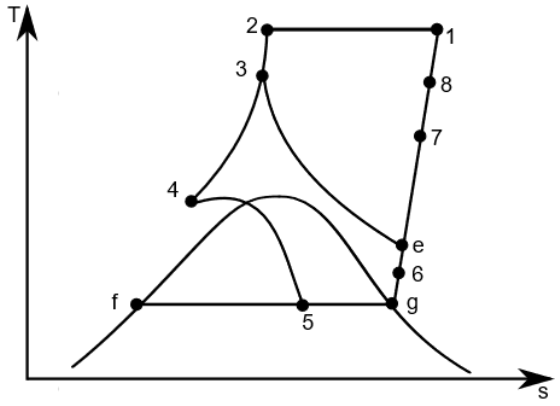

Figure 2.19 Temperature-entropy diagram of Kapitza cycle

For Kapitza cycle, the refrigeration effect per unit mass of the liquefied gas can be expressed as

$$q_L = h_1 - h_f \tag{2.33}$$

The refrigeration effect per unit mass of gas can be written as

$$q_L = h_1 - h_2 + r(h_3 - h_e) \tag{2.34}$$

Equation (2.25) can be applied to Kapitza cycle as well to calculate liquid yield. Energy balances for heat exchanger 1 and 2 are given by

$$h_2 - h_3 = (1-y)(h_8 - h_7) \tag{2.35}$$

$$(1-r)(\mathrm{h}_3 - h_4) = (1-y)(\mathrm{h}_7 - \mathrm{h}_6) \tag{2.36}$$

The gas expanded in the expander is mixed with the uncondensed portion of the gas in the cycle. An energy balance for mixing process can be written as

$$(1-y)\,\mathrm{h}_6 = (1-y-r)\,\mathrm{h}_g + r(h_e) \tag{2.37}$$

Net work input to the cycle can be expressed as

$$w_{net} = h_2 - h_1 - T_0(s_2 - s_1) - r(h_3 - h_e) \tag{2.38}$$

For thermodynamic analysis, gas at atmospheric conditions (25°C and 101.325 kPa) is compressed to a pressure of 700 kPa. Expander flowrate ratio is taken as 0.7. In Table 2.5 performance parameters for various gases are given. Due to low operating pressures, Kapitza cycle produces lower refrigeration effect and have lower liquid yield, COP, and second law efficiency compared with Claude cycle.Kapitza cycle is preferable due to ease of operations due to low pressure.

Table 2.5 Performance data of the Kapitza cycle for various gases

	Air	Nitrogen	Oxygen	Argon	Methane	Fluorine
Liquid Fraction y	0.0992	0.0940	0.0986	0.1098	0.1070	0.09219
Refrigeration Effect q_L (kJ/kg per gas)	42.10	40.93	39.87	29.92	97.35	31.66
Refrigeration Effect q_L (kJ/kg per liquid)	424.4	431.3	404.4	272.5	909.9	343.5
Compressor Work w_{comp} (kJ/kg per gas)	193.35	199.47	174.27	148.2	336.4	145.4
Expander Work w_{exp} (kJ/kg per gas)	37.02	38.11	36.91	27.9	89.04	29.65
Liquefaction work w_{liq} (kJ/kg per liquid)	1576	1716	1393	1095	2314	1255
COP	0.2692	0.2513	0.290	0.2488	0.3932	0.2737
Second Law Efficiency η_{II}	0.4648	0.438	0.4516	0.4313	0.4667	0.4495

In Table 2.6, performance data of the Claude cycle and Kapitza cycle for argon are compared under the same operating conditions (P_2=4 MPa, r=0.7). Kapitza cycle has lower liquid yield, COP, andsecond law efficiency. Because the third heat exchanger is eliminated, the first and second heat exchangers' heat duties are increased. The outlet temperature of the first heat exchanger is decreased. As a result, the,the refrigeration effect produced in the expander of the Kapitza cycle is lower than that in the Claude cycle.

Table 2.6 Performance data of the Claude and Kapitza cycles for argon under same operating conditions

	Claude Cycle	Kapitza Cycle
Liquid Fraction y	0.2675	0.2117
Refrigeration Effect q_L (kJ/kg per gas)	72.89	59.42
Refrigeration Effect q_L (kJ/kg per liquid)	272.5	272.5
Compressor Work w_{comp} (kJ/kg per gas)	226.1	225.9
Expander Work w_{exp} (kJ/kg per gas)	63.14	48.59
Liquefaction work w_{liq} (kJ/kg per liquid)	609.19	837.55
COP	0.4473	0.3351
Second Law Efficiency η_{II}	0.7752	0.5877

CHAPTER 3

ECONOMIC ANALYSIS OF GAS LIQUEFACTION CYCLES

3.1 Introduction

In this chapter, economic analysis of gas liquefaction cycles is performed. Cost models are formed with cost data available in literature for each cycle. Detailed sizing of the plain fin type of heat exchanger are also covered.

Economic analysis of any engineering system is an important design stage. From thermodynamic point of view, the cycle with a high second law efficiency may not be economically viable. For example, heat exchanger with 100% effectiveness gives the best performance from thermodynamic point of view. However, an infinitely large heat transfer area is required for this process to takes place. As a result, the initial cost of the system becomes very high.

Gas liquefaction cycles are massive energy consumers. Daily demand for liquid air products is around 5000 tons from air separation units and other cryogenic plants in UK[39]. First liquid air energy storage demonstration plant was constructed in UK with the capacity of 300 kW/2.5 MWh[40]. On the other hand, the largest single application of liquefaction process is liquefied natural gas (LNG). Global liquefaction capacity has reached 339.7 million tons/year in January 2017 [6]. Also, liquid hydrogen may surpass LNG production in the future. Therefore, with continuous growth in the field, it is important to have a better understanding on the liquefaction economy.

Details of economic analysis of plants can be found elsewhere[41],[42]. To obtain a better understanding on the cost structure of gas liquefaction process, economic models are created for simple Linde-Hampson cycle, precooled Linde-Hampson cycle, Claude cycle, and Kapitza cycle with various gases. To obtain specific cost of the liquefied product, the expenses of liquefaction plant are divided into three categories; capital expenses, operating&maintenance expenses and energy expenses. They are investigated separately. Schematic of the cost structure of the gas liquefaction plant is given in Figure 3.1.

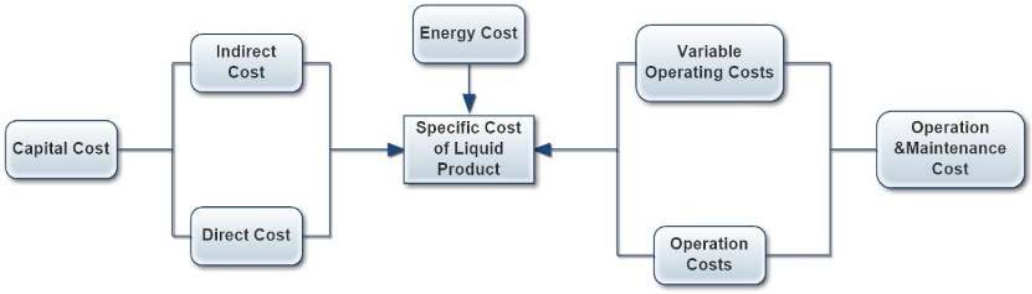

Figure 3.1 Cost structure of the liquefaction plant

Capital cost is divided into direct and indirect costs. Direct cost includes equipment purchasing and installation costs. Indirect cost includes land project execution and construction costs. Purchased costs of equipment are determined from cost function available in literature and compared with vendor's data [43].

Operating & maintenance cost is divided into variable and operating costs. Variable costs include feed gas loses, seal & purge gases, cooling water, refrigerant make-up, etc. Operating cost includes personal, supervision and maintenance costs.

In general, energy cost is investigated under variable operating costs due to its direct relationship with electricity cost. Liquefaction plants are massive energy consumers, and specific cost of liquefied product is mostly affected by energy cost. For this reason, it is better to investigate energy cost separately from the O&M costs.

3.2 Capital Cost

Capital cost is one-time cost unlike O&M and electricity costs which are continuous throughout the operation of the plant. For this reason, the capital cost is treated differently than other costs of the plant.

Capital cost is divided into direct and indirect costs. Direct expenses cover all permanent equipment and their installations besides expenses during the construction of the facility such as land cost, civil, structural and architectural work. Indirect cost is not directly related with the operation of plant but still needed to keep plant operating [4,44]. In Table 3.1, general estimation for both direct and indirect costs are given. The percentages are taken from the given references [4] and [7].

Table 3.1 General cost estimation for liquefaction cycle

Direct Cost	
Purchased Equipment Cost • Compressors • Plate Fin Heat Exchangers • Cryo-Turbines • Refrigeration Units • Storage Tanks	
Purchased Equipment Installation	33% of Purchased Equipment Cost
Piping	35% of Purchased Equipment Cost
Instrumentation and controls	12% of Purchased Equipment Cost
Electrical Equipment and materials	13% of Purchased Equipment Cost
Civil, Structural and architectural work	21% of Purchased Equipment Cost
Service Facilities	35% of Purchased Equipment Cost
Indirect Cost	
Engineering and supervision	8% of Direct Cost
Construction cost	15% of Direct Cost
Contingency	15% of the Engineering and supervision+ Construction Cost

3.2.1 Purchased Equipment Cost Estimation

The first stage of economic analysis is estimating purchased equipment cost. There are several ways to carry out this estimation. The most accurate one is the economic data supplied from the vendor. But this data is not always available and may not be the fastest way to estimate purchased equipment cost. There are other ways such as using scaling factors to estimate cost of equipment with comparing the costs of formerly known equipment's cost with new equipment. This scale factors can be found elsewhere [42]. Also, this method is not always available due to lack of equipment.

The method used in this study is the cost estimation charts, which are cost functions that are available in [45] and [46]. About 25% error is involved in this method due to uncertainties with cost functions. All the cost functions used in this thesis are modified into mid 2017 dollars with Chemical Engineering Plant Cost Index (CEPCI) [47]

$$Cost\ at\ the\ reference\ year = original\ \text{cost}\ \text{X}\left(\frac{Cost\ index\ for\ reference\ year}{Cost\ index\ of\ original\ \text{cost}'s\ year}\right) \qquad (3.1)$$

Compressors and expanders are main components in the gas liquefaction systems. For liquefaction process, screw or reciprocating types of compressors are generally used. It is impractical to use one stage compressor while compressing a gas to high

pressures. In this study, three stage compression is used. The pressure ratio is $(P_n/P_1)^{1/n}$ where n is the number of stages. In addition to producing work, the expanders in liquefaction process are used to produce cooling effect.

The cost functions of the compressor and the expander are calculated from

$$C_{comp} = 10.18(W_{comp})^{(0.61)} \tag{3.2}$$

$$C_{\exp} = 0.54356(W_{\exp})^{(0.81)} \tag{3.3}$$

Equation 3.2 and 3.3 gives the purchased equipment cost for compressor and expander in thousands of dollars K$, where work terms are in horsepower.

Probably, the most crucial components of the gas liquefaction cycles are heat exchangers. The heat exchanger used in a liquefaction process must be compact, have high heat transfer area, be reliable and cost friendly. Mostly aluminum plate fin type of heat exchangers is used in liquefaction process.

Details of the design of the heat exchanger can be found in [48]. In this study, the required surface areas of the heat exchangers are calculated using both ε-NTU and LMTD methods with the help of compact heat exchangers library of the EES software. Design considerations are given in Table 3.2.

Table 3.2 Design Considerations for Heat Exchangers

Heat Exchangers Type	PFHX
Fin Type	Plain
Fin Surface Geometry Designation	3.01
Heat Exchanger Material	Aluminum
Allowable Pressure Drop	2%

In Figures 3.2 and 3.3, temperature profiles of heat exchangers I and II for nitrogen are given for Claude cycle. As can be seen from Figure 3.2, minimum temperature difference occurs at the hot end of the heat exchanger. But in Figure 3.3, the minimum temperature difference occurs inside of the heat exchanger. Around the critical temperature and pressures, specific heats of the substances vary considerably. Due to this reason, conventional effectiveness expression which uses the constant property assumption cannot be used. We need to define the maximum possible heat transferand calculate the required heat transfer area. Maximum possible heat transfer is determined from the smaller of the expressed quantities in the following equations[49].

$$\dot{Q}_{max} = \dot{m}_c(\mathrm{h}_{c,out} - h_{c@(\mathrm{P}_c, T_{h,in})}) \tag{3.4}$$

$$\dot{Q}_{max} = \dot{m}_h(\mathrm{h}_{\mathrm{h,in}} - h_{\mathrm{h}@(\mathrm{P}_h, T_{c,in})}) \tag{3.5}$$

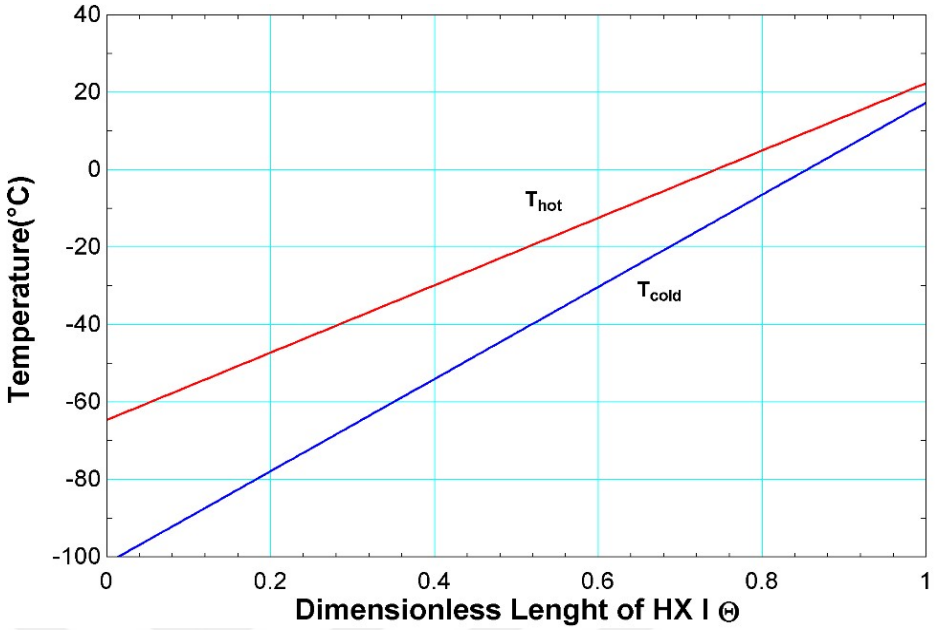

Figure 3.2 Temperature distribution along the heat exchanger I for Claude cycle

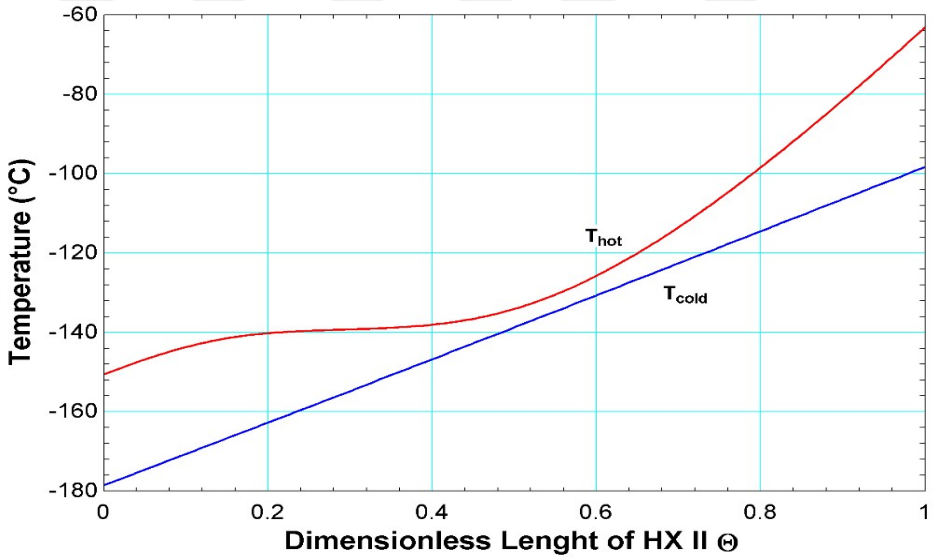

Figure 3.3 Temperature distribution along the heat exchanger II for Claude cycle

Effectiveness of a heat exchanger can be defined as

$$\varepsilon = \frac{\dot{m}_c(h_{c,out} - h_{c,in})}{\dot{Q}_{max}} = \frac{\dot{m}_h(h_{\mathrm{h,in}} - h_{\mathrm{h,out}})}{\dot{Q}_{max}} \tag{3.6}$$

Soyars [50] investigated the applicability of constant properties to cryogenic helium heat exchangers and found that using constant property assumption in sizing cause considerable errors. To size a heat exchanger with internal pinch point, heat

exchanger should be divided into equal parts like finite difference method and for each part UA terms should be calculated.

$$\dot{Q}=UA_i \Delta T_{LMTD,i} \tag{3.7}$$

The overall heat transfer coefficient for plate fin types of heat exchangers is defined as

$$\frac{1}{U}=\frac{1}{\eta_{0h}h_h}+\frac{aA_0}{k_w A_w}+\frac{A_{0h}/A_{0c}}{\eta_{0c}h_c} \tag{3.8}$$

where η_0 is the surface effectiveness, h is the heat transfer coefficient, k is the thermal conductivity and a is the plate thickness.

Cost of the heat exchanger is directly related to heat transfer area. To estimate cost, the cost function taken from [51] and modified into mid 2017 dollars and can be expressed as

$$C_{hx} = 327 A^{0.639} \tag{3.9}$$

where *C* is cost in $ and *A* is heat transfer area. Again, using modified cost function, the cost of storage vessels is estimated based on one hour of liquefied product storage capacity assumption as

$$C_{vessel} = 4.659 \exp[2.631+1.3673(\ln V)-0.06309(\ln V^2)] \tag{3.10}$$

where V is the volume of the product in gallon. The cost of intercoolers is estimated from

$$C_{\text{intercooler}} = 860 Q^{0.65} \tag{3.11}$$

where Q is the heat duty of the intercoolers. The costs of the separator and expansion valve are not considered due to their low values.

3.2.2 Levelized Capital Cost

In order to evaluate cost of the product, after the determination of the capital cost, all expenses of the plant should be levelized throughout the expected economic life. Capital cost can be levelized by

$$U_{capital} = C_{capital} \frac{i}{1-(1+i)^{-n}} \tag{3.12}$$

where $C_{capital}$ is the capital cost, i is the interest rate and n is the expected economic life. In this thesis, interest rate is considered as 8% and expected life is considered as 20 years.

3.3 Operating and Maintenance Cost

There are several factors that affect operating and maintenance cost of the plant such as working regime, maintenance periods, labor cost, etc. O&M cost is divided into variable operating cost and operating costs. Variable operating expenses include instrumental air, necessary lubricants, cooling waters, refrigerant and other make-up gases. Operating costs include operation personnel, supervision, inspections, maintenance, overhauls and repairs.

For gas liquefaction plant, annual operating and maintenance cost can be estimated as 1.5% to 3.5% of the capital cost. In this study, annual operating and maintenance cost is taken as 3.5% of capital cost and given by

$$U_{O\&M} = 0.035 C_{capital} \tag{3.13}$$

3.4 Energy Cost

Generally, energy cost is evaluated as a part of variable operating cost. To liquefy so called permanent gases such as air, hydrogen etc., enormous amount of work is consumed due to nature of the liquefaction process. For this reason, energy cost plays an important role in the evaluation of the cost of liquefied product and investigated separately from the O&M costs.

Cost of the liquefied product is directly affected by the liquefaction work and electricity prices. The annual cost of the liquefied product can be determined from

$$U_{Energy} = \dot{W} H C_e \tag{3.14}$$

where Ẇ is the work consumption in kW, H is the annual operating hours, and C_e are the cost of electricity in \$/kWh. For the economic analysis, the capacity factor is considered as 90% (equivalent of 7884 hours/year) with a unit electricity cost of 0.06 \$/kWh.

3.5 Cost of Liquefied Product

Calculation of the cost of the product is an important step for any economic analysis. In Table 3.3, the parameters used for economic analysis are summarized. Using these values, the annual capital cost, annual O&M cost, and annual energy cost are calculated.

Table 3.3 Economic parameters used in this study

Expected economic life (years)	20
Annual interest rate	8%
Cost of electricity C_e (\$/kWh)	0.06
Capacity factor	90%
Annual operating hours (hours/year)	7884

The calculation of annual costs yields an important result: specific product cost. The specific product cost is the amount of money spent to obtain a unit mass of liquefied product and can be calculated from

$$Specific\ Product\ C\,\mathrm{os}\,t = \frac{U_{energy} + U_{capital} + U_{O\&M}}{\dot{m}_{product}} \tag{3.15}$$

where $\dot{m}_{product}$ is the annual production rate in kg or tons.

Another important economic indicator is the specific energy cost, which has high influence on determination of the specific product cost. Specific energy cost can be calculated from

$$Specific\ Energy\ Cost = \frac{U_{energy}}{\dot{m}_{product}} \tag{3.16}$$

3.6 Economic Analysis of the Cycles

For the economic analysis, all considered cycles are modeled with initial setup with a production capacity of 10 tons/day. The economic analysis is carried out for all considered cycles using the data from the earlier sections. For the economic evaluation, the following assumptions are made for cycle performance:

- Compressors have an isothermal efficiency of 60%.
- Expanders have an isentropic efficiency of 80%.
- Minimum approach temperature for all heat exchangers is 5 K.
- The turbomachinery equipment has mechanical efficiency of 95%.

3.6.1 Economic Analysis of Simple Linde-Hampson Cycle

Simple Linde-Hampson cycle is the first technology used commercially for gas liquefaction. But due to high liquefaction energy required, most of the commercial plants today utilize other cycles. The capital cost for simple Linde-Hampson cycle includes a three-stage compressor with intercoolers and a heat exchanger with a vessel. With the previously stated considerations, the economic analysis of simple Linde-Hampson cycle is carried out. The results are given for 10 tons/day and 1000 tons/day capacities in Table 4.4.

Table 3.4 Results of economic analysis for Simple Linde-Hampson Cycle

Working Fluid	Plant Capacity (tons/day)	Total capital cost (Million $)	Annual capital cost (Million $/year)	Annual O&M cost (Million $/year)	Annual Energy Cost (Million $/year)	Specific cost of liquefied product ($/kg)	Specific cost of energy ($/kg)
Air	10	1.19	0.122	0.042	0.608	0.2115	0.1666
	1000	9.19	0.936	0.321	60.8	0.17	0.1666
Nitrogen	10	1.22	0.125	0.043	0.701	0.2381	0.1921
	1000	10.1	1.02	0.353	70.1	0.1959	0.1921
Oxygen	10	1.11	0.113	0.038	0.399	0.151	0.1094
	1000	6.85	0.698	0.240	39.9	0.1119	0.1094
Argon	10	0.97	0.09	0.033	0.273	0.1113	0.0750
	1000	5.43	0.553	0.190	27.3	0.07705	0.0750
Methane	10	1.69	0.173	0.06	0.393	0.1715	0.1078
	1000	21.27	2.16	0.744	39.3	0.1158	0.1078
Fluorine	10	1.01	0.101	0.035	0.501	0.175	0.1375
	1000	5.13	0.522	0.179	50.1	0.1394	0.1375

The simple Linde-Hampson cycle has the least number of equipment and due to simplicity of its setup, initial cost of the cycle is lower than other considered cycles. However, the simple Linde-Hampson cycle consumes the highest amount of energy to liquefy a unit gas mass which leads to the highest energy cost. Simple Linde-Hampson cycle is not used in large scale applications.

Methane has the highest specific product cost and specific energy cost values and fluorine has the lowest specific product cost and specific energy cost values for both 10 tons/day and 1000 tons/day capacities. Different gases have different cost values due to different thermophysical properties, sizing, power requirement, etc.

Among various cost items, the energy cost has the highest values for both 10 tons and 1000 tons production capacity. As a result, the energy cost plays an important role in the determination of the specific product cost. As the production capacity increases, specific product cost value gets close to the specific energy cost.

3.6.2 Economic Analysis of Precooled Linde-Hampson Cycle

Precooled Linde-Hampson cycle is one of the modifications of the simple Linde-Hampson cycle which uses an auxiliary refrigeration cycle to precool gas before the expansion. The capital cost for the precooled Linde-Hampson cycle includes three-stage compressors with intercoolers, two heat exchangers, a refrigeration unit, and a storage vessel. The results of the economic analysis are given in Table 3.5.

Table 3.5 Results of economic analysis for precooled Linde-Hampson cycle

Working Fluid	Plant Capacity (tons/day)	Total capital cost (Million $)	Annual capital cost (Million $/year)	Annual O&M cost (Million $/year)	Annual Energy Cost (Million $/year)	Specific cost of liquefied product ($/kg)	Specific cost of energy ($/kg)
Air	10	1.21	0.123	0.043	0.331	0.1364	0.0908
	1000	9.53	0.971	0.333	33.15	0.0944	0.0908
Nitrogen	10	1.24	0.127	0.044	0.375	0.1496	0.1028
	1000	10.45	1.64	0.365	37.53	0.1068	0.1028
Oxygen	10	1.12	0.114	0.039	0.223	0.1034	0.0611
	1000	7.15	0.728	0.250	22.32	0.0638	0.0611
Argon	10	0.978	0.096	0.034	0.159	0.0802	0.0436
	1000	5.645	0.574	0.197	15.92	0.0457	0.0436
Methane	10	1.71	0.175	0.06	0.227	0.1267	0.0622
	1000	21.66	2.20	0.758	22.72	0.0703	0.0622
Fluorine	10	1.01	0.103	0.035	0.262	0.1101	0.0719
	1000	5.431	0.553	0.19	26.2	0.0740	0.0719

Adding an auxiliary refrigeration unit to the simple Linde-Hampson cycle increases the initial cost, but more refrigeration effect is produced, and the energy cost is reduced. When compared with the simple Linde-Hampson cycle, precooled Linde-Hampson cycle have lower specific product cost and specific energy cost values due to additional refrigeration cycle. It should be noted that, mass flow rate of the auxiliary refrigeration cycle is determined in order to maximize the heat transfer. Each gas has its own auxiliary refrigerant mass flow rate, and this affects the cost of the auxiliary refrigeration unit. Again, this is due to different thermophysical properties of the working fluids.

3.6.3 Economic Analysis of Claude Cycle

In large scale liquefaction applications, such as air separation plants or hydrogen storage units, Claude cycle or its variations are used. Capital cost for Claude cycle includes the costs of three compressors with intercoolers, three heat exchangers, one expander and one storage vessel. In Table 3.6, the results of economic analysis are presented for Claude cycle.

Table 3.6 Results of economic analysis for Claude cycle

Working Fluid	Plant Capacity (tons/day)	Total capital cost (Million $)	Annual capital cost (Million $/year)	Annual O&M cost (Million $/year)	Annual Energy Cost (Million $/year)	Specific cost of liquefied product ($/kg)	Specific cost of energy ($/kg)
Air	10	2.78	0.283	0.0974	0.141	0.1430	0.03862
	1000	70.03	7.167	2.463	14.11	0.065	0.03862
Nitrogen	10	2.897	0.295	0.1014	0.1507	0.1499	0.04129
	1000	72.53	7.388	2.539	15.07	0.06849	0.04129
Oxygen	10	2.63	0.267	0.0923	0.128	0.1341	0.03517
	1000	67.66	6.891	2.368	12.84	0.06054	0.03517
Argon	10	2.177	0.221	0.076	0.0910	0.1066	0.02495
	1000	58.12	5.985	2.057	9.105	0.04698	0.02495
Methane	10	3.705	0.377	0.129	0.2147	0.1977	0.05881
	1000	88.884	9.04	3.109	21.47	0.0921	0.05881
Fluorine	10	2.49	0.253	0.0871	0.186	0.1258	0.03249
	1000	64.62	6.582	2.262	11.86	0.0567	0.03249

When compared with simple Linde-Hampson and precooled Linde-Hampson cycle, Claude cycle has higher number of equipment. This significantly affect initial cost of the cycle as observed in Table 3.6.

Adding an expander unit increases the refrigeration effect and more liquid is produced. Also, work produced by the expander decreases the compressor work. Therefore, in Claude cycle, more liquid is produced with a smaller work input and energy cost is reduced.

As the production capacity increases, the energy cost becomes much more dominant in the evaluation of specific product cost for liquefaction cycles. Claude cycle has the lowest specific energy cost among all liquefaction cycles and this makes Claude cycle more suitable for large scale applications.

3.6.4 Economic Analysis of Kapitza Cycle

Kapitza cycle is one of the modifications of the Claude cycle operating at lower pressure levels while eliminating the last heat exchanger. Kapitza cycle is mostly used in air separation units. Capital cost of the Kapitza cycle includes three-stage compressor unit with intercoolers, one expander, two heat exchangers, and one storage vessel. Results of the economic analysis for the Kapitza cycle are given in Table 3.7.

Table 3.7 Results of economic analysis for Kapitza cycle

Working Fluid	Plant Capacity (tons/day)	Total capital cost (Million $)	Annual capital cost (Million $/year)	Annual O&M cost (Million $/year)	Annual Energy Cost (Million $/year)	Specific cost of liquefied product ($/kg)	Specific cost of energy ($/kg)
Air	10	3.81	0.88	0.133	0.46	0.271	0.128
	1000	89.2	9.08	3.123	46.9	0.162	0.128
Nitrogen	10	3.93	0.400	0.137	0.494	0.2831	0.135
	1000	91.51	9.321	3.203	49.46	0.1698	0.135
Oxygen	10	3.349	0.341	0.117	0.374	0.2281	0.1025
	1000	80.51	8.20	2.818	37.41	0.1327	0.1025
Argon	10	2.72	0.277	0.0952	0.2711	0.1763	0.0742
	1000	68.17	6.944	2.386	27.11	0.0998	0.0742
Methane	10	4.79	0.488	0.167	0.646	0.3568	0.177
	1000	109	11.1	3.2	64.6	0.2179	0.177
Fluorine	10	3.31	0.337	0.116	0.368	0.2252	0.101
	1000	79.74	8.122	2.791	36.86	0.1309	0.101

When compared with the Claude cycle, Kapitza cycle has higher initial cost, despite having a smaller number of equipment. This is because, Kapitza cycle has lower liquid yield as seen in Table 3.5. A higher amount of gas mass entering the cycle requires larger equipment size.

3.7 Conclusions

Economic analysis is carried out for the considered cycles using engineering economy principles in order to determine specific cost of the liquefied product and specific cost of energy. Results show that the capital, O&M, and energy costs are different for different cycles and working fluids.

Simple Linde-Hampson cycle has the lowest initial and O&M costs but involves the highest amount of liquefaction work. As a result, energy cost is high. For large scale applications, simple Linde-Hampson cycle is not a suitable choice.

Precooled Linde-Hampson cycle is a modification to the simple Linde-Hampson cycle with the addition of an auxiliary refrigeration cycle. With some increase to the initial cost, precooled Linde-Hampson cycle has the lowest specific product cost among all considered cycles for 10 tons/day production capacity. This makes it suitable for small scale applications.

As the production capacity increases, energy cost plays a much dominant role in determination of the specific cost of the product. As the production capacity increases, the specific product cost value becomes close to the specific energy cost value.

Claude cycle has the lowest specific product cost for 1000 tons/day applications. This makes it suitable for large scale applications. On the other hand, Kapitza cycle

does not have any significant advantages over other cycles due to higher initial cost and lower liquid yield.

CHAPTER 4

PARAMETRIC STUDIES ON GAS LIQUEFACTION CYCLES

4.1 Introduction

In this chapter, we investigate effects of operating and design parameters on the thermodynamic and economic performance of the cycles. Effects of compressor inlet temperature, compressor outlet pressure, compressor isothermal efficiency, expander isentropic efficiency and minimum approach temperatures in heat exchangers on the liquid yield, liquefaction work, second law efficiency, and specific product cost are investigated.

4.2 Parametric Studies on Simple Linde-Hampson Cycle

In Chapters 2 and 3, thermodynamic and economic analysis of simple Linde-Hampson cycle were carried out. In this section, the results of parametric studies on the cycle are presented.

4.2.1 Effect of Compressor Inlet Temperature

Effect of compressor inlet temperature on the liquid yield, COP, liquefaction work and second law of efficiency are given in Figures 4.1 to 4.5 for various gases. As shown in Figure 4.1, as the compressor inlet temperature decreases, the temperature at the valve inlet decreases, and the liquefaction effect produced by the valve increases. Thus, the liquid yield increases with a decrease in compressor inlet temperature.

In Figure 4.2, the effect of the compressor inlet temperature on the liquefaction work is depicted. The compressor inlet temperature affects the liquefaction work in two ways: As the compressor inlet temperature increases, the compressor work increases. This increases the inlet temperature of the J-T valve, and thus it decreases the liquid yield. As the compressor inlet temperature decreases, the isothermal compressor work also decreases. Also, an increase in liquid yield decreases the liquefaction work. This is because, more liquid can be produced with the same work consumption.

The effect of the compressor inlet temperature on the COP and second law efficiency of the simple Linde-Hampson cycle is given in Figures 4.3 and 4.4. As the inlet temperature of the compressor decreases, the refrigeration effect produced per unit gas mass decreases, and the liquefaction work decreases. Therefore, the

COP of the cycle increases as the inlet temperature decreases. As the COP increases, the cycle performance gets closer to the ideal performance which in turn increases the second law efficiency.

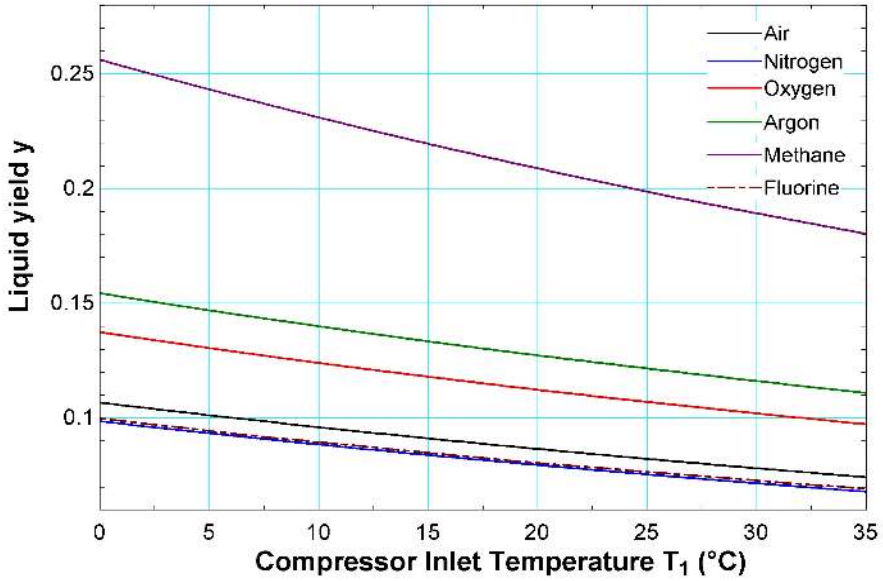

Figure 4.1 Effect of compressor inlet temperature on liquid yield for simple Linde-Hampson cycle

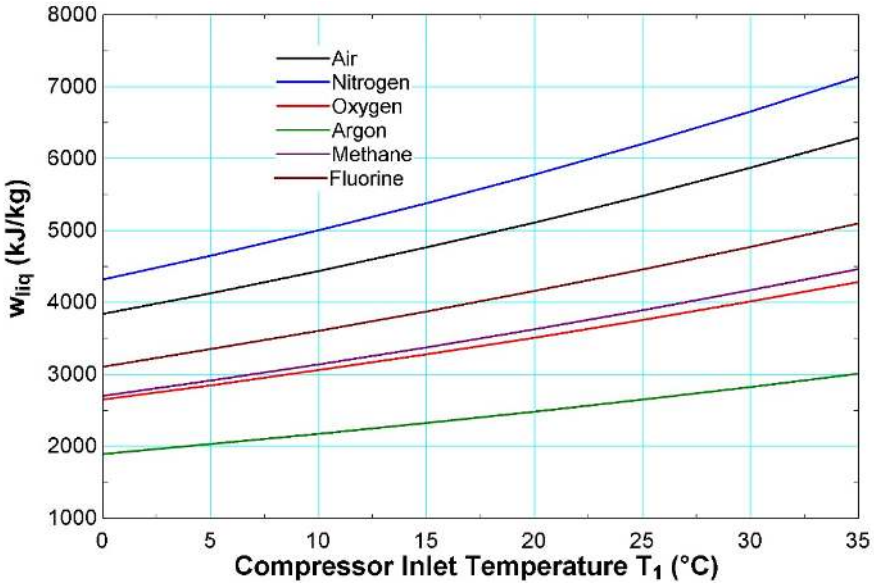

Figure 4.2 Effect of compressor inlet temperature on liquefaction work for simple Linde-Hampson cycle

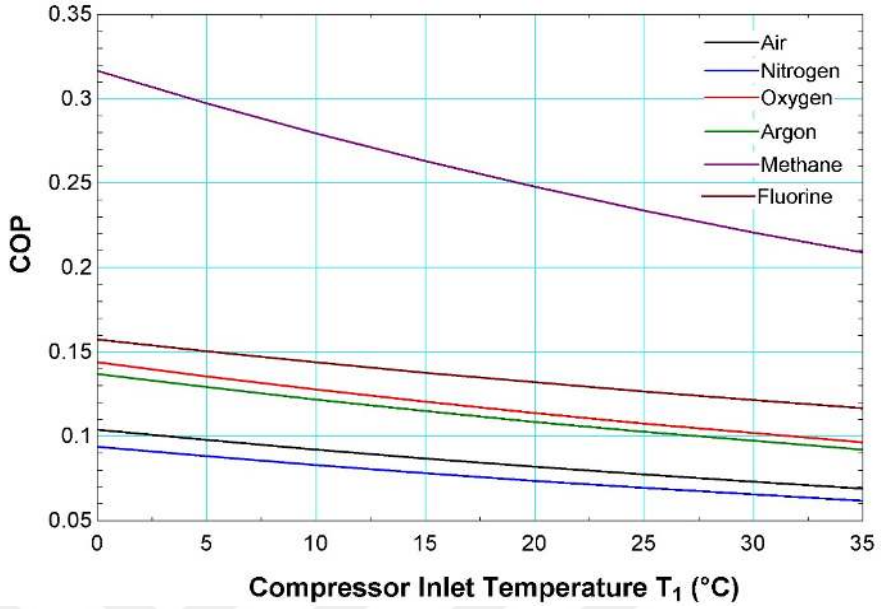

Figure 4.3 Effect of compressor inlet temperature on coefficient of performance (COP) for simple Linde-Hampson cycle

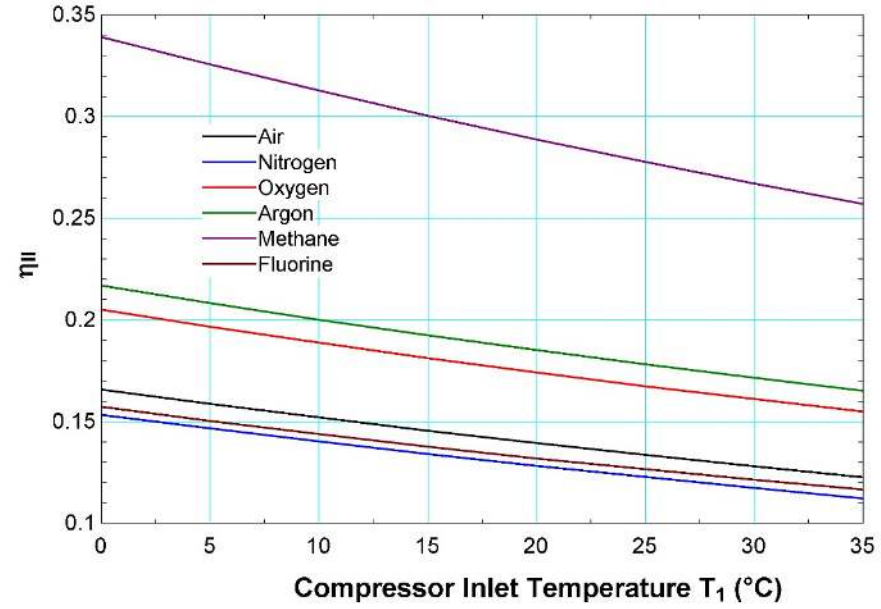

Figure 4.4 Effect of compressor inlet temperature on second law efficiency for simple Linde-Hampson cycle

In Figures 4.5 and 4.6, effect of compressor inlet temperature on the specific product cost and specific energy cost are given. It should be noted that the compressor inlet temperature of the actual liquefaction plants is generally the atmospheric temperature. In this thesis, the required refrigeration unit to cool down inlet temperature is not considered in our economic calculations. As the compressor

inlet temperature decreases, the liquefaction work decreases. As a result, the specific energy cost and specific product cost also decrease.

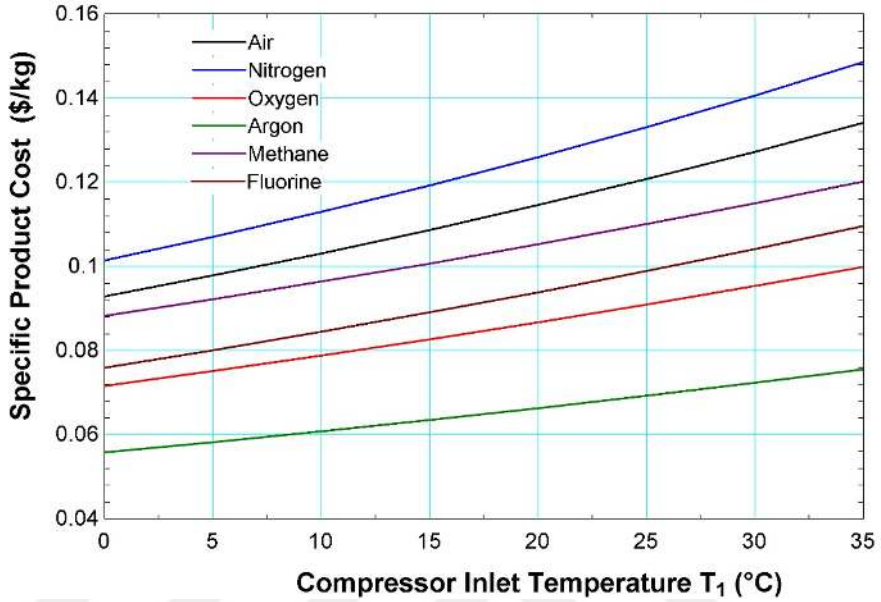

Figure 4.5 Effect of compressor inlet temperature on specific product cost for simple Linde-Hampson cycle

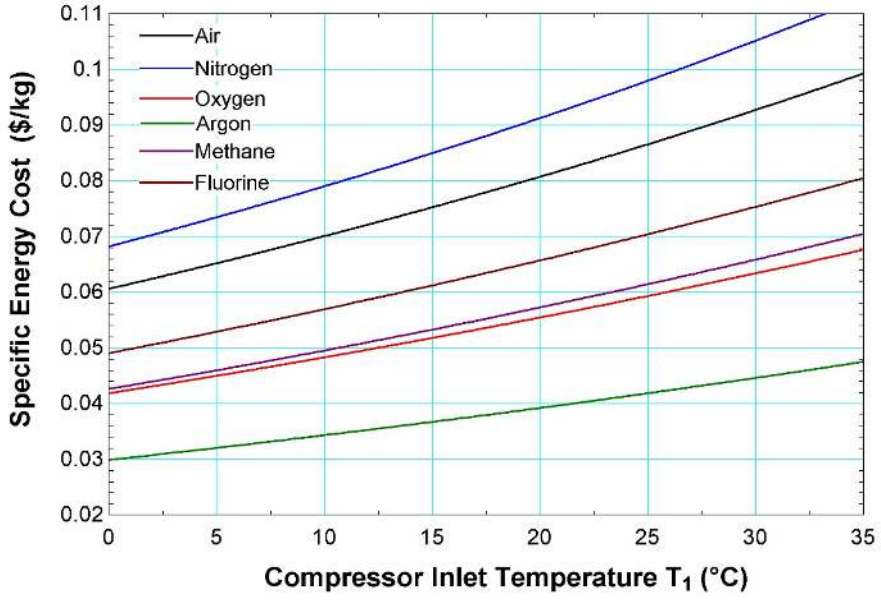

Figure 4.6 Effect of compressor inlet temperature on specific energy cost for simple Linde-Hampson cycle

4.2.2 Effect of Compressor Outlet Pressure

Figure 4.7 shows the effect of compressor outlet pressure on the liquid yield. After the inversion line is reached, the liquid yield is decreased with an increase in the outlet pressure. To obtain maximum liquid yield, the operating pressure should be selected such that it lies within the inversion line. For air, this value is 0.1076 which occurs at 42.85 MPa.

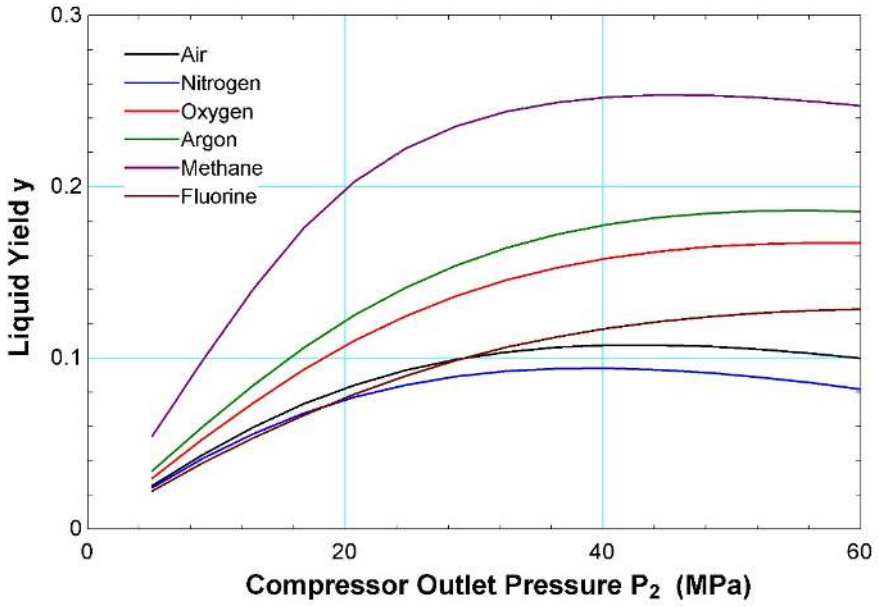

Figure 4.7 Effect of compressor outlet pressure on liquid yield for simple Linde-Hampson cycle

The effect of compressor outlet pressure on the liquefaction work, COP and second law of efficiency are given in Figures 4.8 to 4.10. As the pressure increases, there is a significant decrease in the liquefaction work until optimum point is reached. Also, the COP and second law efficiency increase until the optimum point is reached. Due to the natural logarithmic behavior of the isothermal work, after optimum value is reached, there is a slight increase in the liquefaction work and a decrease in the COP and second law efficiency.

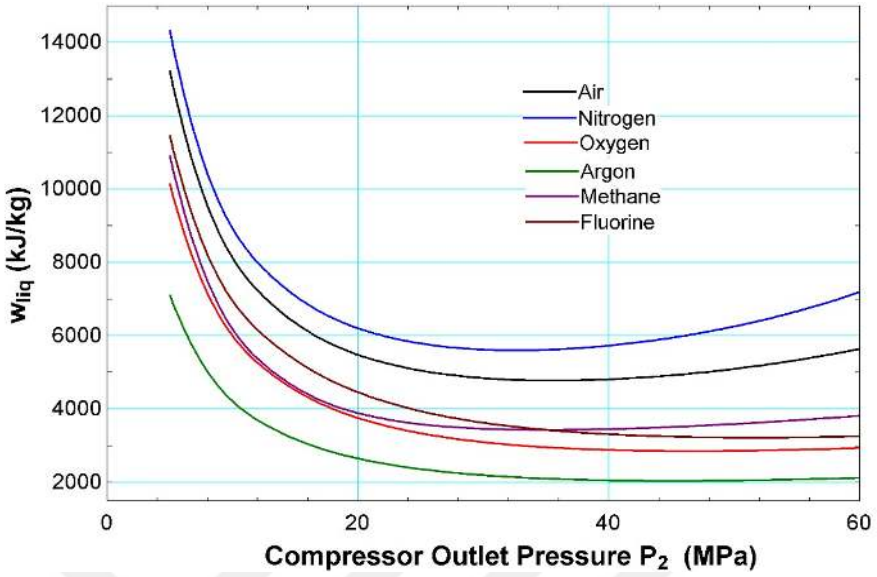

Figure 4.8 Effect of compressor outlet pressure on liquefaction work for simple Linde-Hampson cycle

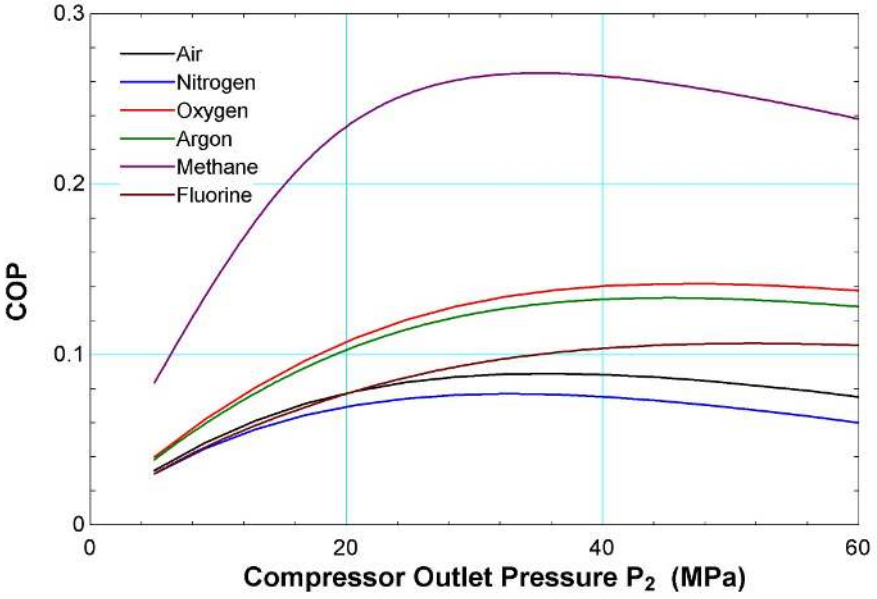

Figure 4.9 Effect of compressor outlet pressure on COP for simple Linde-Hampson cycle

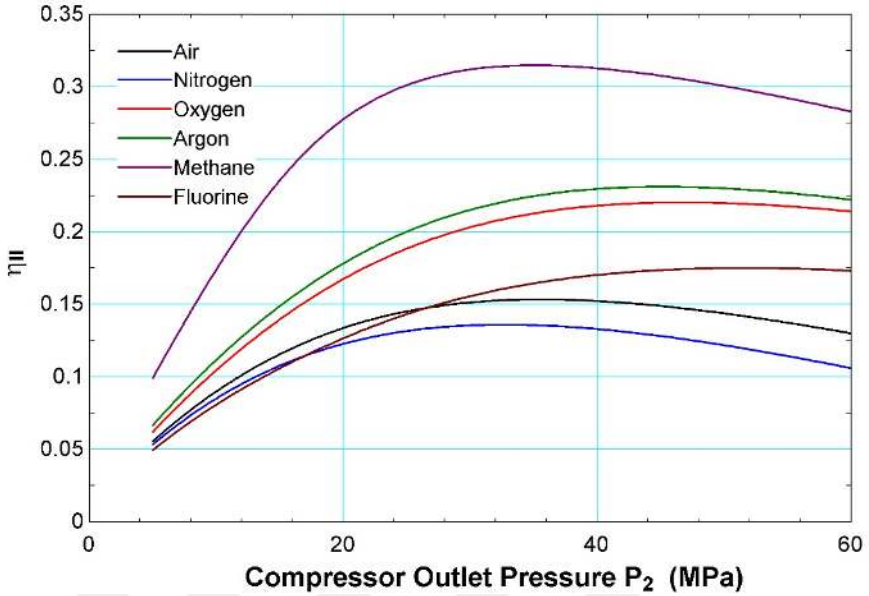

Figure 4.10 Effects of compressor outlet pressure to second law efficiency for simple Linde-Hampson cycle

In Figures 4.11 and 4.12, the effect of compressor outlet pressure on the specific product cost and specific energy cost are given. These two economic performance indicators are directly related to the liquefaction work, and thus they have similar trends as the liquefaction work.

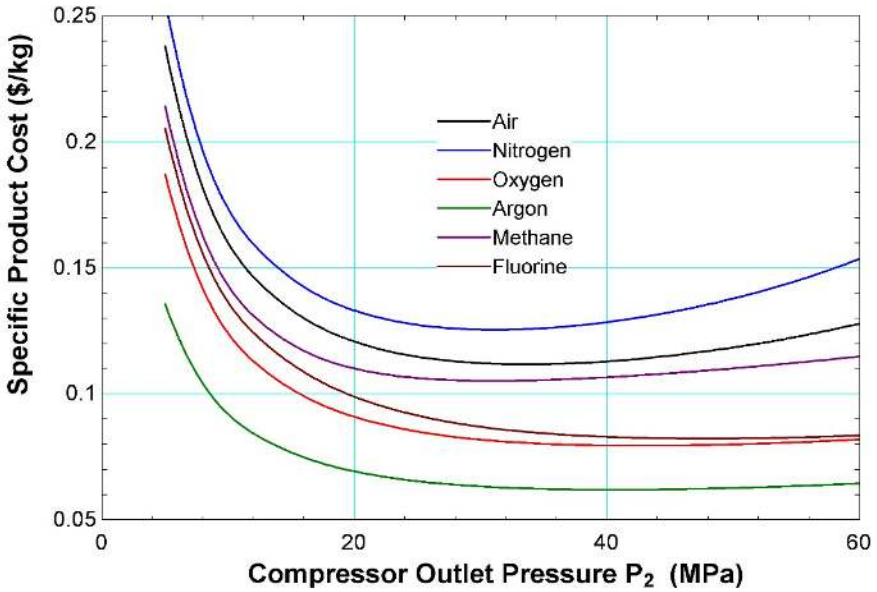

Figure 4.11 Effect of compressor outlet pressure on specific product cost for simple Linde-Hampson cycle

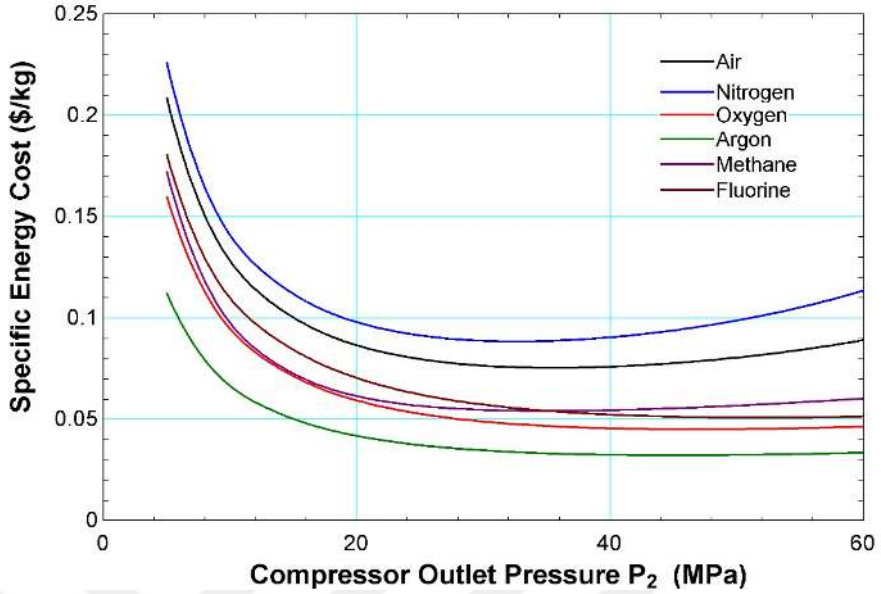

Figure 4.12 Effect of compressor outlet pressure on specific energy cost for simple Linde-Hampson cycle

4.2.3 Effect of Isothermal Compressor Efficiency

The isothermal efficiency of the compressor does not affect the liquid yield of the cycle, but it affects other performance indicators. The effect of isothermal compressor efficiency on the liquefaction work, COP and second law efficiency are given in Figures 4.13 to 4.16. As the isothermal efficiency decreases, the liquefaction work increases and the COP decreases. Also, as a result of decreasing the isothermal efficiency, the cycle deviates further from the ideal liquefaction cycle performance and this decreases the second law efficiency.

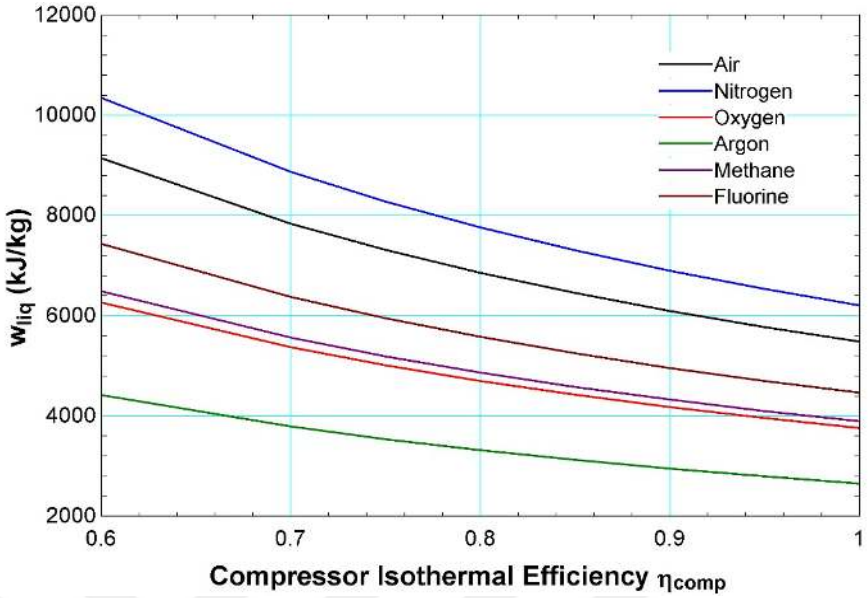

Figure 4.13 Effect of isothermal efficiency of compressor on liquefaction work for simple Linde-Hampson cycle

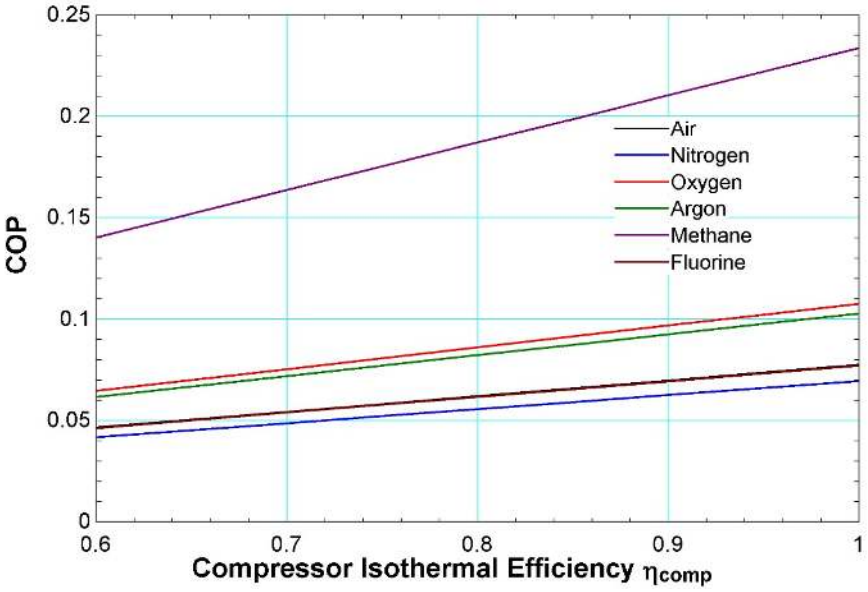

Figure 4.14 Effect of isothermal efficiency of compressor on COP for simple Linde-Hampson cycle

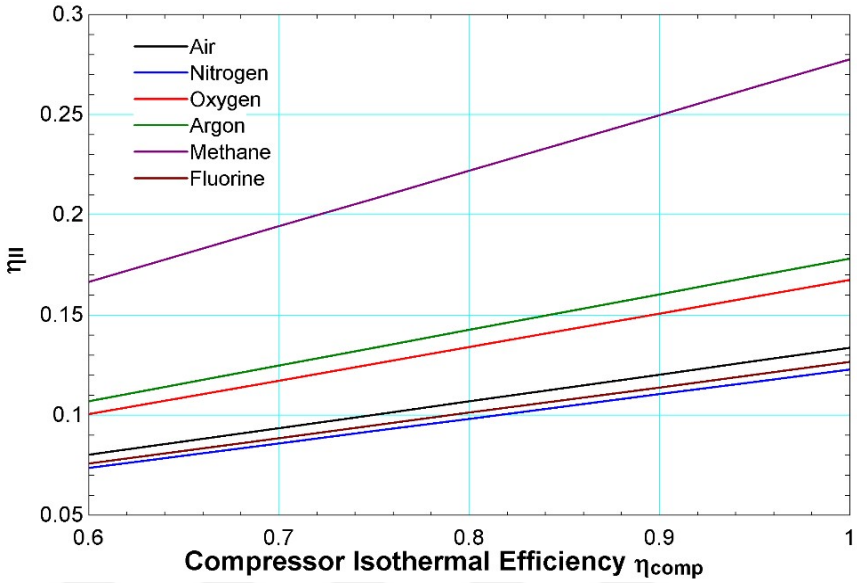

Figure 4.15 Effect of isothermal efficiency of compressor on second law efficiency for simple Linde-Hampson cycle

Figures 4.16 and 4.17 show the effect of isothermal compressor efficiency on the specific product cost and specific energy cost. As the isothermal compressor efficiency increases, both specific product cost and specific energy cost decrease. Increasing isothermal compressor efficiency decreases the compressor work but increases the cost of intercoolers, which in turn increases the initial cost of the plant. However, the specific product cost ultimately decreases with an increase in isothermal efficiency due to the more significant effect with the decrease in the energy cost.

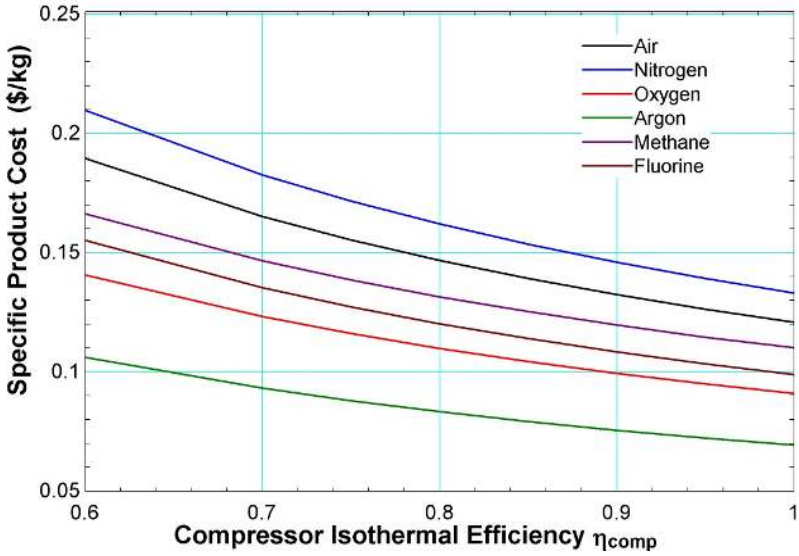

Figure 4.16 Effect of isothermal efficiency of compressor on specific product cost for simple Linde-Hampson cycle

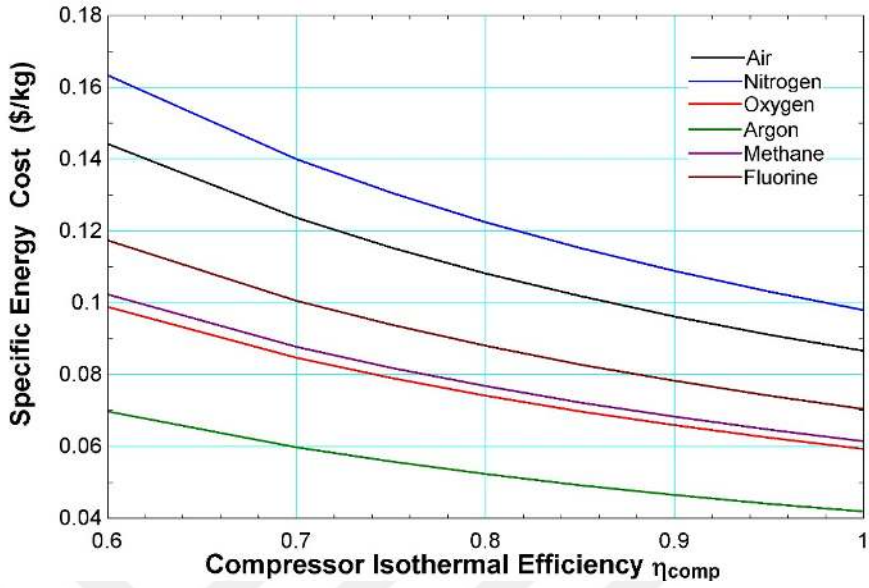

Figure 4.17 Effect of isothermal efficiency of compressor on specific energy cost for simple Linde-Hampson cycle

4.2.4 Effect of Minimum Approach Temperature in the Heat Exchanger

The effect of minimum approach temperature on the liquid yield is given in Figure 4.18. As the minimum temperature difference increases in the heat exchanger, the temperature at the inlet of the J-T valve increases. As a result, the liquid yield decreases. A result of lower liquid yield is higher liquefaction work, as shown in Figure 4.19. Another consequence is a lower COP value, as shown in Figure 4.20. As the minimum temperature difference decreases, the cycle's performance further deviates from the ideal performance, as shown by the second-law efficiency in Figure 4.21.

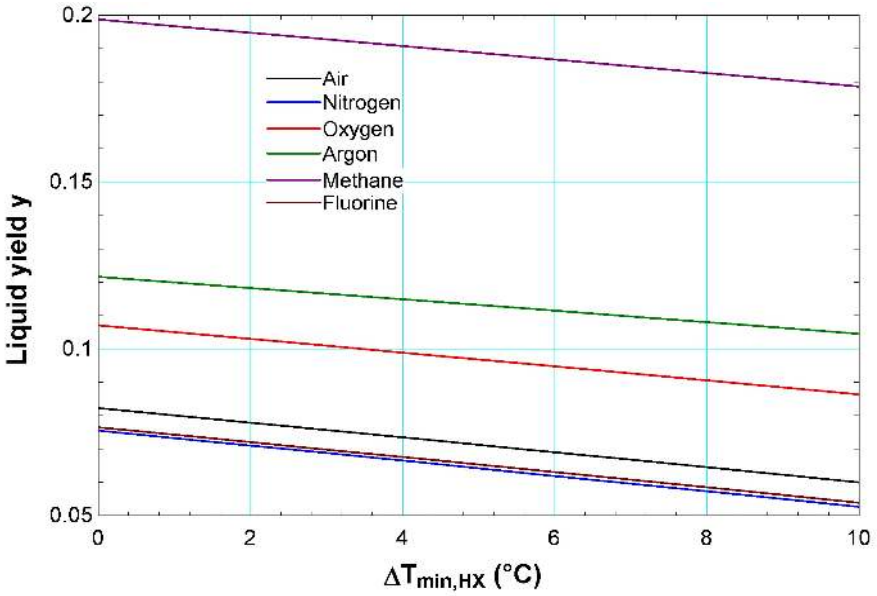

Figure 4.18 Effect of minimum approach temperature on liquid yield for simple Linde-Hampson cycle

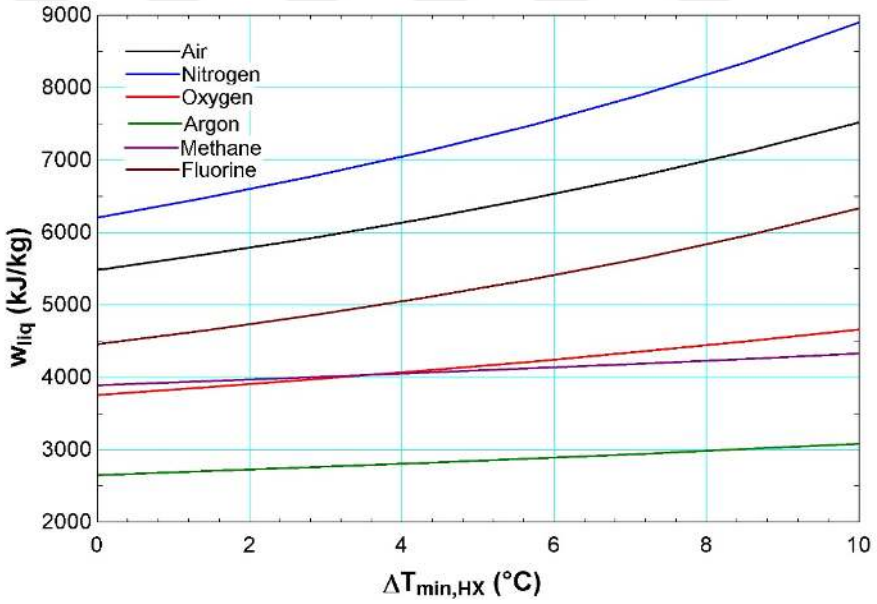

Figure 4.19 Effect of minimum approach temperature on liquefaction work for simple Linde-Hampson cycle

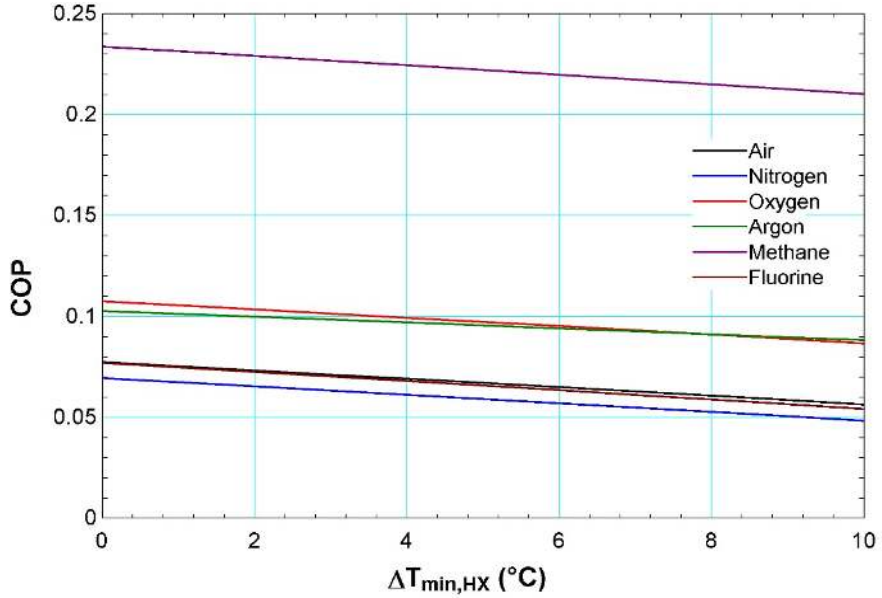

Figure 4.20 Effect of minimum approach temperature on COP for simple Linde-Hampson cycle

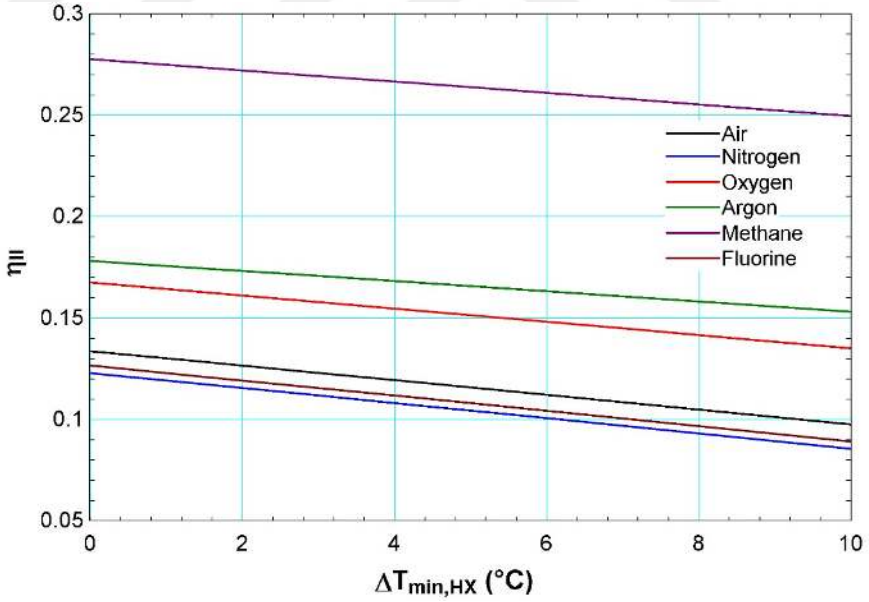

Figure 4.21 Effect of minimum approach temperature on the second law efficiency for simple Linde-Hampson cycle

Figures 4.22, 4.23 and 4.24 show the effect of minimum approach temperature on the capital cost of the heat exchanger, specific product cost, and specific energy cost, respectively. In order to maintain smaller temperature difference in the heat exchanger, higher heat transfer areas must be used. Therefore, as the temperature difference decreases, the initial cost increases. However, the effect of initial cost on

the product cost is not as pronounced as the effect of energy cost. Thus, both the specific product cost and specific energy cost decrease with a decrease in minimum approach temperature.

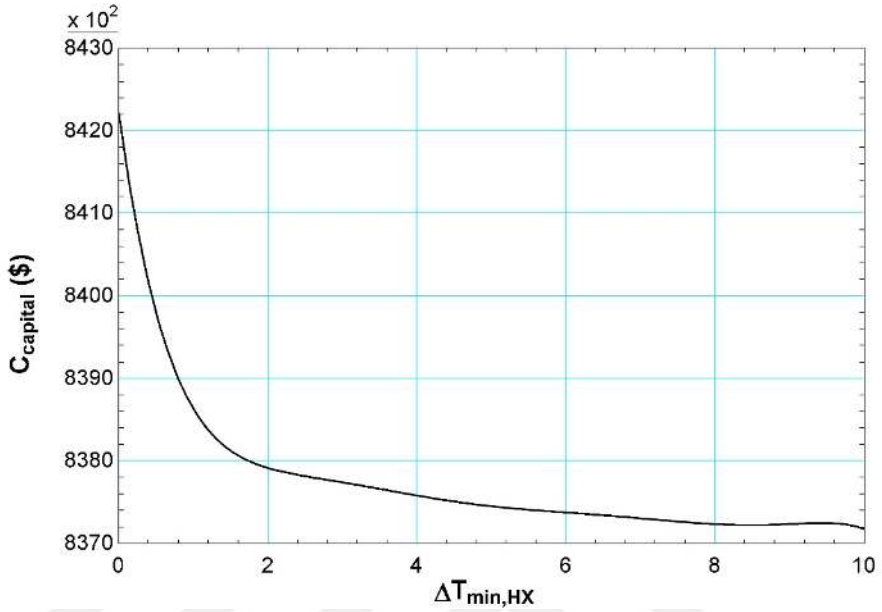

Figure 4.22 Effect of minimum approach temperature on capital cost for oxygen for simple Linde-Hampson cycle

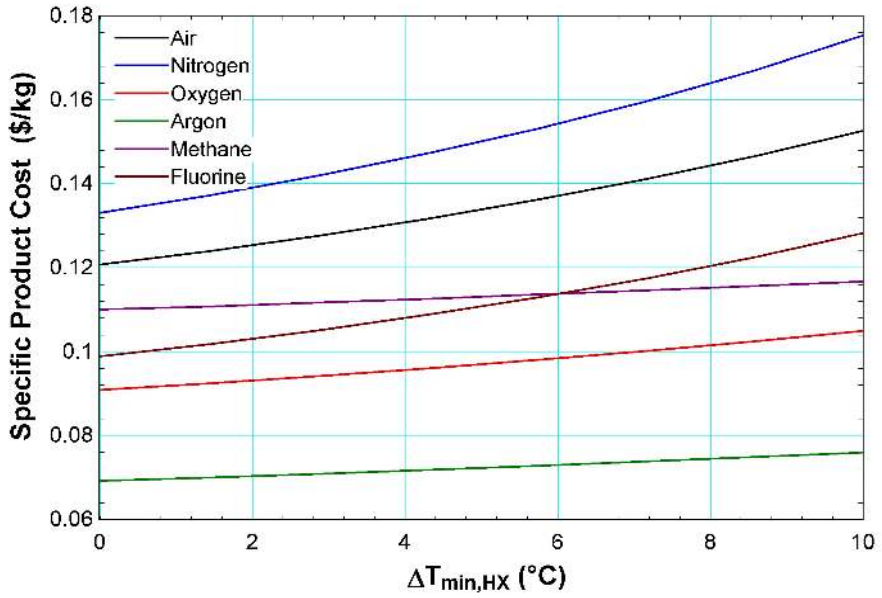

Figure 4.23 Effect of minimum approach temperature on specific product cost for simple Linde-Hampson cycle

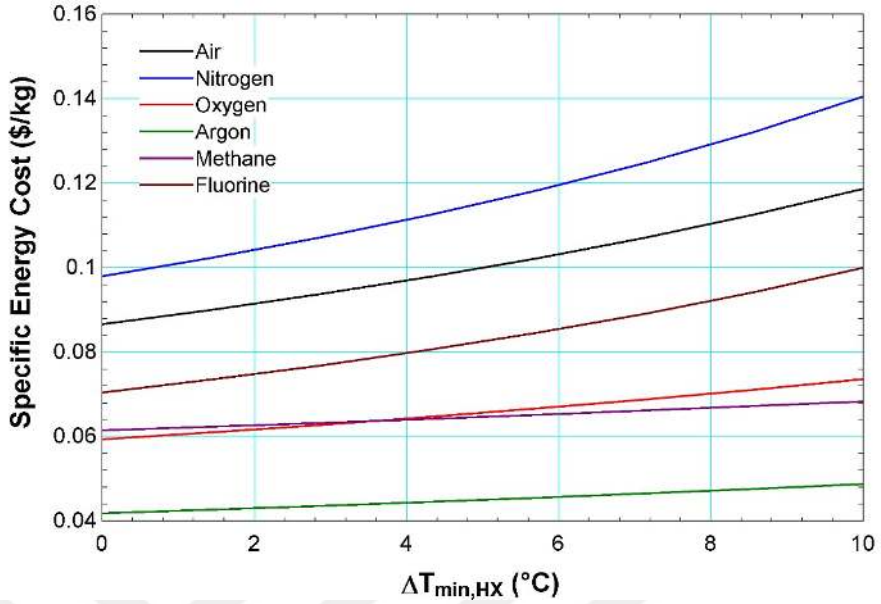

Figure 4.24 Effect of minimum approach temperature on specific energy cost for simple Linde-Hampson cycle

4.2.5 Effect of Production Capacity

In Figure 4.25, effect of daily production capacity on the specific product and specific energy costs are given. As the production capacity increases, the specific energy cost remains constant, but the specific product cost sharply decreases and approach to the specific energy cost up to a capacity of 200 tons/day. The specific product cost remains fairly constant after this value.

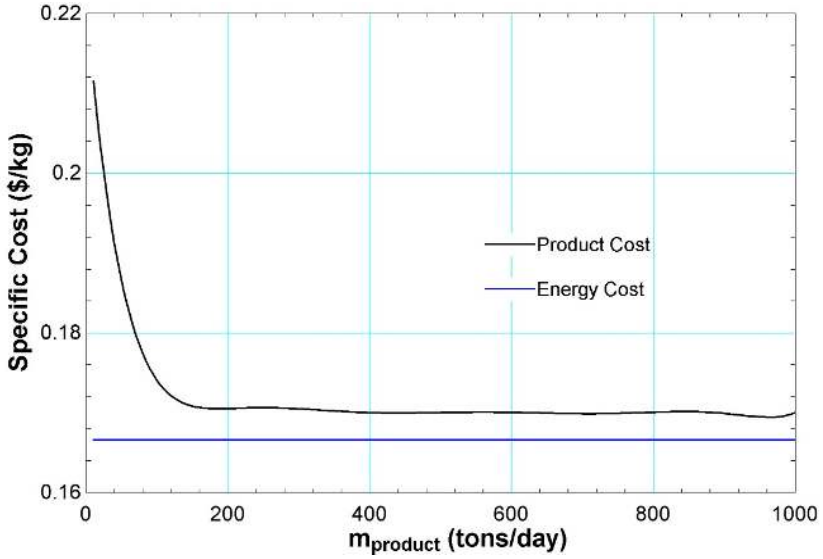

Figure 4.25 Effect of production capacity on specific cost for simple Linde-Hampson cycle

4.3 Parametric Studies on Precooled Linde-Hampson Cycle

In Chapters 2 and 3, thermodynamic and economic analysis of precooled Linde-Hampson cycle were performed. In this section, parametric studies are done to study effects of certain operating and design parameters on the thermodynamic and economic performance of the cycle.

4.3.1 Effect of Compressor Inlet Temperature

The effect of compressor inlet temperature on the auxiliary refrigerant flow rate ratio, liquefaction work, COP and second law efficiency are given in Figures 4.26 to 4.29. As stated in Equation 2.20, maximum liquid yield can be obtained using the optimum auxiliary refrigerant flow rate ratio. This maximum liquid yield only depends on the boiling point of the auxiliary refrigerant. As a result, unlike the other cycles, the compressor inlet temperature does not have any effect on the liquid yield. However, as the compressor inlet temperature increases, the auxiliary refrigeration cycle flow rate ratio increases, as shown in Figure 4.26.

In Figure 4.27, effect of compressor inlet temperature on the liquefaction work is presented. The compressor inlet temperature affects the liquefaction work in two ways. As the compressor inlet temperature increases, the compressor work input to the liquefaction system, the mass flow rate ratio, and the compressor work of the auxiliary refrigeration cycle increase.

The effect of compressor inlet temperature on the COP of the cycle is given in Figure 4.28. With an increase in the liquefaction work, less refrigeration effect is produced by the system. As a result, the COP decreases with an increase in the compressor inlet temperature.

Figure 4.29 shows how the second law efficiency of the cycle changes with the compressor inlet temperature. As the compressor inlet temperature increases, there is a slight increase in second law efficiency for all gases. This can be explained as follows: The reversible work increases at a higher rate than the actual liquefaction work when the compressor inlet temperature increases for a given liquid yield.

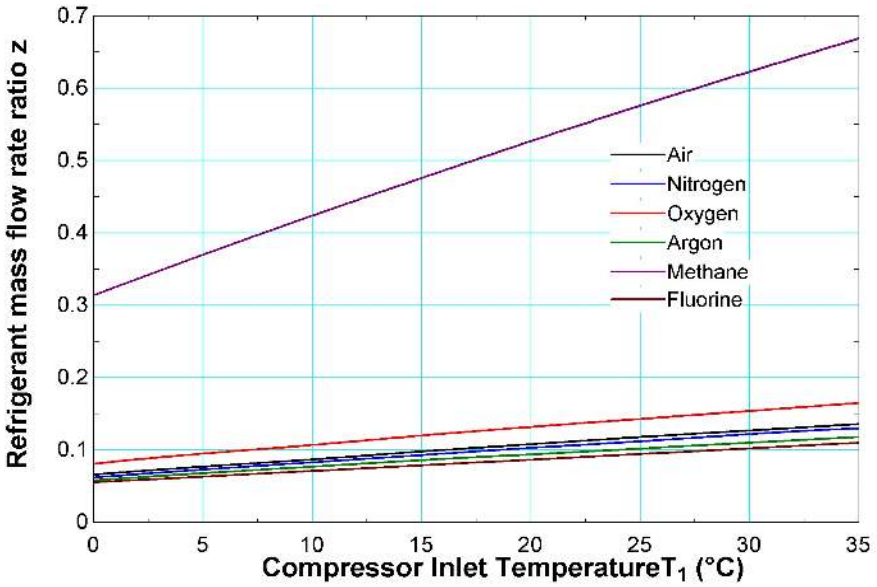

Figure 4.26 Effect of compressor inlet temperature on refrigerant mass flow rate ratio for precooled Linde-Hampson cycle

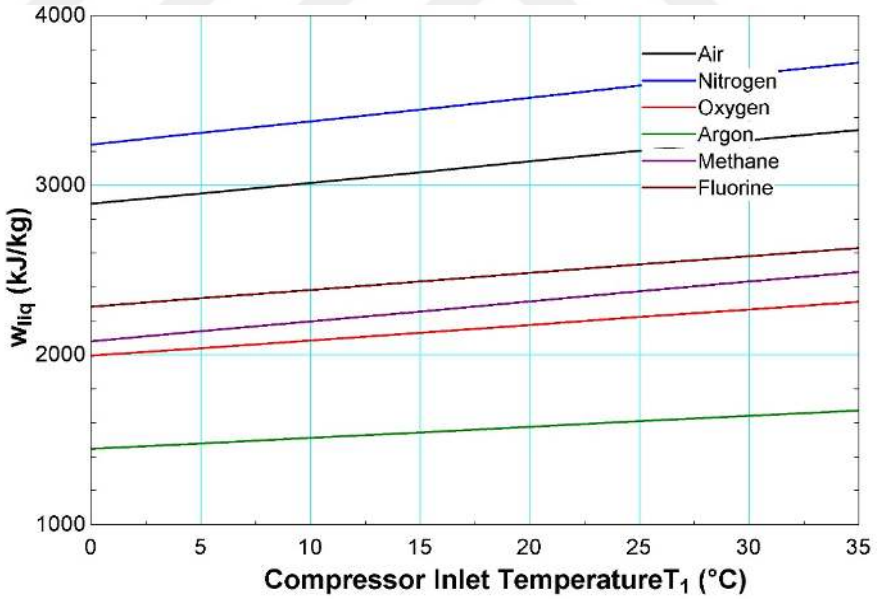

Figure 4.27 Effect of compressor inlet temperature on liquefaction work for precooled Linde-Hampson cycle

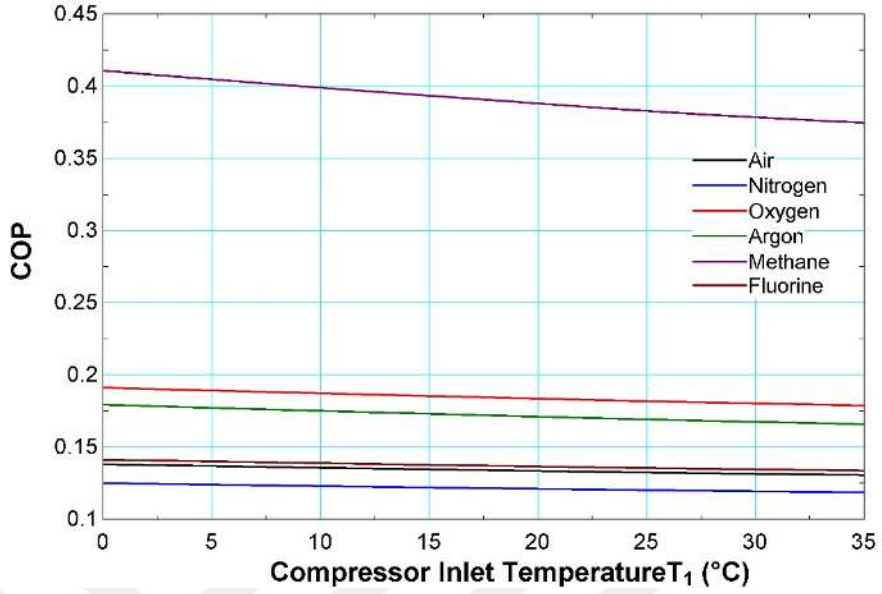

Figure 4.28 Effect of compressor inlet temperature on COP for precooled Linde-Hampson cycle

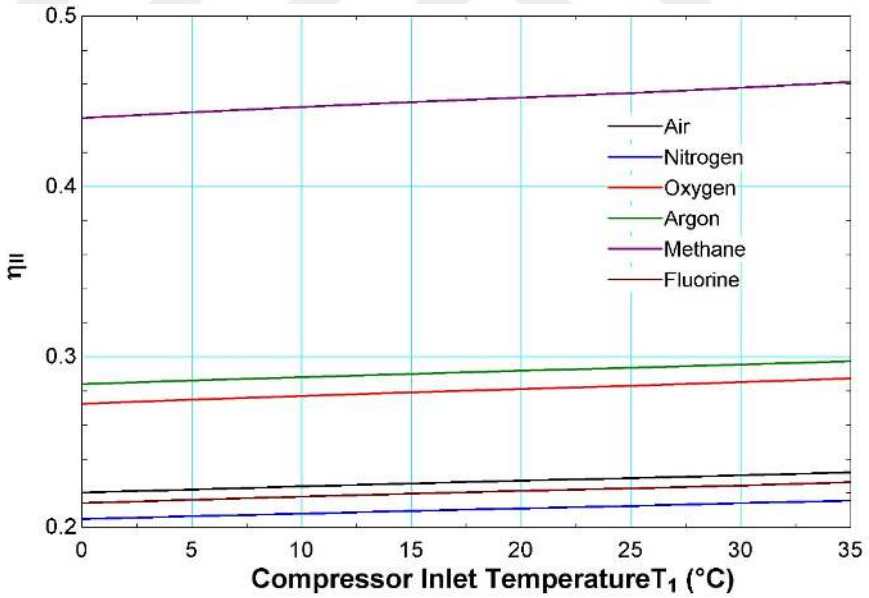

Figure 4.29 Effect of compressor inlet temperature on second law efficiency for precooled Linde-Hampson cycle

Effects of compressor inlet temperature on the specific product cost and specific energy cost are given in Figures 4.30 and 4.31. As the compressor inlet temperature increases, the specific product cost increases due to an increase in the cost of the refrigeration unit as well as an increase in the specific energy cost, as shown in Figure 4.29.

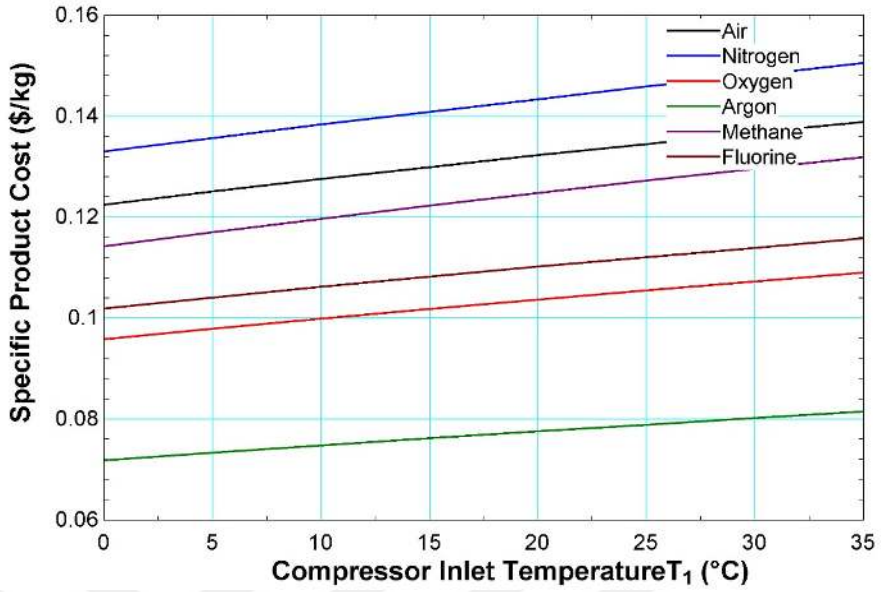

Figure 4.30 Effect of compressor inlet temperature on specific product cost for precooled Linde-Hampson cycle

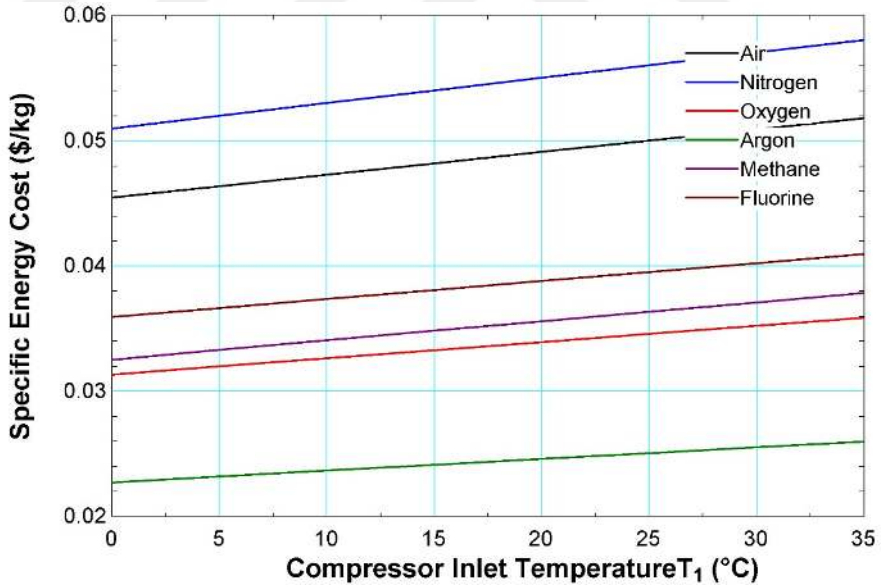

Figure 4.31 Effect of compressor inlet temperature on the specific energy cost for precooled Linde-Hampson cycle

4.3.2 Effect of Compressor Outlet Pressure

The performance of precooled Linde-Hampson cycle in terms of compressor outlet pressure is investigated and the results are shown in Figures 4.32 to 4.35 for various gases. The effect of compressor outlet pressure on the liquid yield, liquefaction work, COP and second law efficiency are studied. The results are similar to those

obtained for simple Linde-Hampson cycle. As the compressor outlet pressure increases, the liquid yield, COP and second law efficiency increase up to a certain point and start decreasing. On the other hand, the liquefaction work decreases with an increase in the pressure up to a certain value and remains almost constant with further increase in the pressure. The trend for the liquefaction work is due to Joule-Thompson coefficient effect mentioned earlier.

Figures 4.36 and 4.37 show the effect of compressor outlet pressure on the specific product cost and specific energy cost. It appears that the trends for specific product cost and specific energy cost are very similar to that for the liquefaction work.

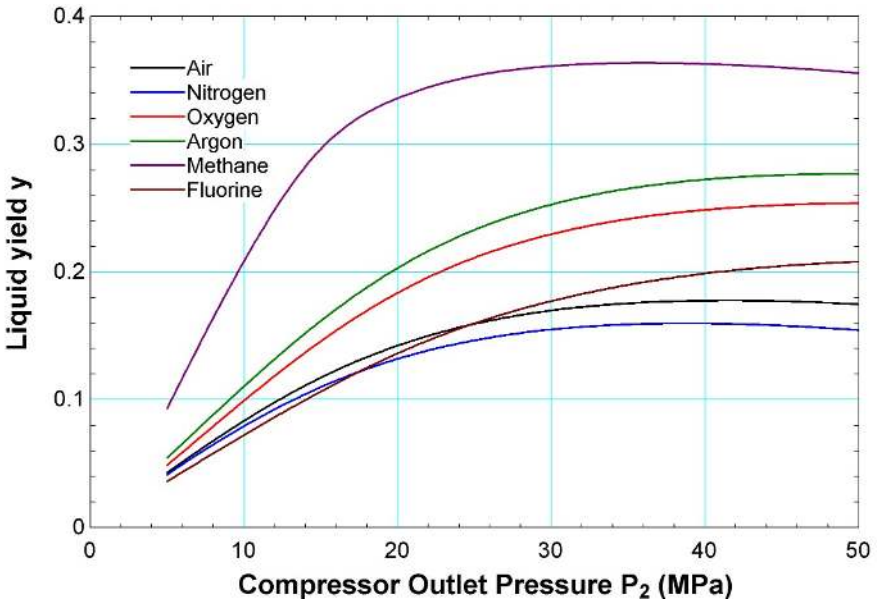

Figure 4.32 Effect of compressor outlet pressure on liquid yield for precooled Linde-Hampson cycle

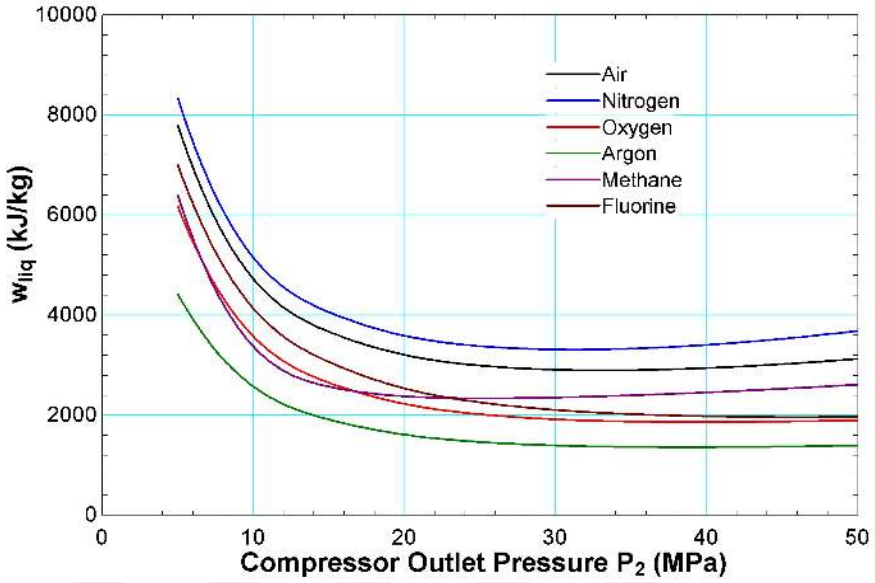

Figure 4.33 Effect of compressor outlet pressure on liquefaction work for precooled Linde-Hampson cycle

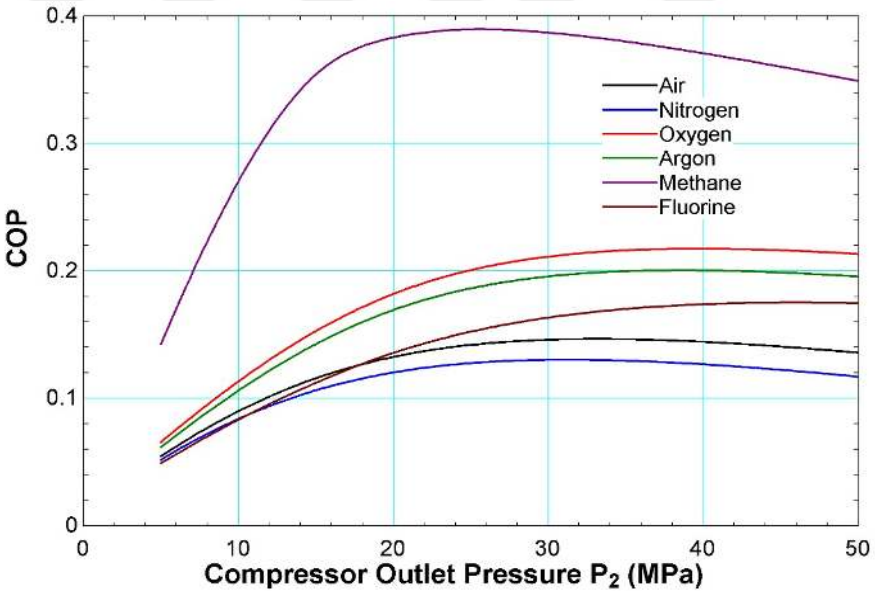

Figure 4.34 Effect of compressor outlet pressure on COP for precooled Linde-Hampson cycle

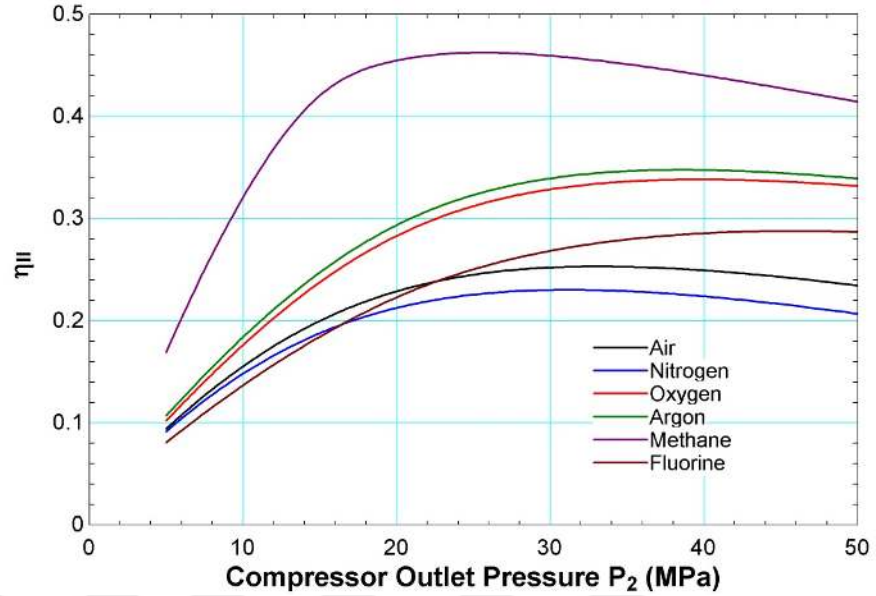

Figure 4.35 Effect of compressor outlet pressure on second law efficiency for precooled Linde-Hampson cycle

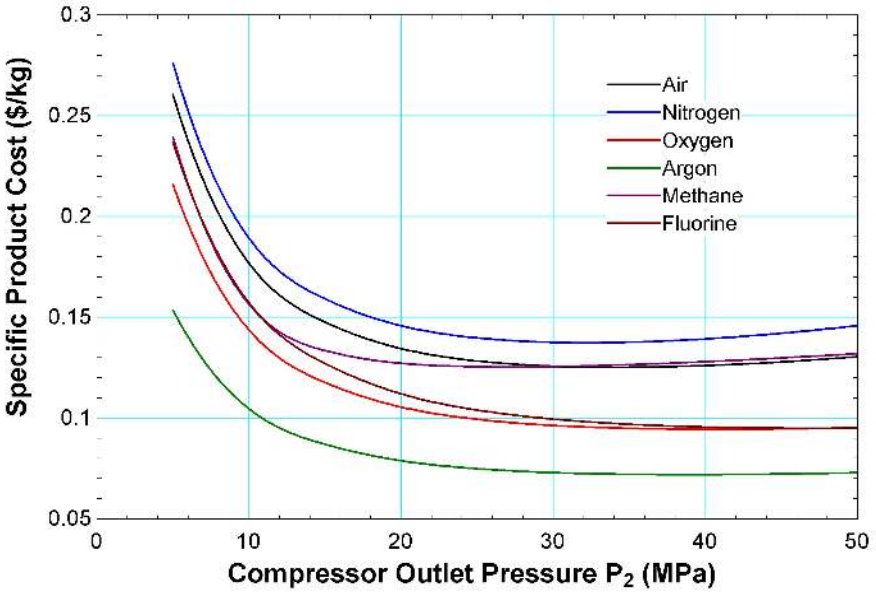

Figure 4.36 Effect of compressor outlet pressure on specific product cost for precooled Linde-Hampson cycle

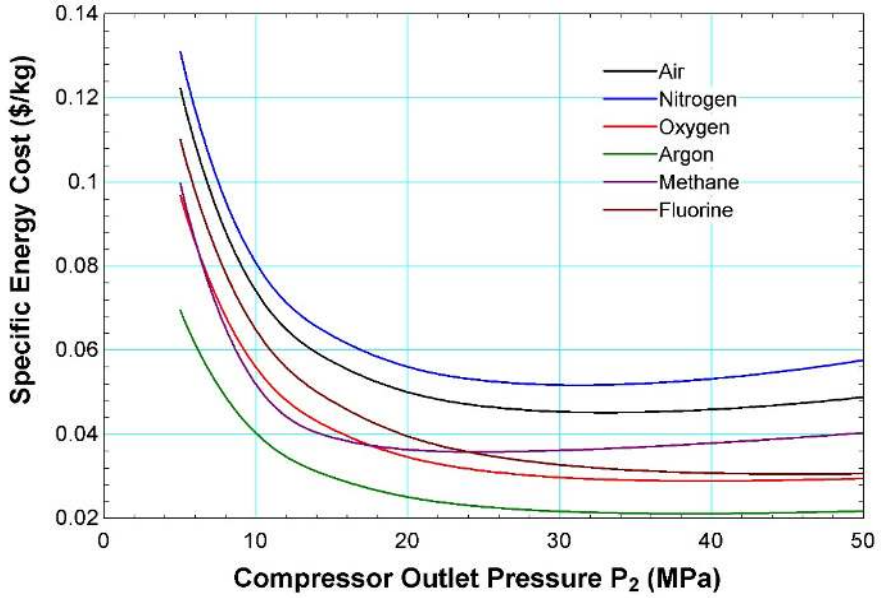

Figure 4.37 Effect of compressor outlet pressure on specific energy cost for precooled Linde-Hampson cycle

4.3.3 Effect of Minimum Approach Temperatures in the Heat Exchangers

Effect of minimum approach temperature in the first heat exchanger on the auxiliary refrigerant flow rate ratio is given in Figure 4.38. The minimum approach temperature in the first heat exchanger does not affect the liquid yield but as the minimum approach temperature increases, auxiliary refrigerant flow rate ratio increases. In Figure 3.39, the effect of minimum approach temperature of first heat exchanger on the liquefaction work is given. As the minimum temperature difference in first heat exchanger increases, the liquefaction work slightly increases due to increase in auxiliary refrigerant flow rate, which in turn increases the compressor work of the auxiliary refrigeration cycle. Figure 4.40 shows the effect of the minimum approach temperature on the specific product cost. The specific product cost decreases up to around 3 K for all gases and it remains fairly constant after that point. This is because the cost of the heat exchanger and the cost of the refrigeration unit compensate each other.

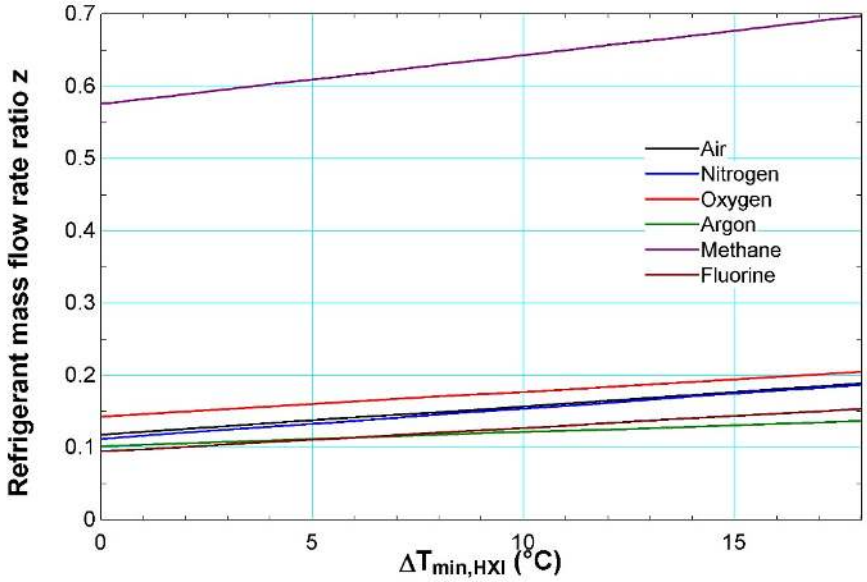

Figure 4.38 Effect of minimum approach temperature in first heat exchanger on refrigerant mass flow rate ratio for precooled Linde-Hampson cycle

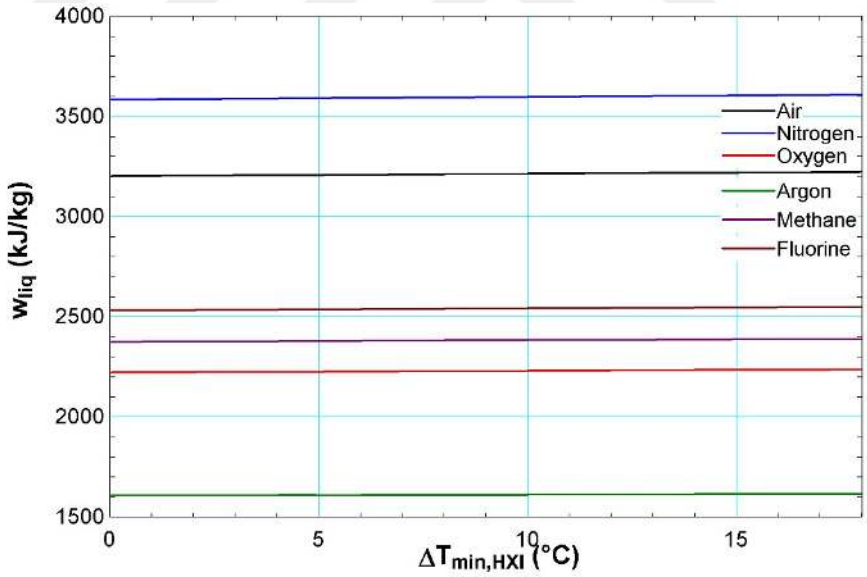

Figure 4.39 Effect of minimum approach temperature in first heat exchanger on liquefaction work for precooled Linde-Hampson cycle

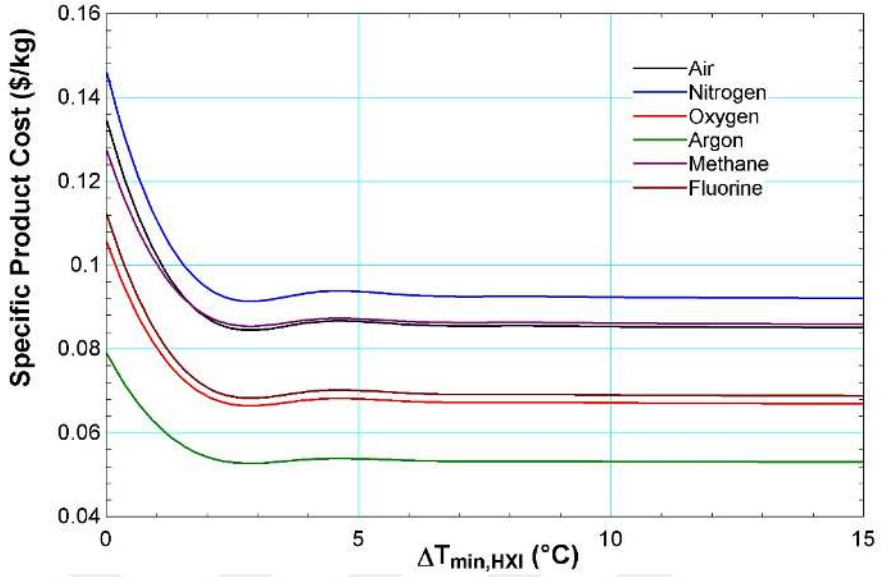

Figure 4.40 Effect of minimum approach temperature in first heat exchanger on the specific product cost for precooled Linde-Hampson cycle

Figures 4.41 through 4.44 show the effect of minimum approach temperature on the liquid yield, liquefaction work, COP and second law efficiency. As the minimum approach temperature decreases, the temperature at the inlet of J-T valve increases, and as a result, lower amounts of liquid are produced. The liquefaction work increases because more work is consumed per unit mass of liquid. The COP also decreases as the minimum approach temperature decreases, and the cycle deviates further from the ideal performance. The trend for the second law efficiency also indicates this behavior.

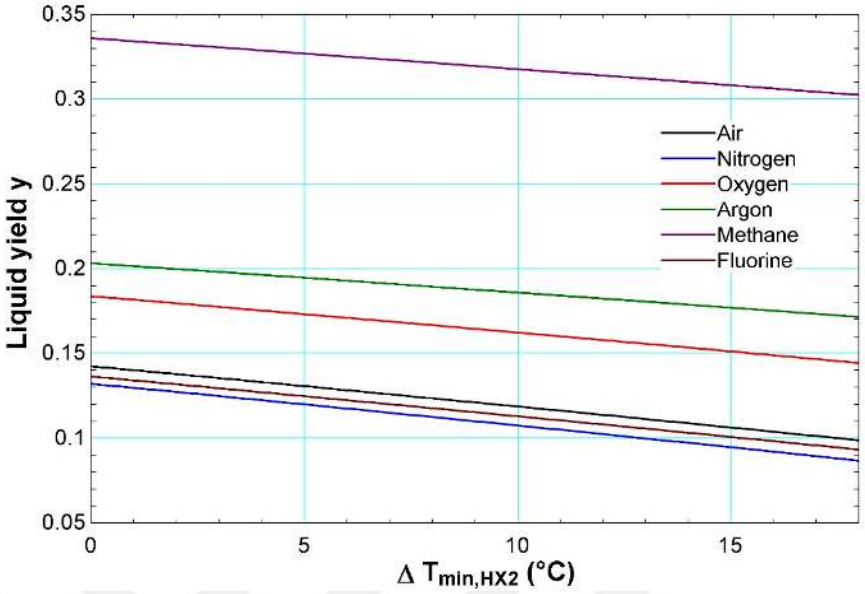

Figure 4.41 Effect of minimum approach temperature in second heat exchanger on liquid yield for precooled Linde-Hampson cycle

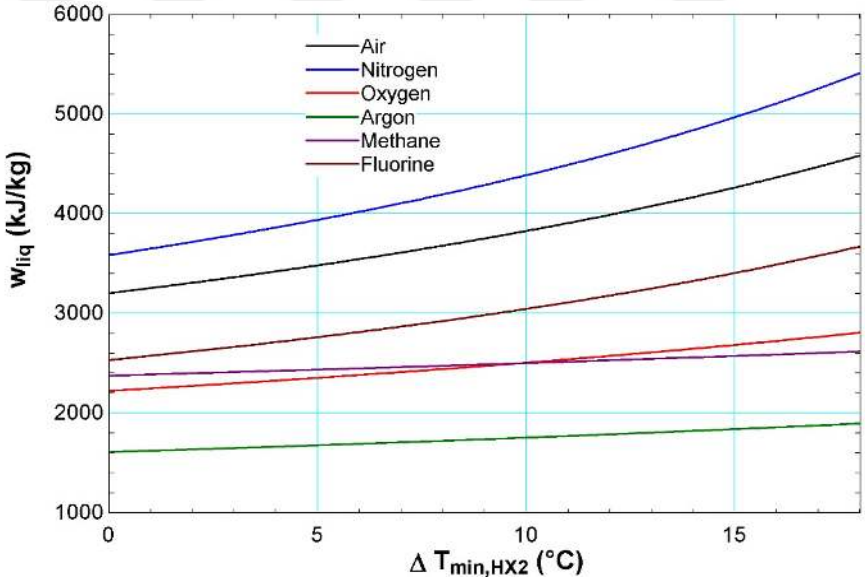

Figure 4.42 Effect of minimum approach temperature in second heat exchanger on liquefaction work for precooled Linde-Hampson cycle

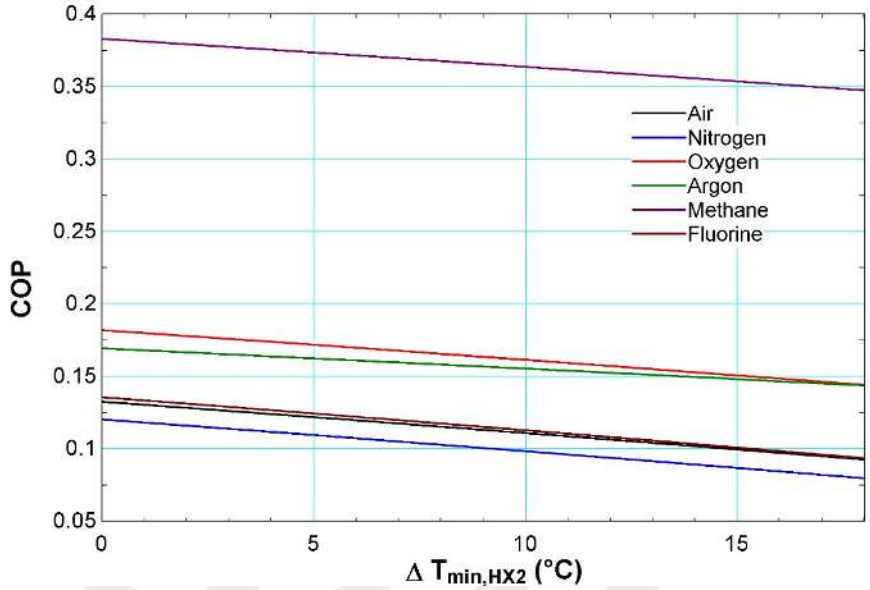

Figure 4.43 Effect of minimum approach temperature in second heat exchanger on COP for precooled Linde-Hampson cycle

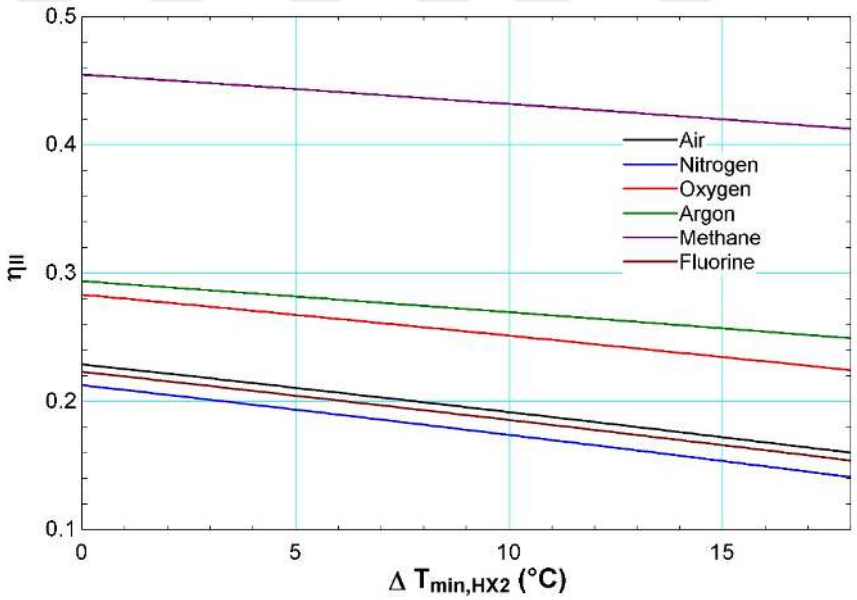

Figure 4.44 Effect of minimum approach temperature in second heat exchanger on second law efficiency for precooled Linde-Hampson cycle

Effect of the minimum approach temperature on the specific product cost and specific energy cost are given in Figures 4.45 and 4.46. As the minimum temperature difference decreases, a larger heat transfer area is required, and this increases capital cost and specific product cost. Once the optimum point is reached, the specific product cost slightly increases due to increase in specific energy cost, as shown in Figure 4.44.

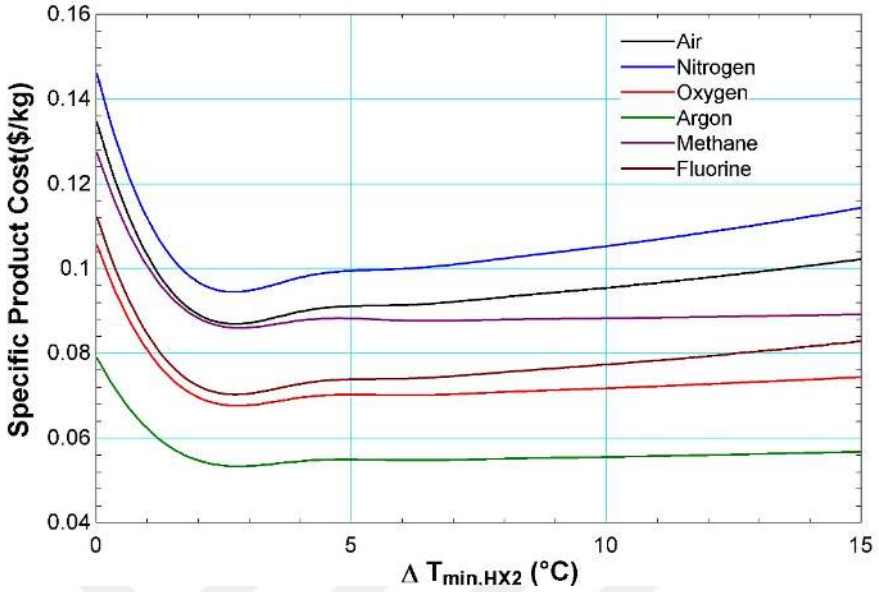

Figure 4.45 Effect of minimum approach temperature in second heat exchanger on specific product cost for precooled Linde-Hampson cycle

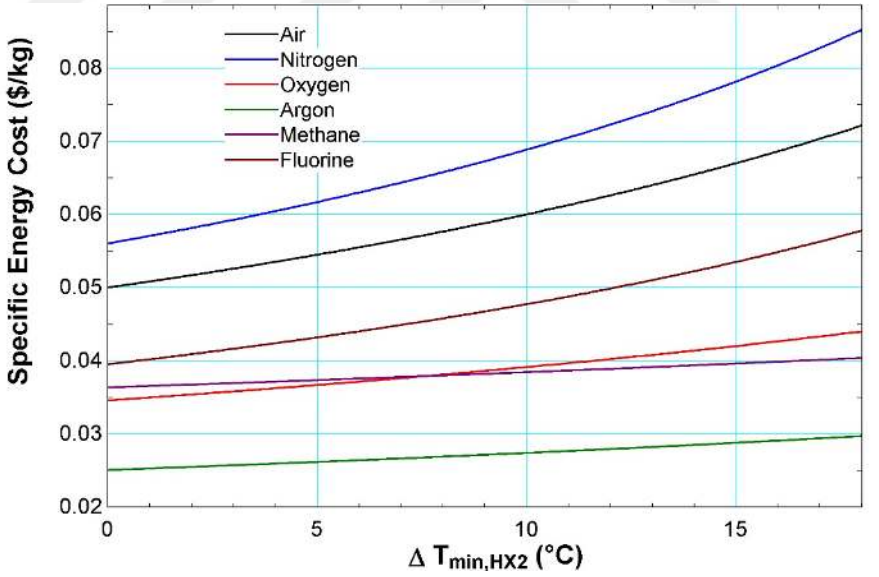

Figure 4.46 Effect of minimum approach temperature in second heat exchanger on specific energy cost for precooled Linde-Hampson cycle

4.3.4 Effect of Production Capacity

The production capacity of a liquefaction cycle is directly related to the size of the plant and capital cost. In Figures 4.47 through 4.49, the effect of production capacity on the annualized capital cost, O&M cost, annual energy cost, annual total cost, specific product cost, and specific energy cost are given. As the production capacity increases, all annual expanses increase. However, as seen in Figure 4.46,

energy cost plays a dominant role on the annual expenses. The specific product cost decreases as the production capacity increases up to 200 tons/day and remains almost constant after this value.

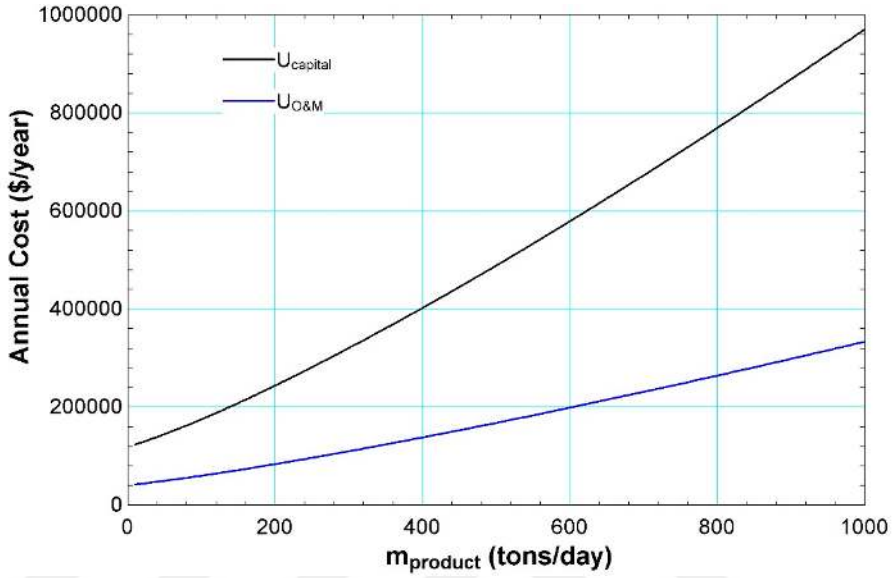

Figure 4.47 Effect of production capacity on the annual O&M and annualized capital cost for precooled Linde-Hampson cycle

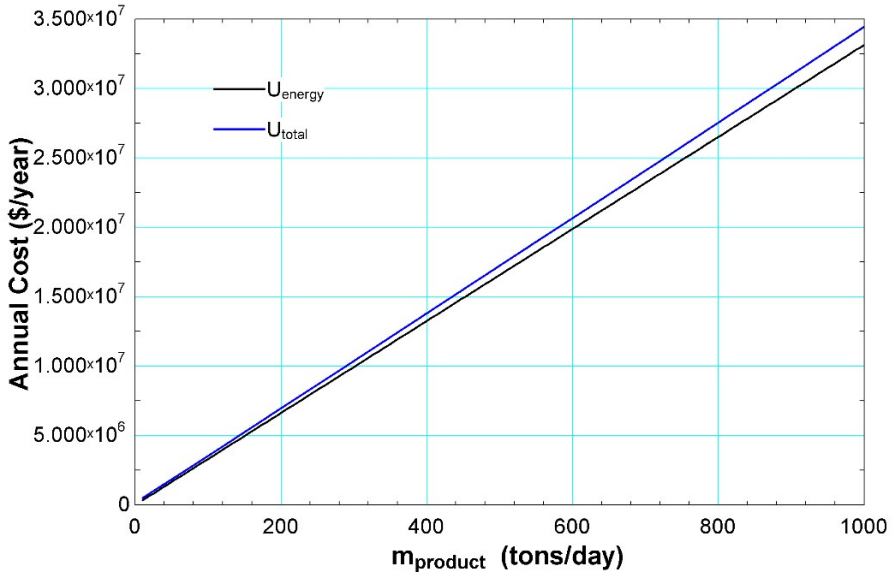

Figure 4.48 Effect of production capacity on the annual energy and total cost for precooled Linde-Hampson cycle

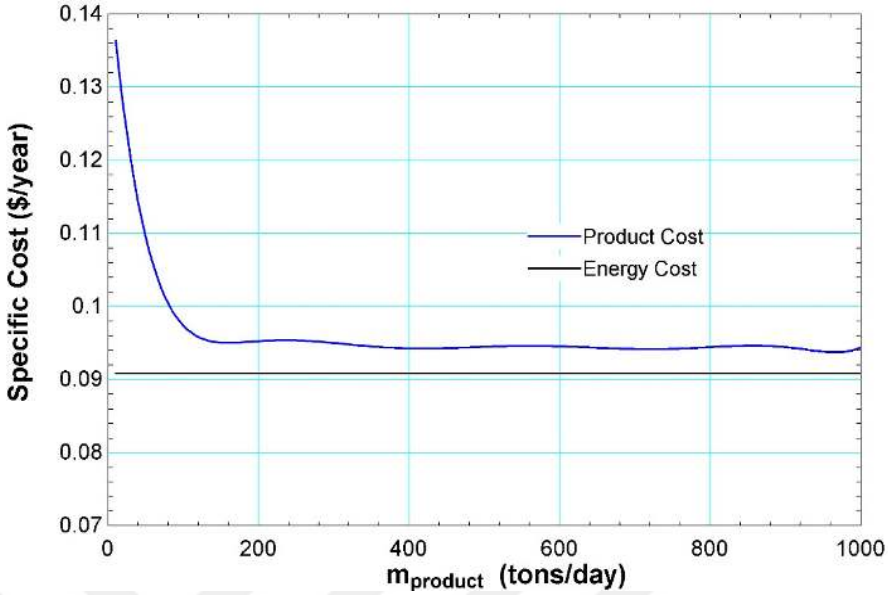

Figure 4.49 Effect of production capacity on the specific product and specific energy costs for precooled Linde-Hampson cycle

4.4 Parametric Studies on Claude and Kapitza Cycles

Thermodynamic and economic analysis of Claude and Kapitza cycle were performed in Chapters 2 and 3. Due to similar characteristics of Claude and Kapitza cycles, the parametric studies of only Claude cycle are given in this section. The trends for Kapitza cycle are very similar.

4.4.1 Effect of Compressor Inlet Temperature

Effect of compressor inlet temperature on the liquid yield, liquefaction work, COP and second law efficiency are given in Figures 4.50 through 4.53. As the compressor inlet temperature increases, the liquid yield decreases due to higher temperature at the valve inlet. The compressor work also increases with more refrigeration effect. The work produced by the expander will be higher due to higher temperature at the expander inlet. However, this refrigeration effect is not enough to increase the liquid yield. The liquefaction work increases, and the COP and second law efficiency decrease as the compressor inlet temperature increases.

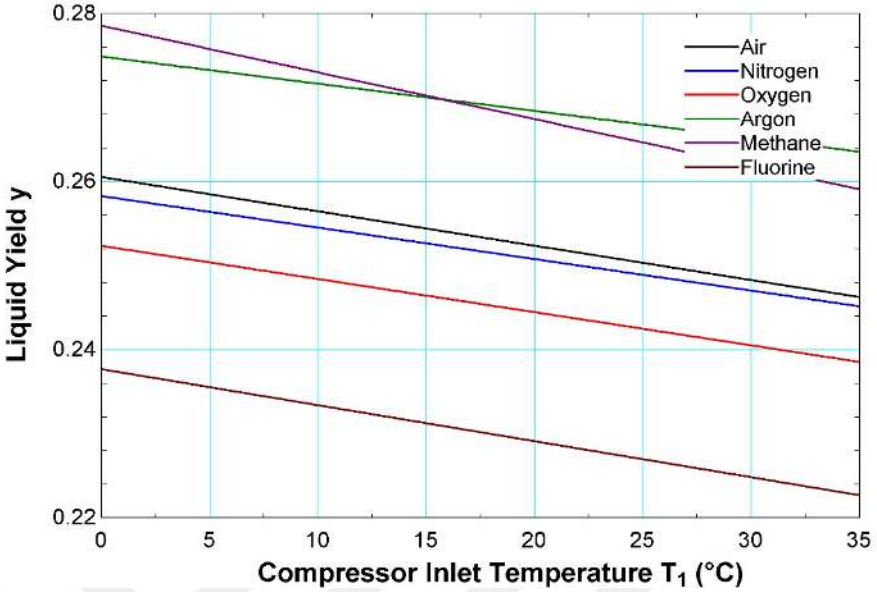

Figure 4.50 Effect of compressor inlet temperature on the liquid yield for Claude cycle

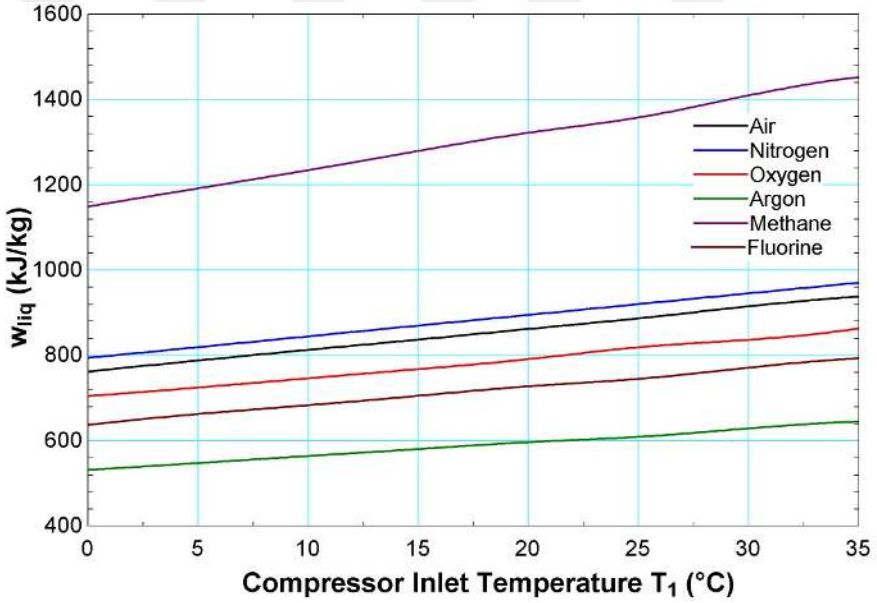

Figure 4.51 Effect of compressor inlet temperature on the liquefaction work for Claude cycle

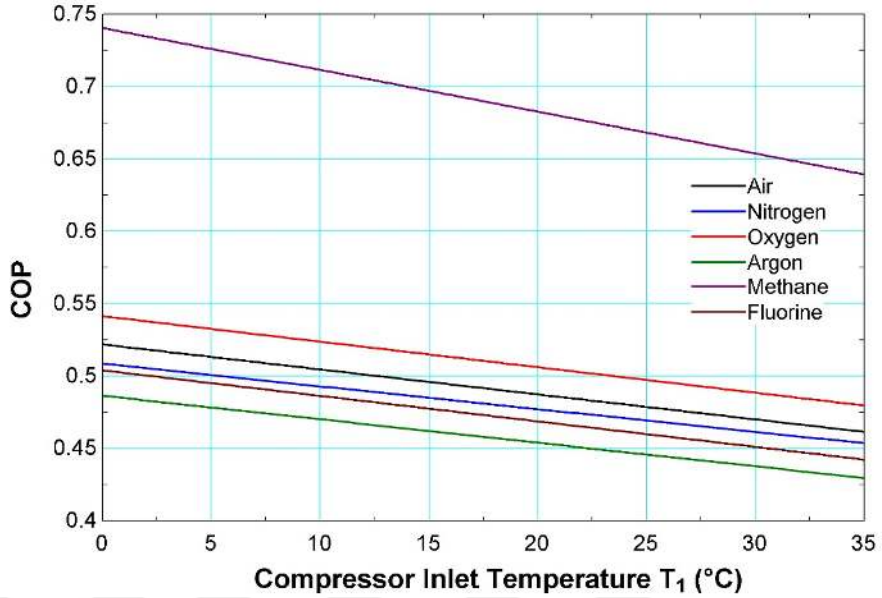

Figure 4.52 Effect of compressor inlet temperature on COP for Claude cycle

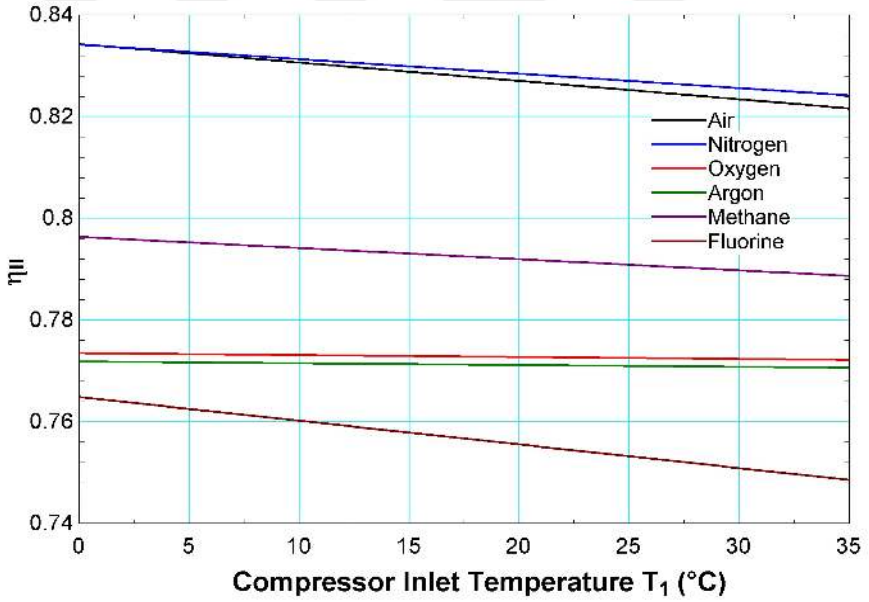

Figure 4.53 Effect of compressor inlet temperature on the second law efficiency for Claude cycle

In Figures 4.54 and 4.55, the effect of compressor inlet temperature on the specific product cost and specific energy cost are given. As the compressor inlet temperature increases, the cost of the compressor increases and due to more work consumed, specific energy cost also increases.

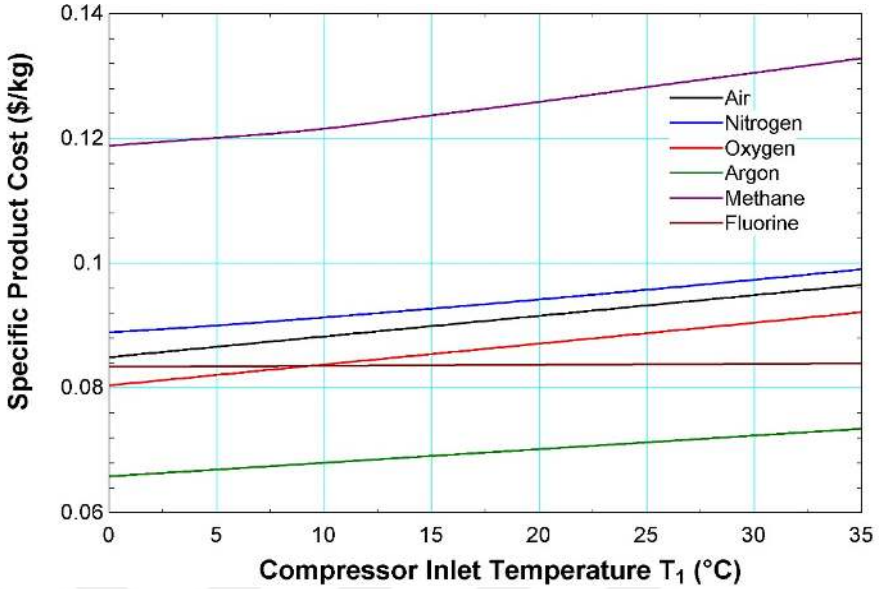

Figure 4.54 Effect of compressor inlet temperature on the specific product cost for Claude cycle

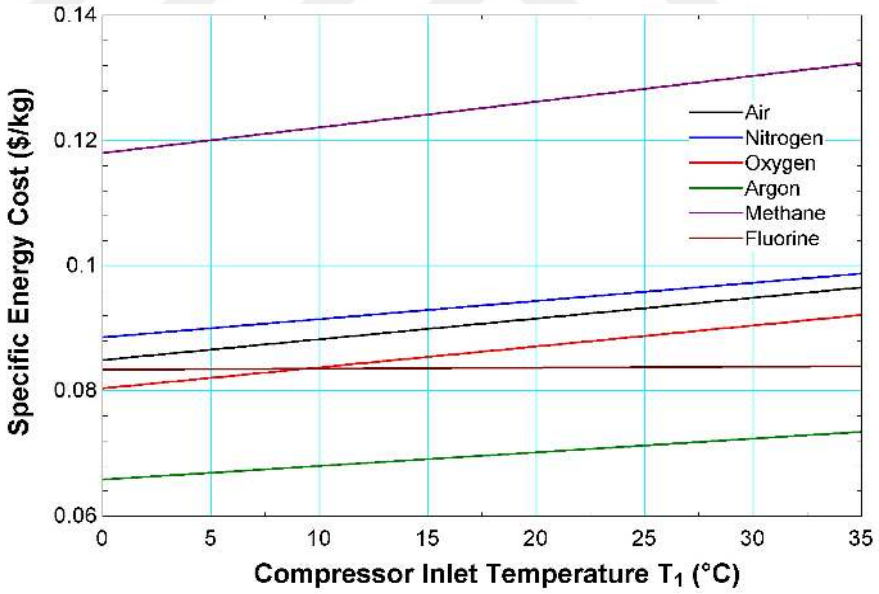

Figure 4.55 Effect of compressor inlet temperature on the specific energy cost for Claude cycle

4.4.2 Effect of Compressor Isothermal Efficiency

Effect of compressor isothermal efficiency on the liquefaction work, COP and second law efficiency are given in Figures 4.56 to 4.58. As the isothermal efficiency decreases, the compressor work increases, which increases the liquefaction work and decreases the COP and second law efficiency.

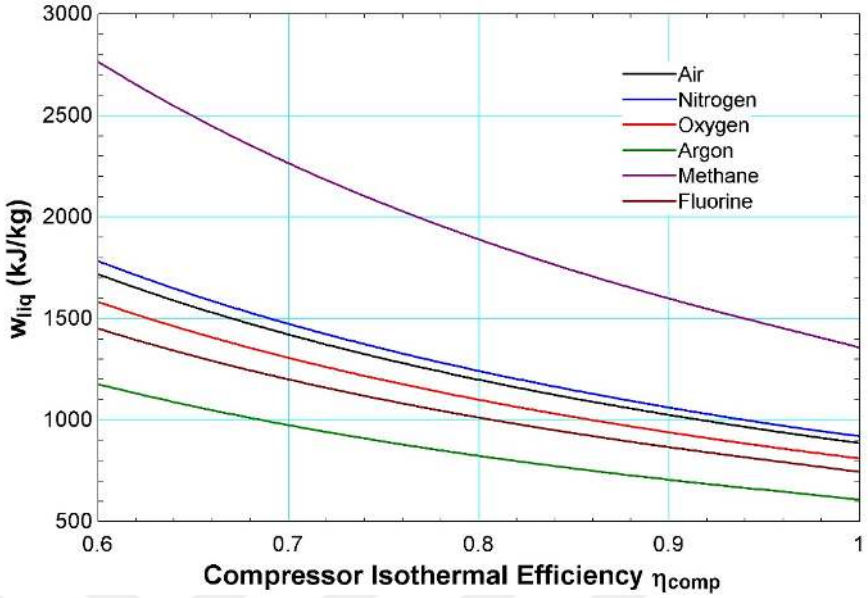

Figure 4.56 Effect of compressor isothermal efficiency on the liquefaction work for Claude cycle

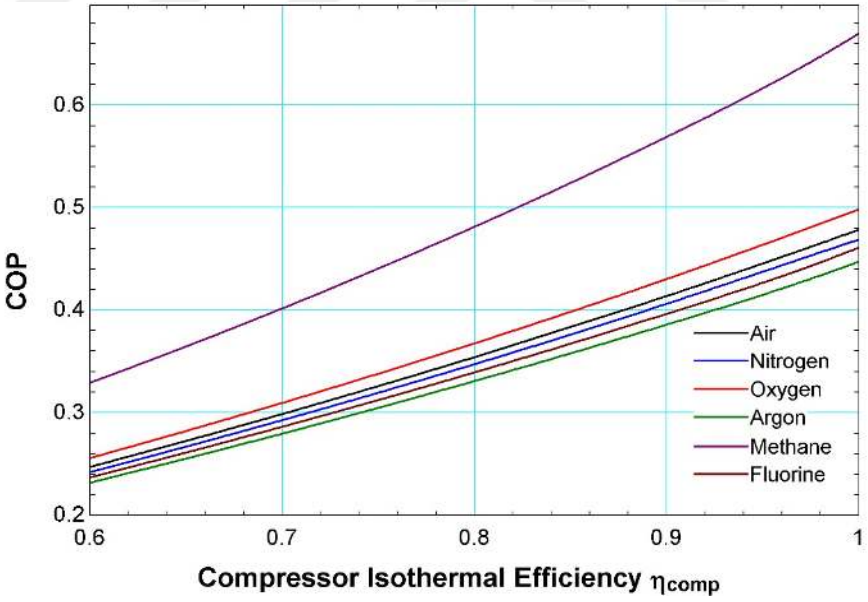

Figure 4.57 Effect of compressor isothermal efficiency on COP for Claude cycle

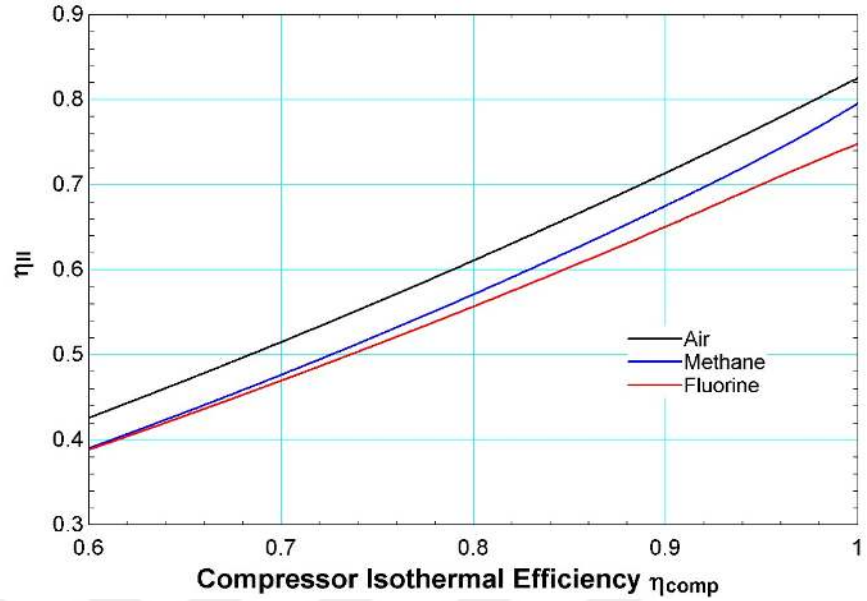

Figure 4.58 Effect of compressor isothermal efficiency on the second law efficiency for Claude cycle

Figures 4.59 and 4.60 show the effect of isothermal compressor efficiency on the specific product cost and specific energy cost. As the efficiency increases, more cooling is required by intercoolers, and this increases the capital cost. The specific product cost and specific energy cost decrease due to lower work consumption in the compressor.

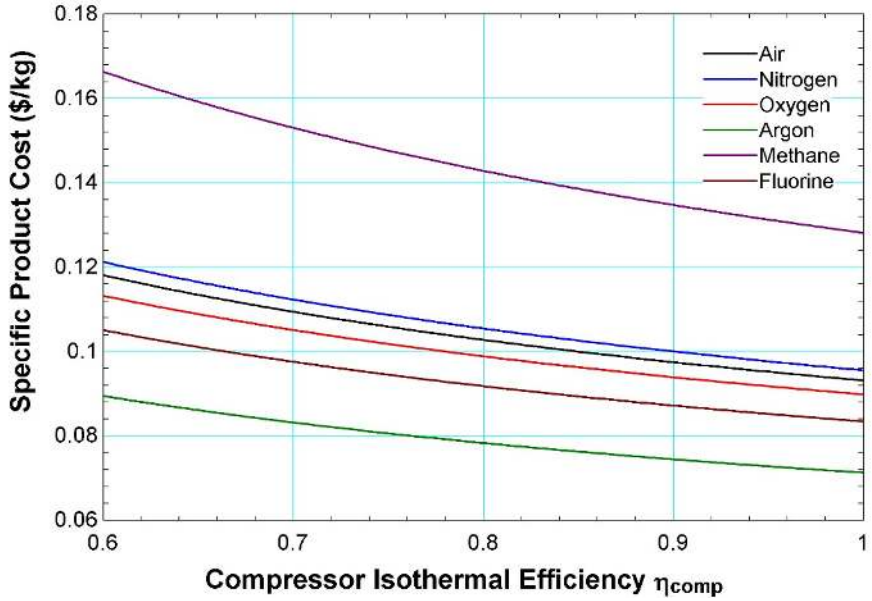

Figure 4.59 Effect of compressor isothermal efficiency on specific product cost for Claude cycle

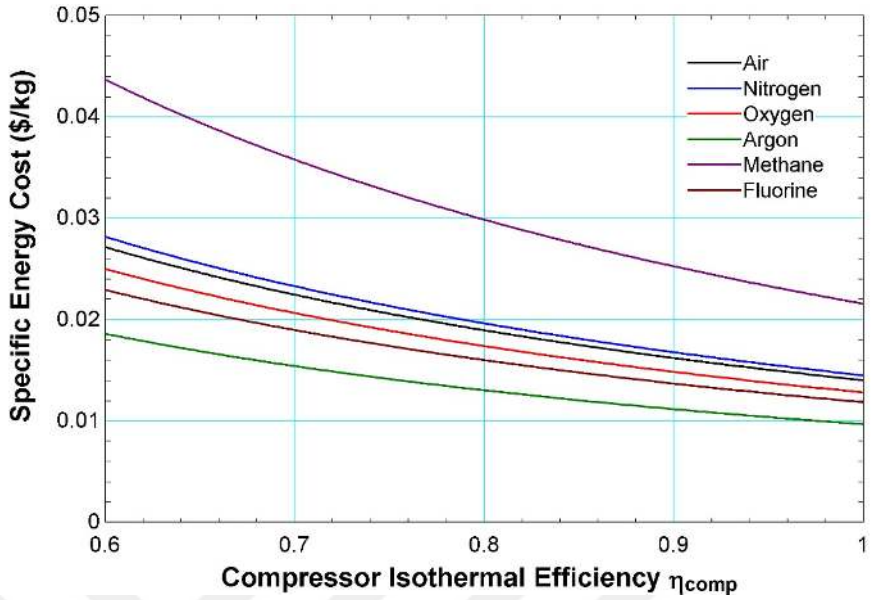

Figure 4.60 Effect of compressor isothermal efficiency on specific energy cost for Claude cycle

4.4.3 Effect of Compressor Outlet Pressure

Effect of compressor outlet pressure on the liquid yield, liquefaction work, COP and second law efficiency are given in Figures 4.61 to 4.64. With the additional refrigeration effect produced by the expander unit, Claude and Kapitza cycles can reach higher liquid yield than simple Linde-Hampson and precooled Linde-Hampson cycles. As seen in Figure 4.61, as the outlet pressure increases, liquid yield increases until an optimum pressure value which is around 5-10 MPa for different gases. After the optimum point, the liquid yield slightly decreases with increase in pressure due to behavior of the gases at high pressures.

In Figure 4.62, effect of compressor outlet pressure on the liquefaction work is presented. As the compressor outlet pressure increases, the compressor work and refrigeration effect produced by the expander increase but the refrigeration effect produced by the expander is not affected. At higher pressures than about 5-10 MPa, the liquefaction work increases with decrease in liquid yield and this also negatively affect the COP and second law efficiency, as shown in Figures 4.63 and 4.64.

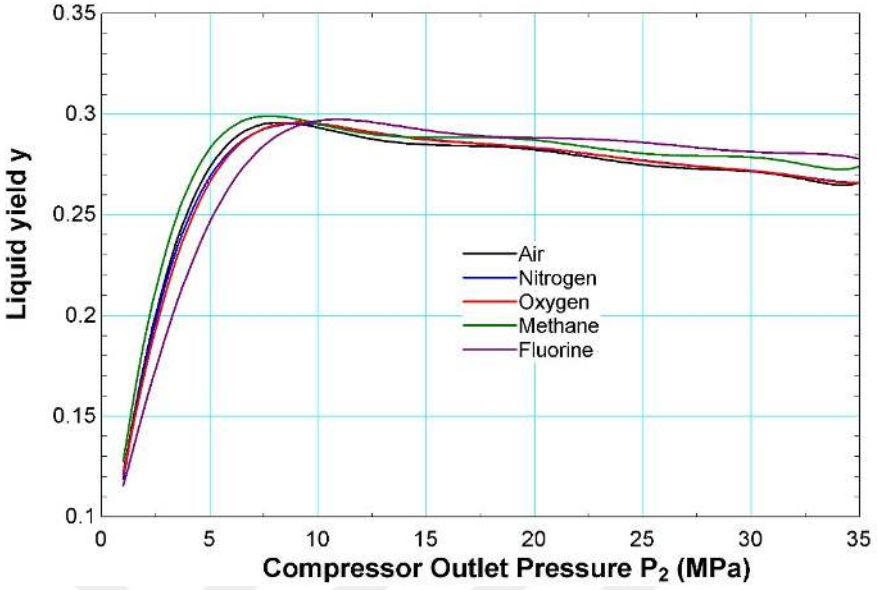

Figure 4.61 Effect of compressor outlet pressure on liquid yield for Claude cycle

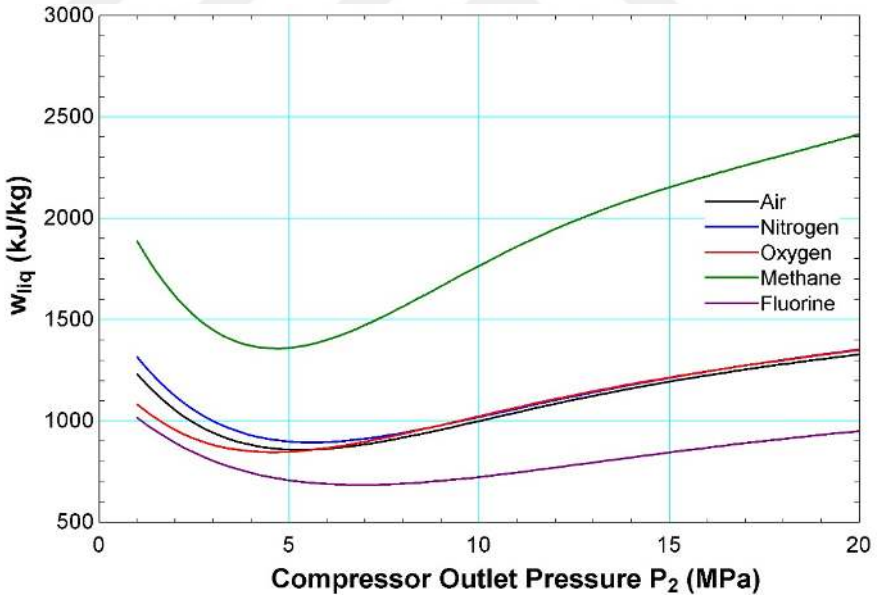

Figure 4.62 Effect of compressor outlet pressure on liquefaction work for Claude cycle

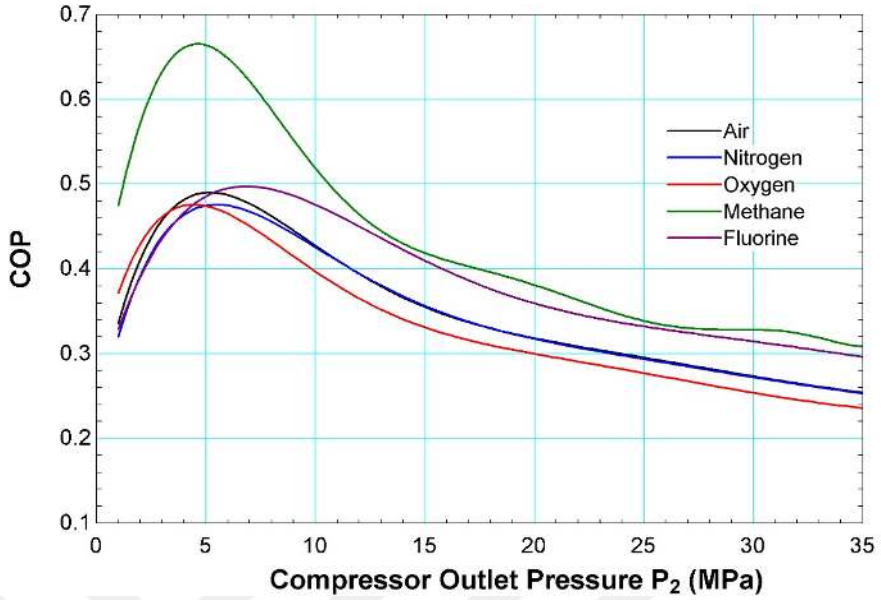

Figure 4.63 Effect of compressor outlet pressure on COP for Claude cycle

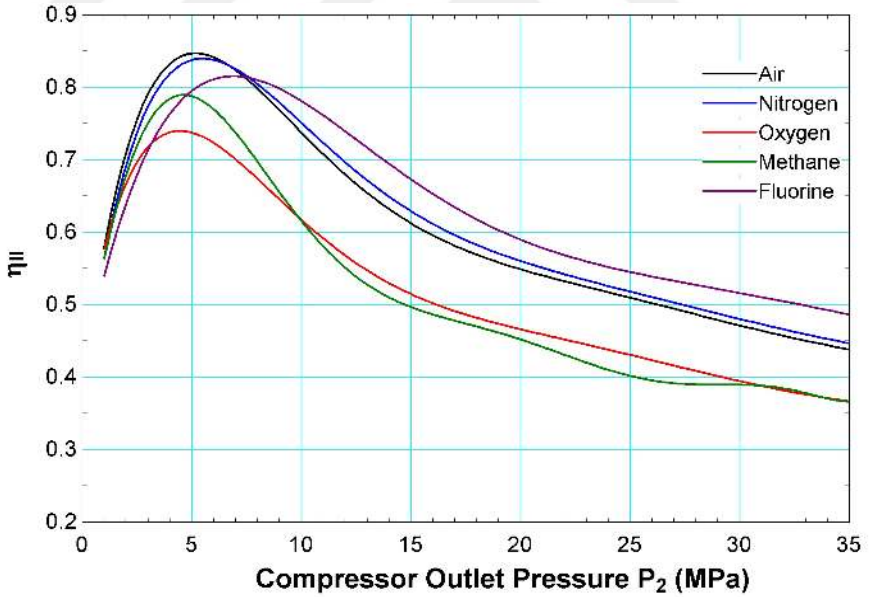

Figure 4.64 Effect of compressor outlet pressure on second law efficiency for Claude cycle

Effect of compressor outlet pressure on the specific product cost and specific energy cost is given in Figures 4.65 and 4.66. As the compressor outlet pressure increases, the size of the compressor unit also increases negatively affecting the initial cost of the compressor. Due to high influence of liquefaction work on the product and energy costs, the trends for specific product cost and specific energy cost are very similar to that for the work.

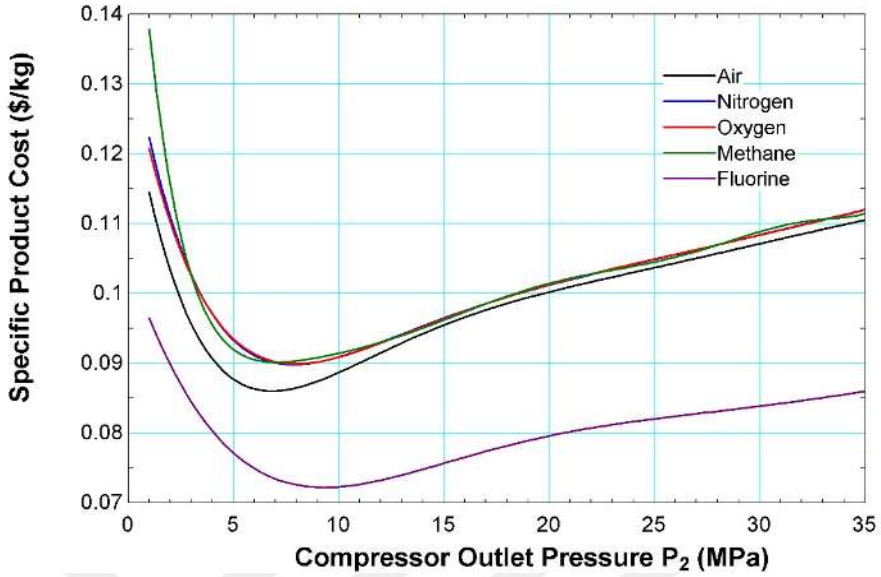

Figure 4.65 Effect of compressor outlet pressure on specific product cost for Claude cycle

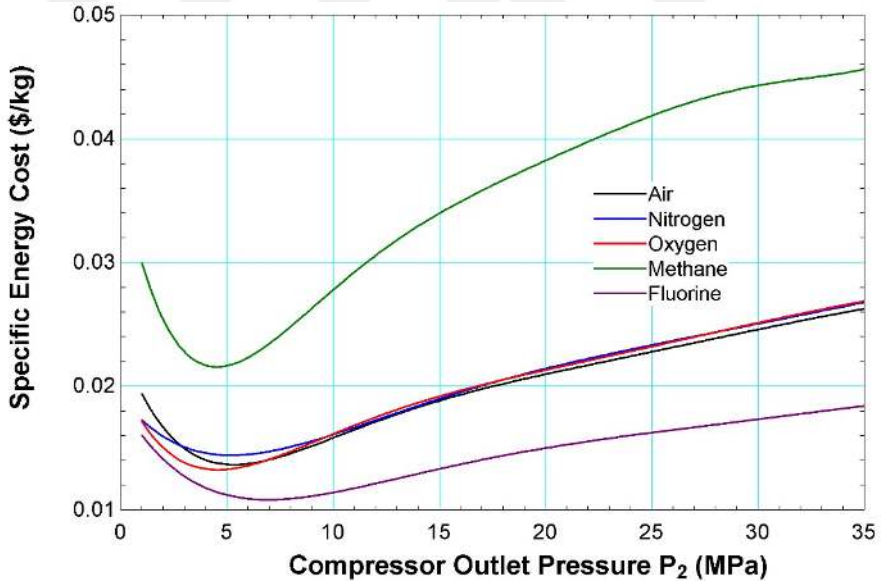

Figure 4.66 Effect of compressor outlet pressure on specific energy cost for Claude cycle

4.4.4 Effect of Expander Flow Rate Ratio

Expander flow rate ratio is an important parameter for both Claude and Kapitza cycles because it is directly related to the refrigeration effect produced by the expander. In Figures 4.67 to 4.70, the effect of expander flow rate ratio on the liquid

yield, liquefaction work, COP and second law efficiency are given. The liquid yield first increases as the flow ratio increases up to a value of about 0.70-0.75 and then decreases. The results clearly show the existence of an optimum flow ratio to maximize the liquid yield, the COP, and the second law efficiency, and minimize the liquefaction work.

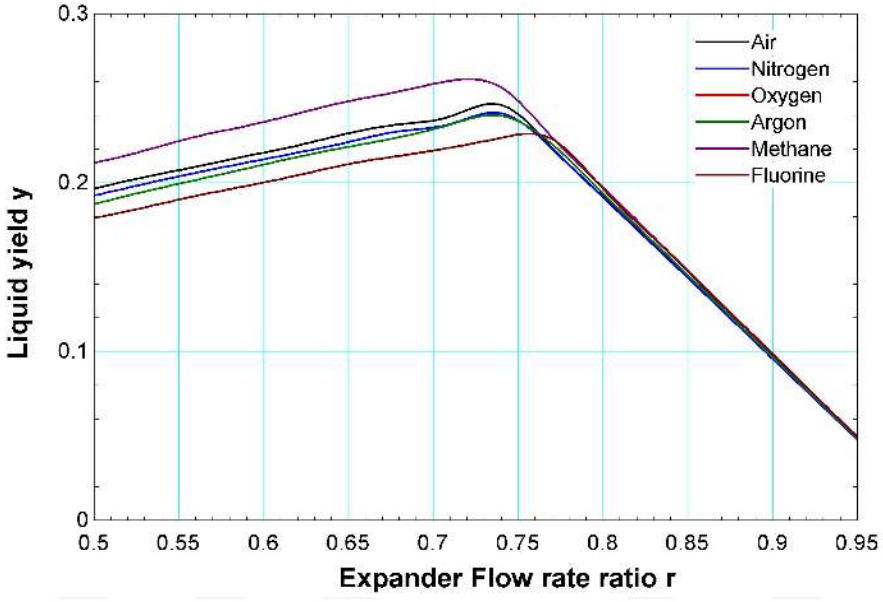

Figure 4.67 Effect of expander flow ratio on liquid yield for Claude cycle

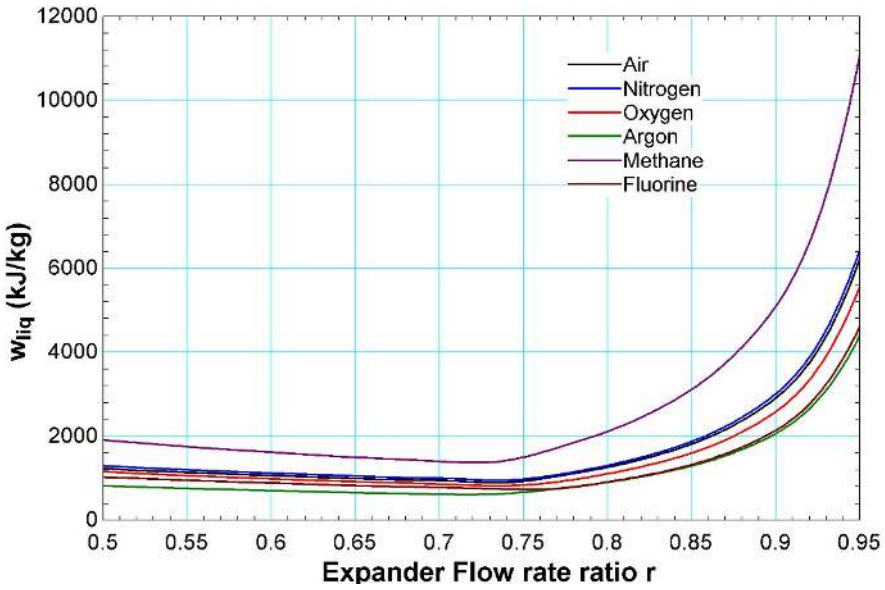

Figure 4.68 Effect of expander flow ratio on liquefaction work for Claude cycle

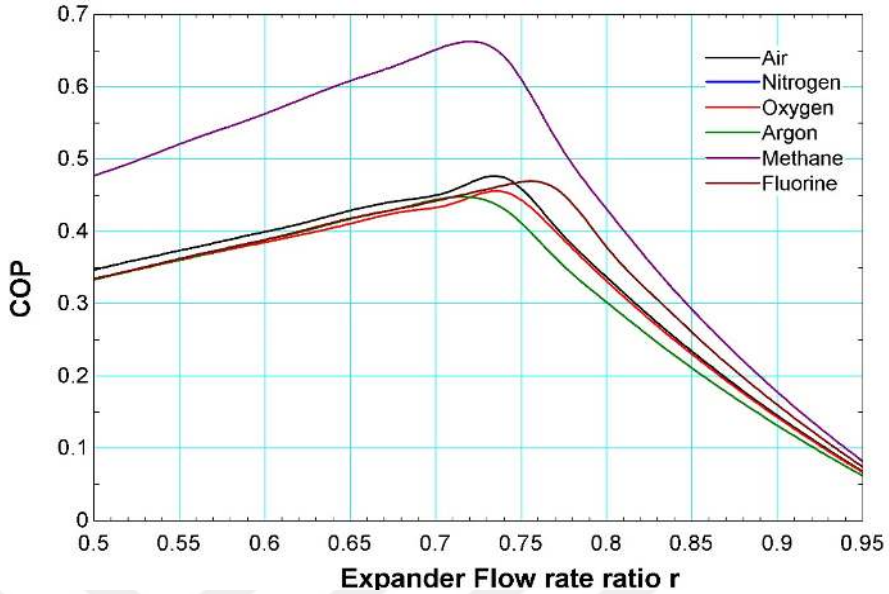

Figure 4.69 Effect of expander flow ratio on COP for Claude cycle

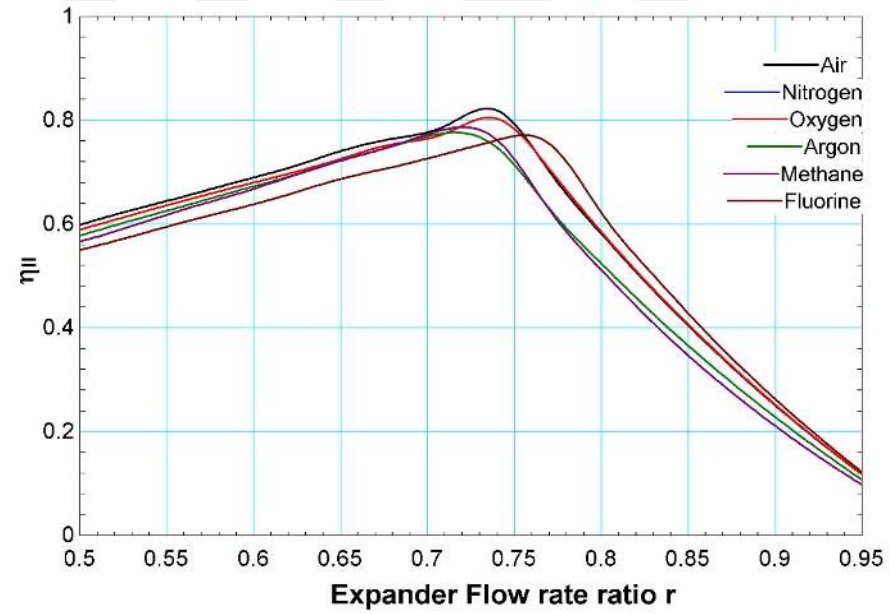

Figure 4.70 Effect of expander flow ratio on second law efficiency for Claude cycle

Figures 4.71 and 4.72 show the effect of expander flow rate ratio on the specific product cost and specific energy cost. As the flow rate to the expander increase, the specific product cost and specific energy cost first decrease up to a certain point and start increasing. Therefore, the specific costs are minimized at an optimum value of flow ratio.

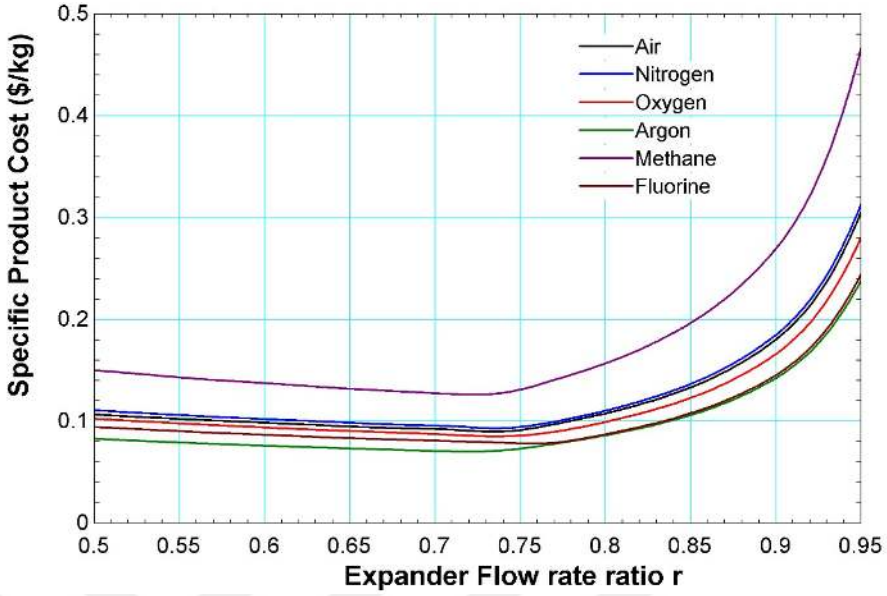

Figure 4.71 Effect of expander flow ratio on specific product cost for Claude cycle

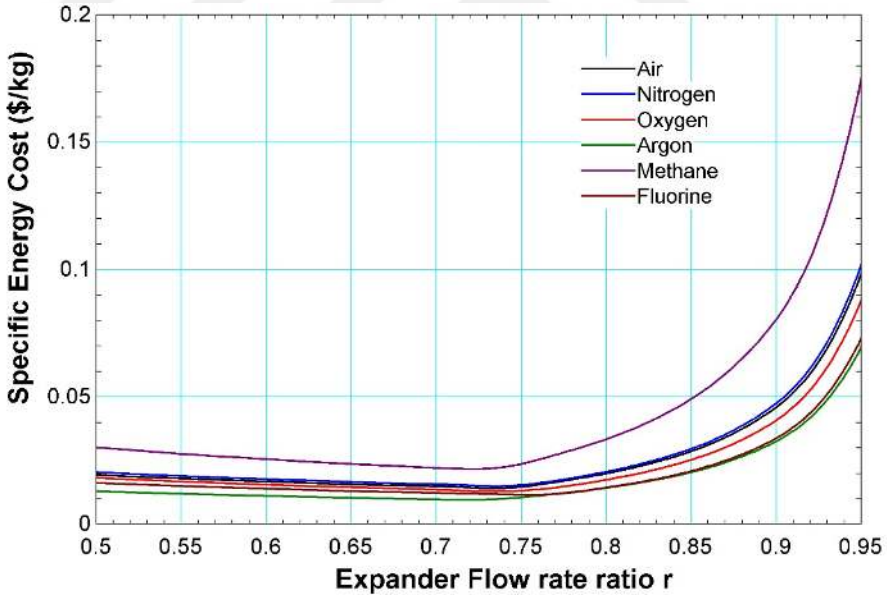

Figure 4.72 Effect of expander flow ratio on specific energy cost for Claude cycle

4.4.5 Effect of Expander Isentropic Efficiency

An expander is used in Claude cycle to produce work and cooling effect. The effect of expander isentropic efficiency on the liquid yield is given in Figure 4.73. As the isentropic efficiency decreases, the liquid yield also decreases due to lower refrigeration effect produced by the expander. This increases the temperature at the J-T valve inlet, which in turn decreases the liquid yield. Figures 4.74, 4.75 and 4.76 show the effect of expander isentropic efficiency on the liquefaction work, COP and

second law efficiency. As the expander efficiency increases, the COP and second law efficiency increase and the liquefaction work decreases.

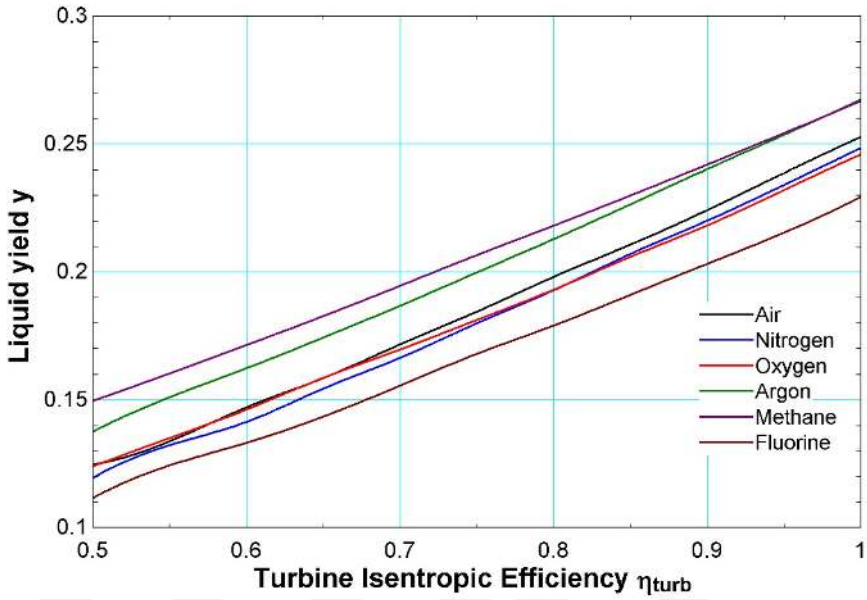

Figure 4.73 Effect of expander isentropic efficiency on the liquid yield for Claude cycle

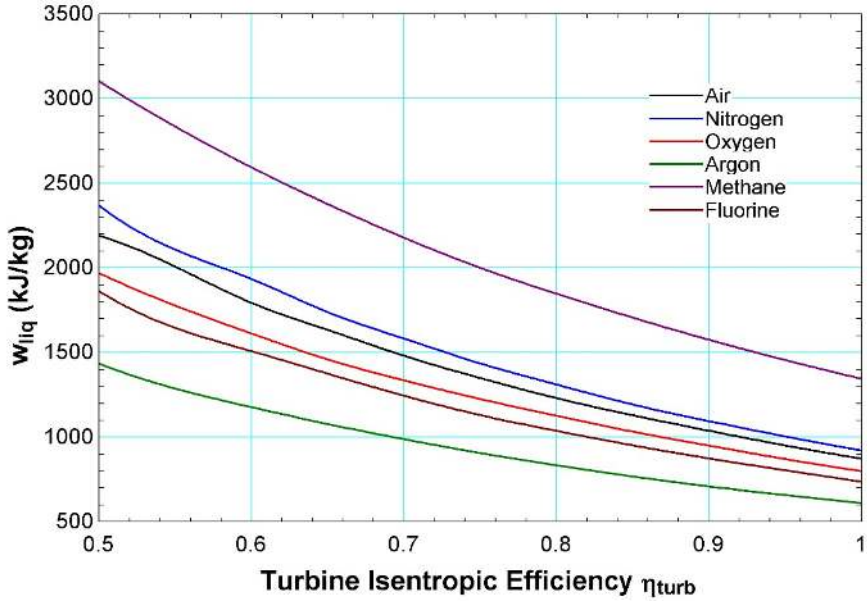

Figure 4.74 Effect of expander isentropic efficiency on liquefaction work for Claude cycle

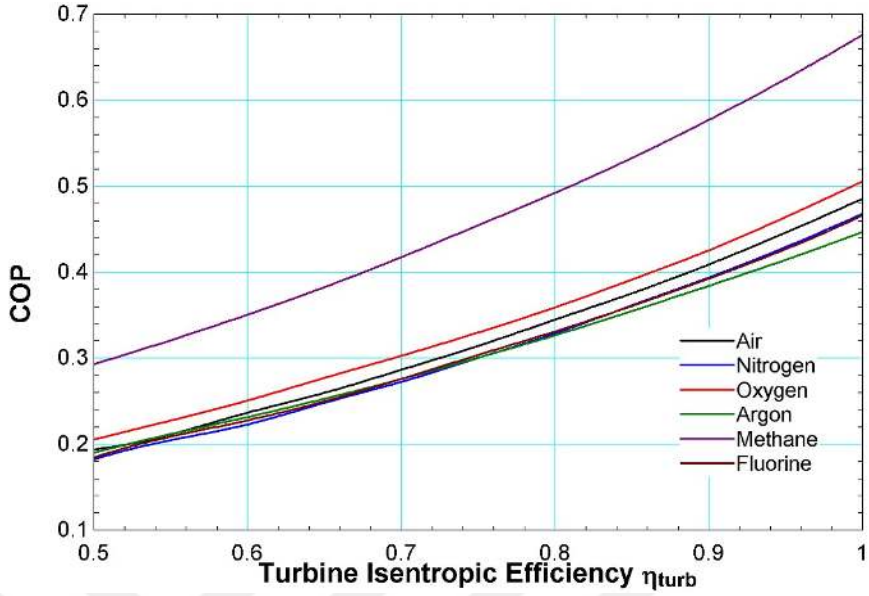

Figure 4.75 Effect of expander isentropic efficiency on COP for Claude cycle

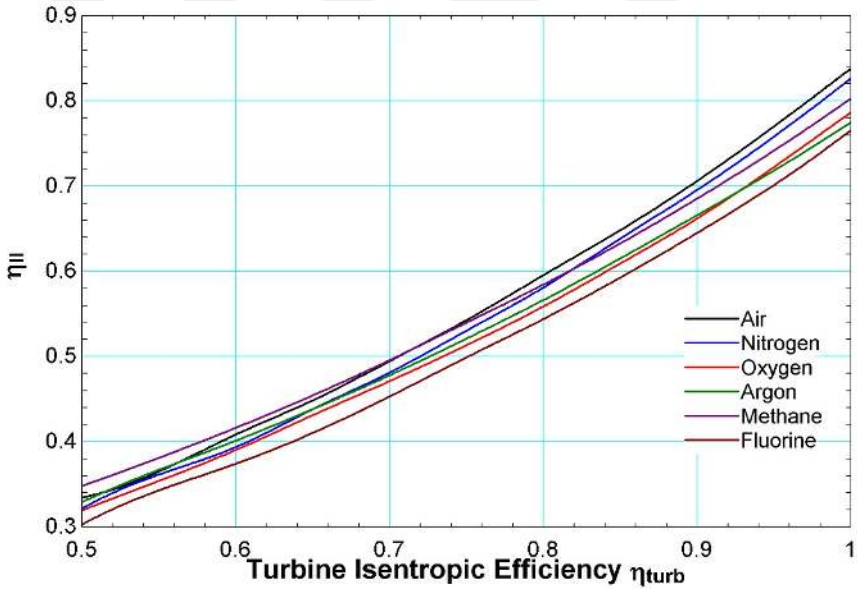

Figure 4.76 Effect of expander isentropic efficiency on second law efficiency for Claude cycle

In Figures 4.77 and 4.78, the effect of isentropic efficiency on the specific product cost and specific energy cost are given. As the isentropic efficiency decreases, lower amounts of liquid are produced, and more liquefaction work is consumed. The result is an increase in both specific energy cost and specific product cost.

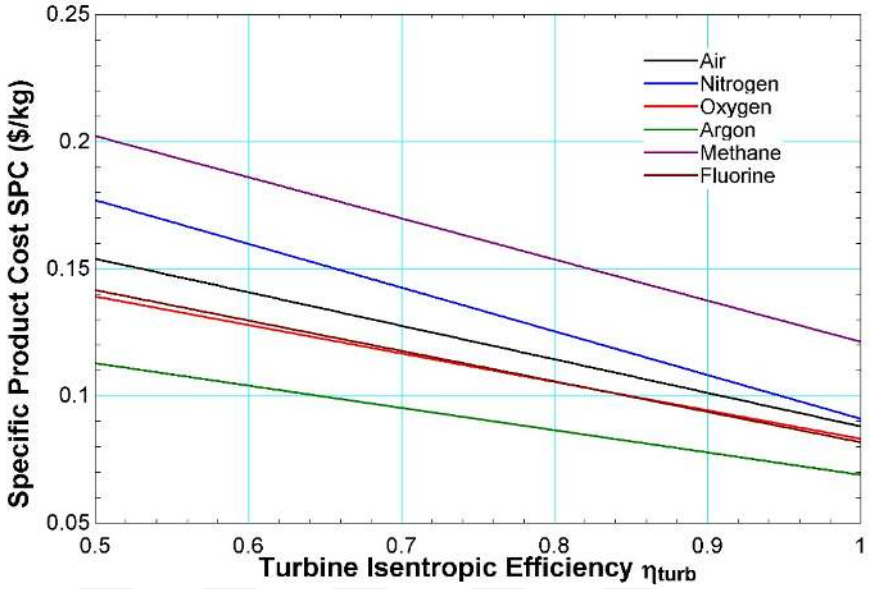

Figure 4.77 Effect of expander isentropic efficiency on specific product cost for Claude cycle

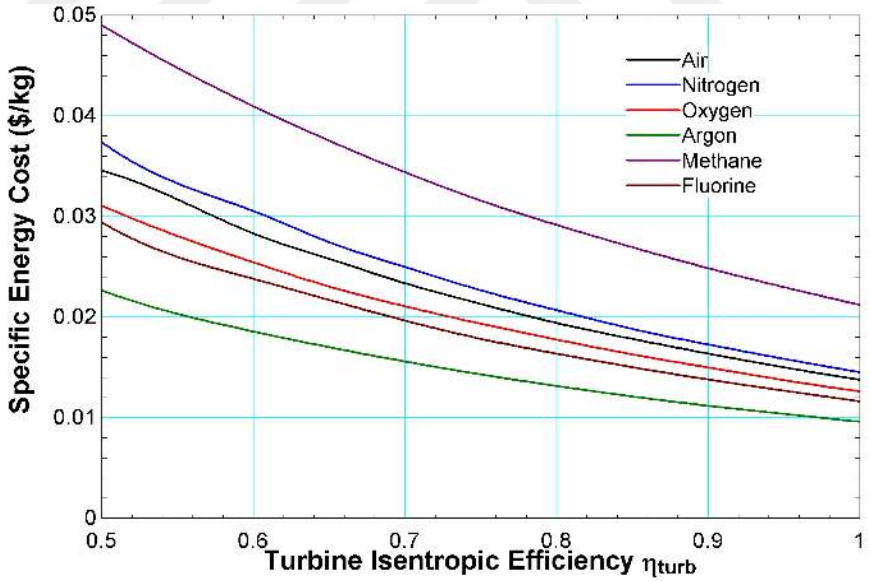

Figure 4.78 Effect of expander isentropic efficiency on specific energy cost for Claude cycle

4.4.6 Effect of Minimum Approach Temperatures in Heat Exchangers

Effect of minimum approach temperature in the heat exchanger on the liquid yield is presented for heat exchanger I, II and III in Figures 4.79, 4.80, and 4.81, respectively. Heat exchangers I and II are crucial components of the liquefaction process for Claude and Kapitza cycles. Heat exchanger I performance directly

affects the refrigeration effect produced by the expander since hot outlet stream of heat exchanger I is diverted to the expander. As the minimum approach temperature increases, the refrigeration effect produced by the expander also increases but this is not enough to decrease temperature at the J-T valve inlet. As a result, the liquid yield decreases with an increase in minimum approach temperature in heat exchanger I.

The second heat exchanger has the highest heat duty in the cycle due to condensation taking place. Again, as the minimum approach temperature increases in this heat exchanger, the inlet temperature to the J-T valve also increases, and this leads to a decrease in liquid yield.

Heat exchanger III has the lowest heat duty among the heat exchangers. Therefore, it has no significant effect on liquid yield or other performance indicators. Then, heat exchanger III can be eliminated in the Claude cycle, and the result of this modification is Kapitza cycle.

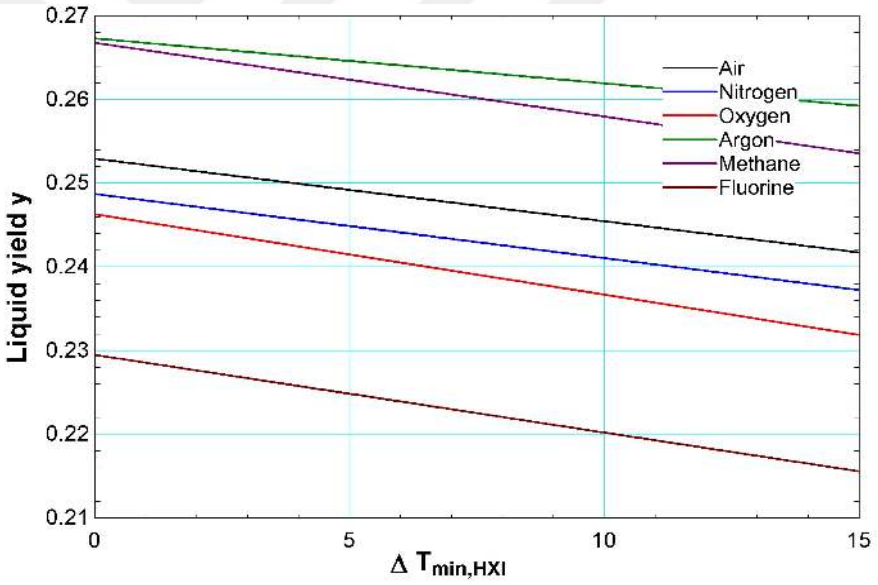

Figure 4.79 Effect of minimum approach temperature of HX I on liquid yield for Claude cycle

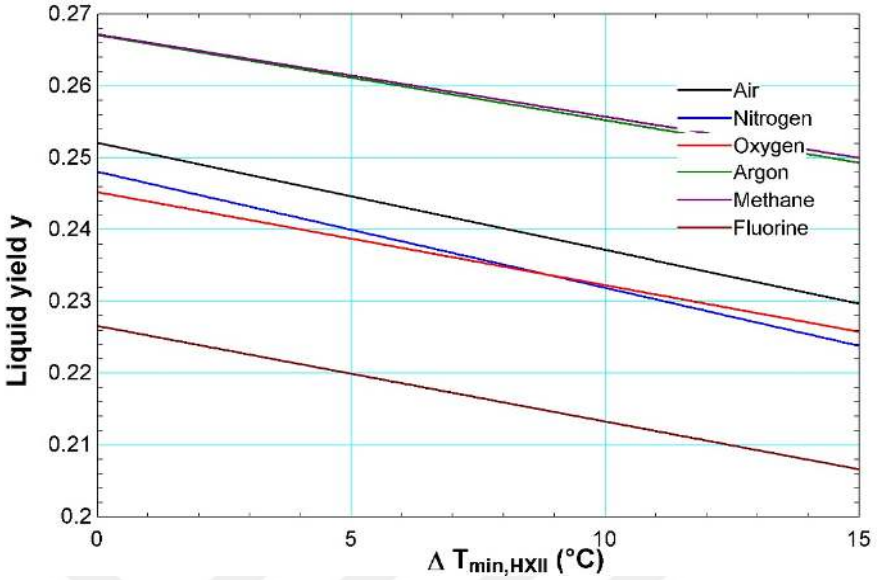

Figure 4.80 Effect of minimum approach temperature of HX II on the liquid yield for Claude cycle

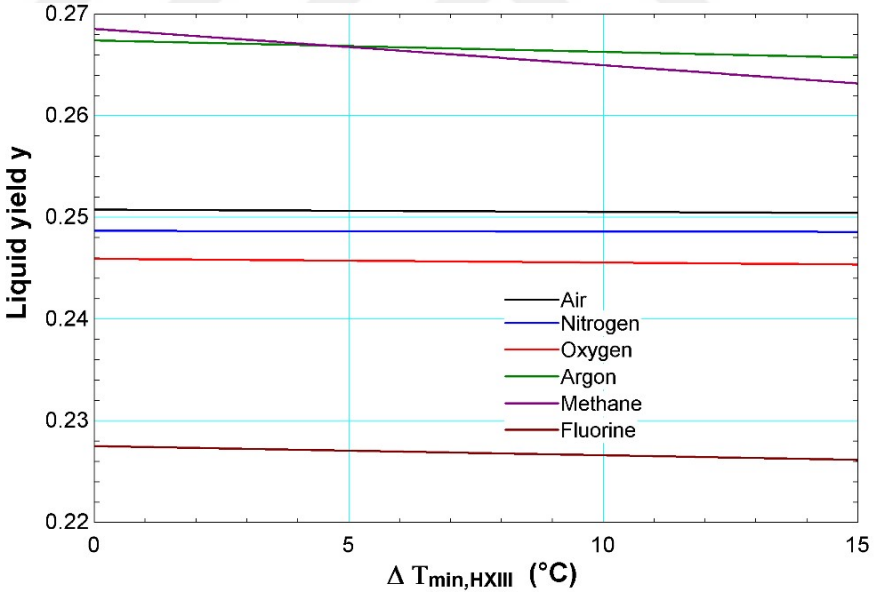

Figure 4.81 Effect of minimum approach temperature of HX III on liquid yield for Claude cycle

Figures 4.82 and 4.83 show the effect of minimum approach temperature on the liquefaction work for heat exchangers I and II, respectively. As the minimum approach temperature increases, there is a slight increase in the liquefaction work. The resulting effect on the COP and second law efficiency are given in Figures 4.84 to 4.87. As the minimum approach temperature increases, the COP and second law efficiency decrease. However, this decrease is not significant. The increase in the

liquefaction work as a result of increasing the minimum approach temperature is more significant in the second heat exchanger. This is because as the minimum approach temperature increases

in the first heat exchanger, the refrigeration effect and work produced by the expander also increases.

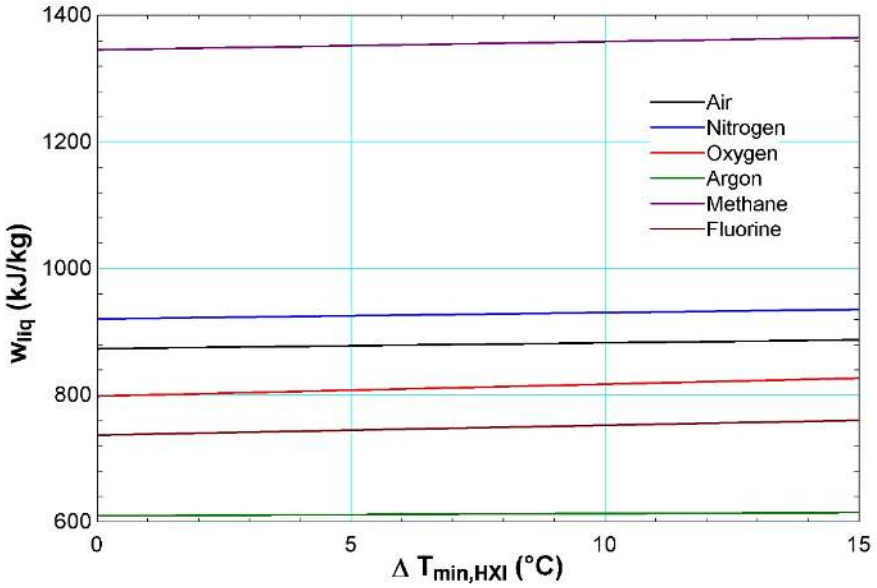

Figure 4.82 Effect of minimum approach temperature of HX I on liquefaction work for Claude cycle

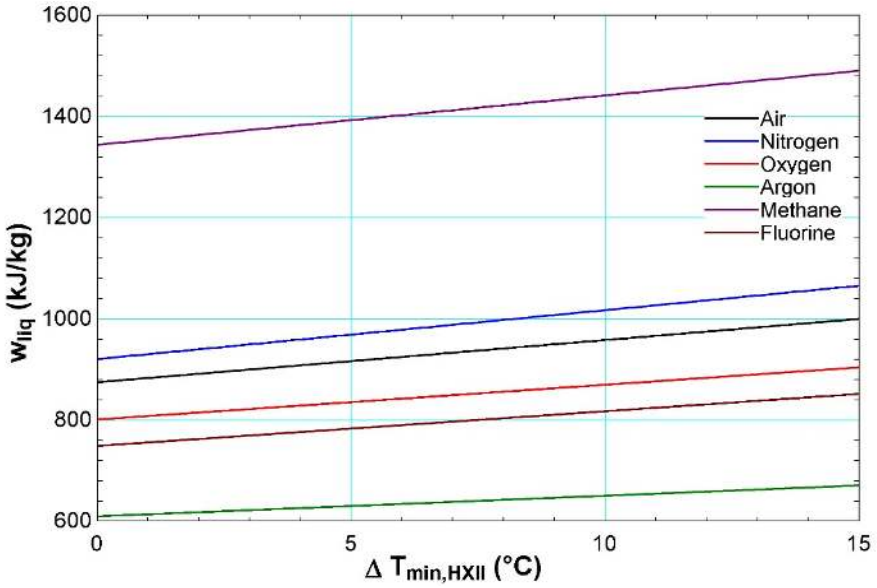

Figure 4.83 Effect of minimum approach temperature of HX II on liquefaction work for Claude cycle

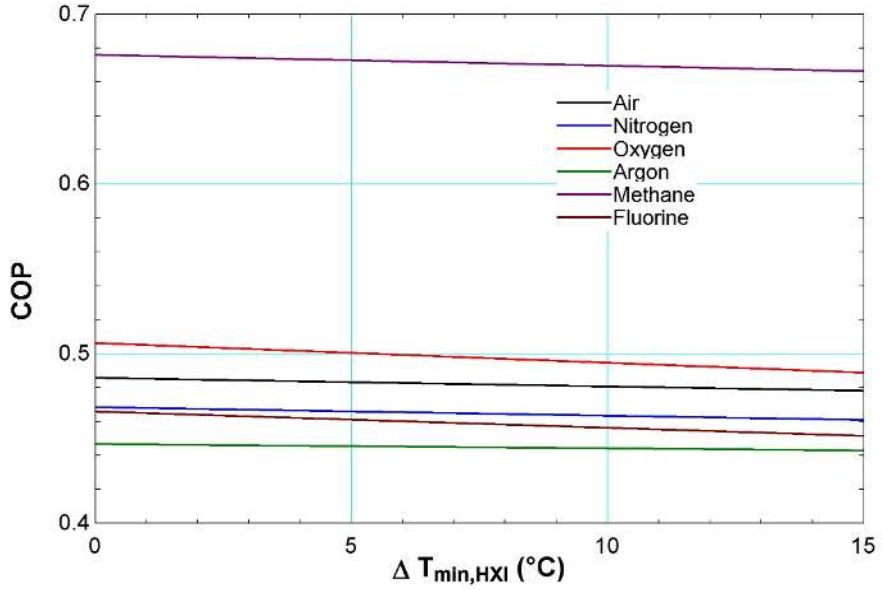

Figure 4.84 Effect of minimum approach temperature of HX I on COP for Claude cycle

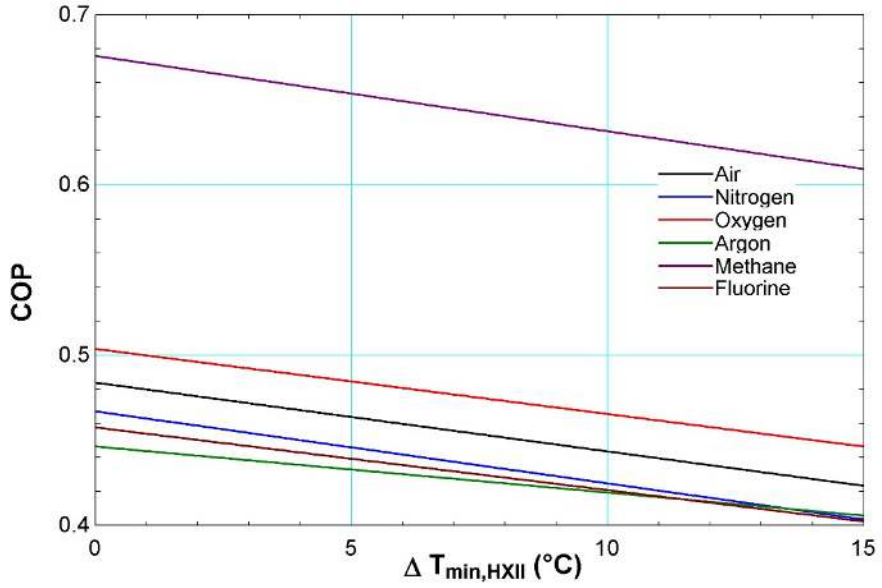

Figure 4.85 Effect of minimum approach temperature of HX II COP for Claude cycle

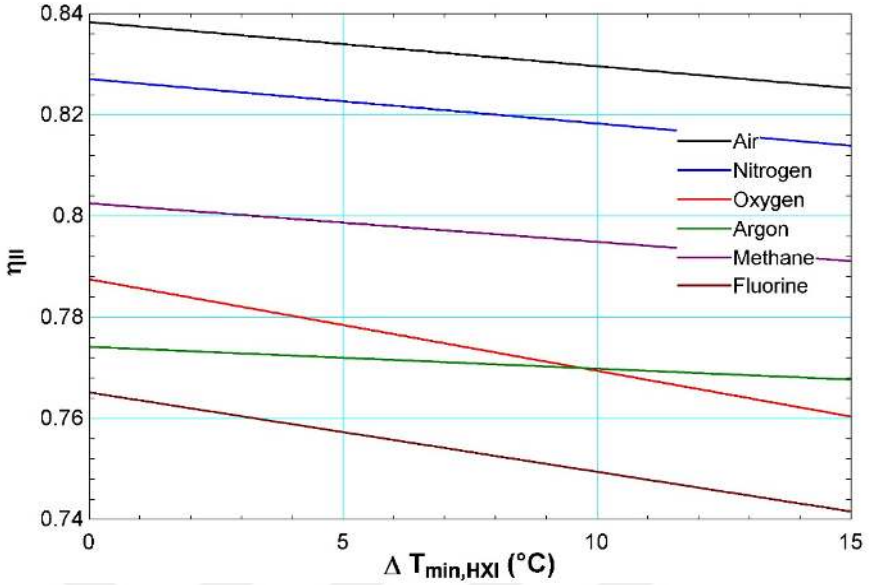

Figure 4.86 Effect of minimum approach temperature of HX I on second law efficiency for Claude cycle

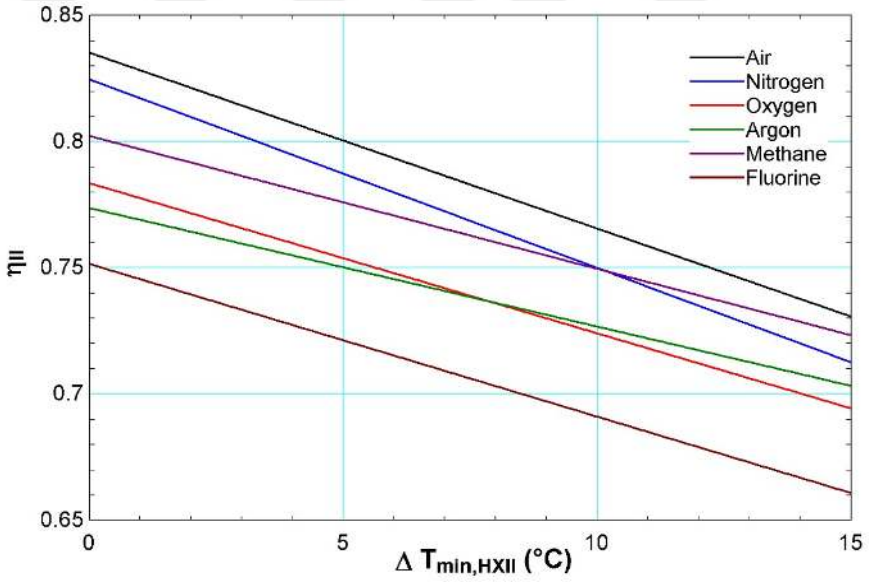

Figure 4.87 Effect of minimum approach temperature of HX II on second law efficiency for Claude cycle

In Figure 4.88, the effect of minimum approach temperature of HX I on the specific product cost for air is given. As can be seen from the figure, as the approach temperature goes to zero, the required heat transfer area goes to infinity, and this affects the capital cost of the system. When the minimum approach temperature is around 2 K for air, the specific product cost reaches its minimum value. After this point, specific product cost increases again, as shown in Figure 4.89.

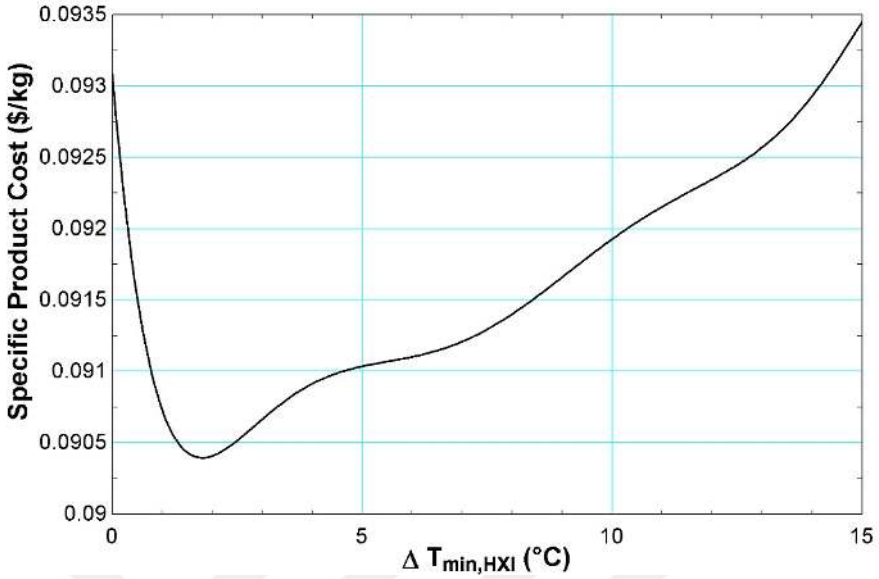

Figure 4.88 Effect of minimum approach temperature of HX I on specific product cost for Claude cycle for air

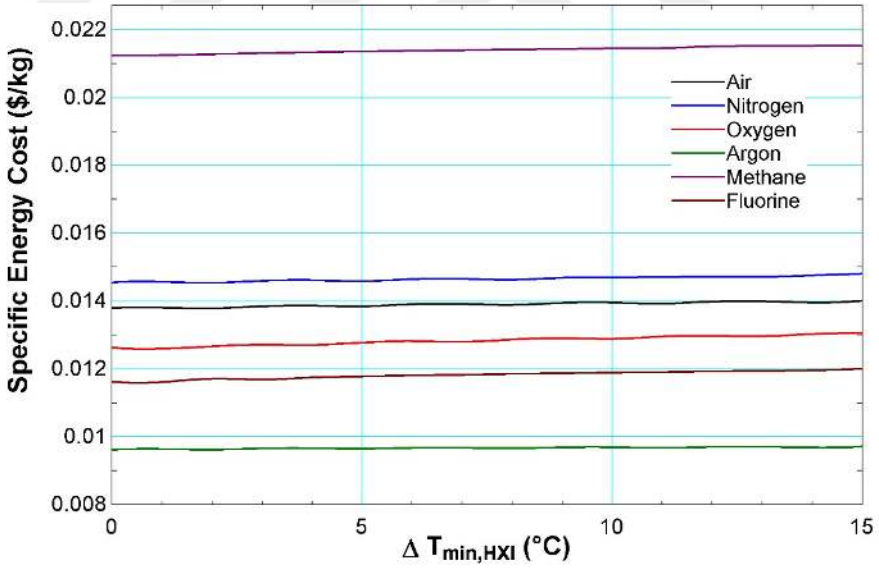

Figure 4.89 Effect of minimum approach temperature of HX I on specific energy cost for Claude cycle

Effect of minimum approach temperature of HX II on the specific product cost and specific energy cost are given in Figures 4.90 and 4.91. Unlike HX I, the minimum approach temperature occurs inside of heat exchanger II. As a result, the effectiveness of heat exchanger II cannot reach unity and the heat transfer area does not converges to infinity. Because of this characteristic, the specific energy and product costs increase as the minimum approach temperature increases.

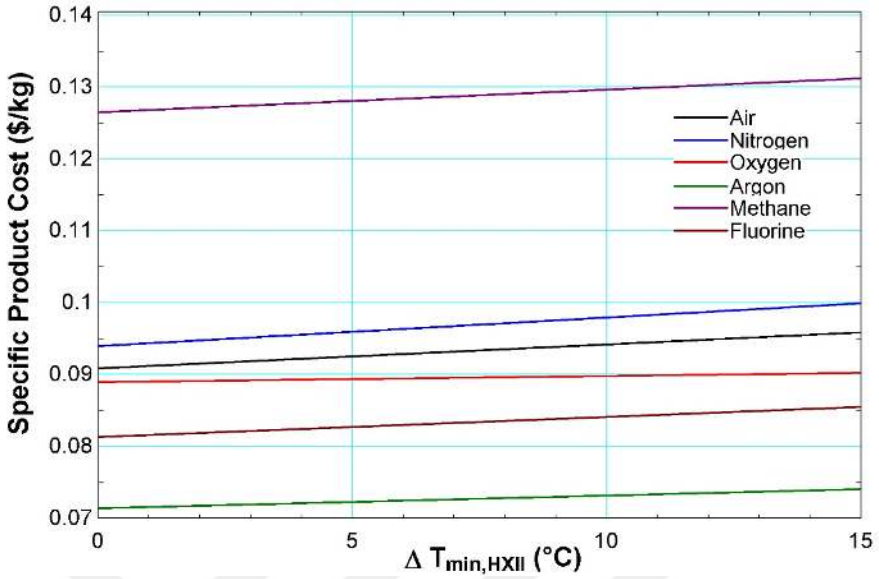

Figure 4.90 Effect of minimum approach temperature of HX II on specific product cost for Claude cycle

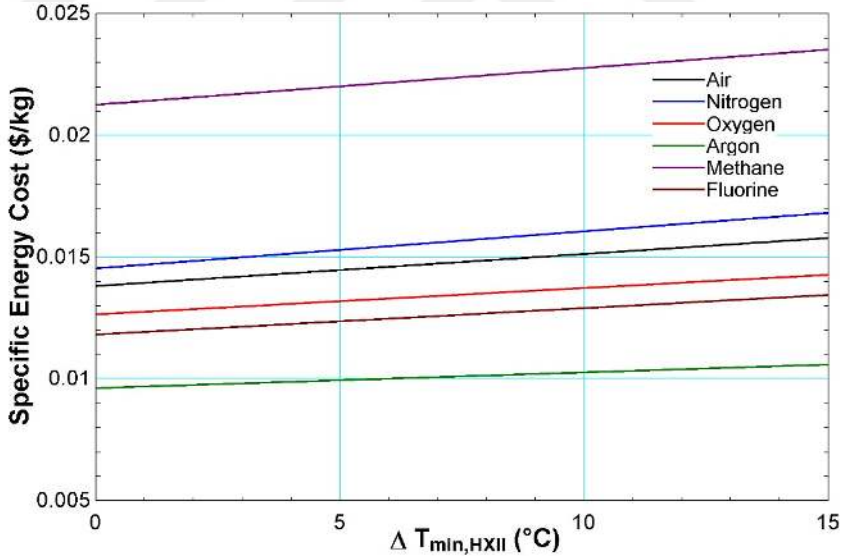

Figure 4.91 Effect of minimum approach temperature of HX II on specific energy cost for Claude cycle

4.4.7 Effect of Production Capacity

Effect of production capacity on the annual capital and O&M costs are given for air in Figure 4.92. As the production capacity increases, the size of the equipment and their cost as well as O&M expenses increase. In Figure 4.93, the effect of production capacity on the total annual energy cost is given. As the production capacity increases, the annual energy cost increases. In Figure 4.94, the effect of production capacity on the specific product and specific energy costs are given. The

specific product cost gets closer to the specific energy cost for capacities up to 400 tons/day. After that point, the specific product cost remains fairly constant. The specific energy cost remains constant at all capacities because it is evaluated per unit mass basis.

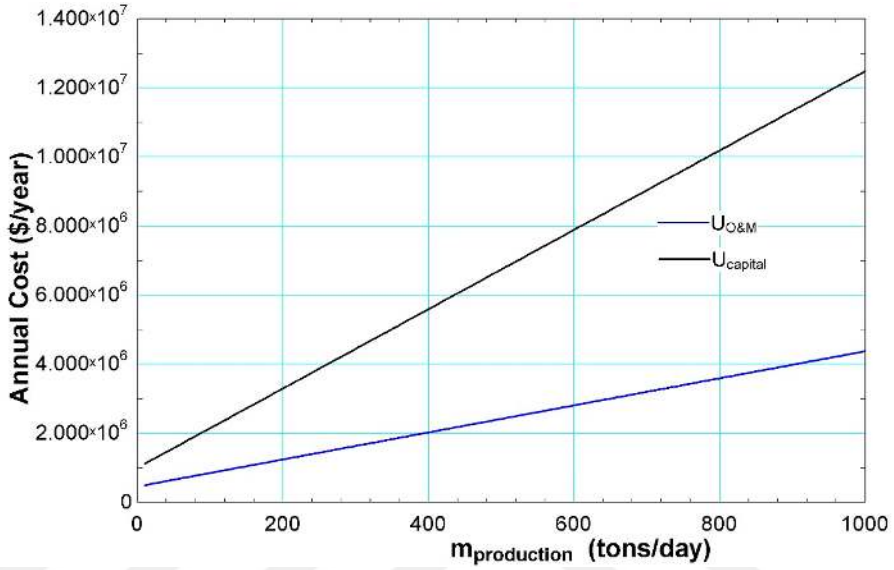

Figure 4.92 Effect of production capacity on annual O&M and capital costs for Claude cycle with air

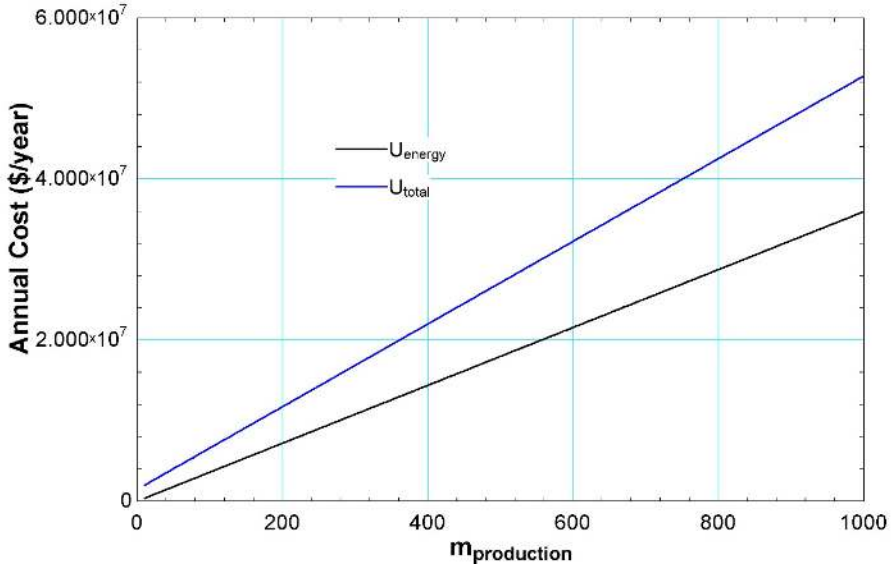

Figure 4.93 Effect of production capacity on annual energy and total costs for Claude cycle with air

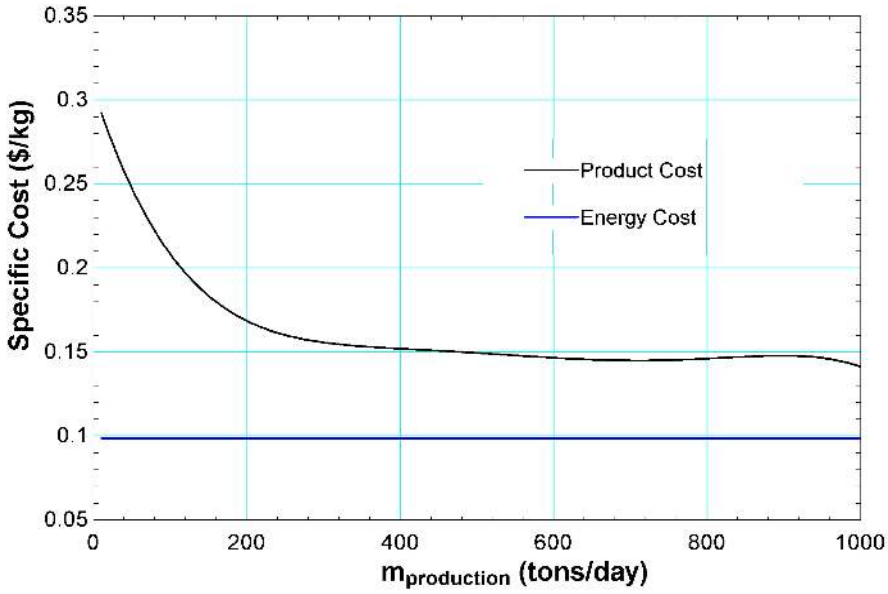

Figure 4.94 Effect of production capacity on specific product and specific energy costs for Claude cycle with air

4.5 Conclusions

In this chapter, we performed parametric studies for commonly used gas liquefaction cycles considering various gases. Effects of compressor inlet temperature, compressor isothermal efficiency, compressor outlet pressure, minimum approach temperature in the heat exchangers, expander isentropic efficiency, and flow rate ratio to the expander on various thermodynamic and economic performance indicators are investigated.

The results show that for optimum thermodynamic performance (highest second law efficiency and liquid yield), the compressor inlet temperature should be decreased as much as possible; the isothermal efficiency of the compressor and isentropic efficiency of the expander should be as high as possible; and the minimum approach temperatures should be as low as possible. On the other hand, economic considerations require that the minimum approach temperature should not be zero as this requires a heat exchanger with an infinite surface area. Therefore, the operating and design parameters of the cycles should be selected to maximize thermodynamic performance while meeting economic limitations.

CHAPTER 5

CONCLUSIONS

Gas liquefaction cycles are an important application of cryogenics and liquefied gases are used in variety of industries from transportation of natural gas to the freezing of foods. However, gas liquefaction cycles are massive energy consumers. Their design and operation should be optimized thermodynamically and economically to minimize the energy consumption.

In this thesis, commonly used gas liquefaction cycles; simple Linde-Hampson, Precooled Linde-Hampson, Claude and Kapitza cycles, are modeled thermodynamically and economically in a computer environment for various gases. Performance parameters of the cycles are determined under realistic operating conditions. In parametric studies, effects of compressor inlet pressure, compressor outlet pressure, compressor isothermal efficiency, minimum approach temperatures in the heat exchangers, expander flow rate ratio, expander isentropic efficiency, and plant capacity on certain thermodynamic and economic performance parameters are investigated. The performance parameters considered are liquid yield, liquefaction work, COP, second law efficiency, specific production cost, and specific energy cost. Parametric analysis indicates how the performance of the cycles change with the design and operating parameters, and thus indicate optimum operating parameters.

The findings from this study can be summarized as follows:

- The fraction of the gas that is liquefied (i.e., liquid yield) is determined to be in the range of 0.07 - 0.20, 0.13 - 0.33, 0.22 - 0.26, and 0.09 - 0.1 for simple Linde-Hampson, precooled Linde-Hampson, Claude and Kapitza cycles, respectively. The second law efficiencies are determined to be 0.12 - 0.27, 0.22 - 0.45, 0.76 - 0.82 and 0.43 - 0.46 for the same cycles, respectively.
- Thermodynamic analysis shows that Claude cycle provides the maximum liquid yield, minimum liquefaction work, maximum COP and second law efficiency for all considered gases.
- Adding an auxiliary refrigeration cycle to the existing system significantly increases the amount of liquid produced, the COP and second law efficiency while decreasing the liquefaction work.
- The expander used in Claude and Kapitza cycles provide additional cooling of the gas which reduce the temperature at the inlet of J-T valve, and increases the liquid yield, COP and second law efficiency.

- Economic analysis shows that simple Linde-Hampson cycle has the lowest initial cost, which is followed by precooled Linde-Hampson cycle, Claude cycle and Kapitza cycle. Kapitza cycle has the highest specific product cost, which is followed by simple Linde-Hampson cycle, precooled Linde-Hampson cycle and Claude cycle.
- Results of the parametric studies shows that as the compressor inlet temperature decreases, more liquid is produced due to the decrease in temperature at Joule-Thompson valve inlet.
- The isothermal efficiency of the compressor does not affect amount of liquid obtained in the cycle, but the liquefaction work increases as the compressor isothermal efficiency decreases.
- Compressor outlet pressure is an important parameter which directly affects the liquid obtained and the liquefaction work. The analysis shows that different cycles have different optimum pressures depending on the gas. For simple and precooled Linde-Hampson cycles, the optimum pressure value varies between 20 and 40 MPa. For Claude and Kapitza cycles, the optimum pressure varies between 6 and 10 MPa. Lower optimum pressure values in these cycles is due to the effect of the expander which provides additional cooling effect.
- Heat exchangers are crucial components in liquefaction systems. Minimum approach temperature in the heat exchangers directly affects thermodynamic performance of the cycles. As the minimum approach temperature in the heat exchangers decreases, the system performance gets closer to the ideal performance. However, decreasing the minimum approach temperature requires a larger heat exchanger, which may not be feasible economically. The analysis indicates that for economically optimum operation, the minimum approach temperature should not exceed 5 K.
- The use of an expander in Claude and Kapitza cycles positively affect the cycle performance as it increases the liquid yield, COP and second law efficiency. As the isentropic efficiency of the expander increases, the expander provides more cooling, which decreases the inlet temperature to the J-T valve. As the isentropic efficiency increases, the specific product cost and specific energy cost decrease.
- Expander flow rate ratio is another operating parameter affecting the magnitude of refrigeration effect produced by the expander and J-T valve. For an optimum system operation from a thermodynamic and economic point of view, the expander flow rate ratio should be between 0.65 and 0.75 depending on the gas to be liquefied.
- Economic analysis of various liquefaction cycles shows that specific product cost is dominated by specific energy cost. The specific product cost decreases as the production capacity of the plant increases up to a value of about 200 tons/day for simple Linde-Hampson and 400 tons/day for Claude and Kapitza cycles. It remains fairly constant after these capacities. At high capacities, the specific product cost becomes very close to specific energy cost as the contribution of other cost items becomes less and less significant with higher capacities.

REFERENCES

[1] Çengel YA, Boles MA. (2015). Thermodynamics : an engineering approach. 8th edition. New York : McGraw-Hill Education,

[2] Vance RW. (1962). Applied cryogenic engineering. New York: Wiley.

[3] Venkatarathnam G, Timmerhaus KD. (2008). Cryogenic mixed refrigerant processes New York: Springer.

[4] Timmerhaus KD.(1989). Cryogenic process engineering. New York : Plenum Press.

[5] Wark K. (1995). Advanced thermodynamics for engineers. New York : McGraw-Hill.

[6] Chevron Co. 2017. IGu 2017 World LNG Report. New York: *PR Newswir*

[7] Smith EM. (2005) Advances in thermal design of heat exchangers : a numerical approach : direct-sizing, step-wise rating, and transients. Hoboken, NJ : Wiley.

[8] Klein S , Alvarado F. 2018.EES, Engineering Equation Solver, *F-Chart Software*

[9] KN Features.2018 UniSim ® Design Suite R450.

[10] Barron RF.(1985). Cryogenic Systems. Oxford University Press.

[11] Kanoglu, M. Dincer, I., Rosen, MA. (2008). Performance analysis of gas liquefaction cycles. *International Journal of Energy Research*, **32**(1), 35–43.

[12] Maytal, BZ. (2006) Maximizing production rates of the Linde-Hampson machine. *Cryogenics*, **46**(1), 49–54.

[13] Syed, MT., Sherif, SA., Veziroglu TN., Sheffield, JW. (1998) An economic analysis of three hydrogen liquefaction systems. *International Journal of Hydrogen Energy*, **23**(7), 565-576.

[14] Thomas, RJ., Ghosh, P., Chowdhury K., (2011). Role of expanders in helium liquefaction cycles: Parametric studies using Collins cycle *Fusion Engineering and Design,* **86**(4–5), 318–324.

[15] Thomas, RJ., Ghosh, P., Chowdhury K., (2012). Role of heat exchangers in helium liquefaction cycles: Simulation studies using Collins cycle. *Fusion Engineering and Design,* **87**(1),39–46.

[16] Cammarata G., Fichera A., Guglielmino D.,(2001) Optimization of a liquefaction plant using genetic algorithms. *Applied. Energy*, **68**(1),19–29.

[17] Nandi TK., Sarangi S. (1993) Performance and optimization of hydrogen liquefaction cycles. *International Journal of Hydrogen Energy,* **18**(2),131–139.

[18] Cardella C., Decker L., Sundberg J., Klein H.(2017). Process optimization for large-scale hydrogen liquefaction. *International Journal of Hydrogen Energy,* **42**(17), 12339–12354.

[19] Cardella C., Decker L., Sundberg J., Klein H. (2017). Economically viable large-scale hydrogen liquifaction. *IOP Conference Series on Material Science and Engineering*, vol. 171.

[20] Cardella U., Decker L.(2017). Roadmap to economically viable hydrogen liquefaction. *International Journal of Hydrogen Energy*, **42**(19),13329–13338.

[21] Kanoğlu M. (2002). Exergy analysis of multistage cascade refrigeration cycle used for natural gas liquefaction. *International Journal of Energy Research*, **26**(8), 763–774.

[22] Castle WF., (2002). Air separation and liquefaction: recent developments and prospects for the beginning of the new millennium. *International Journal of Refrigeration*, **25**,158–172.

[23] Atrey, MD,. (1998). Thermodynamic analysis of Collins helium liquefaction cycl*e. Cryogenics,* **38**,1199-1206.

[24] Hasan MF., Karimi IA., Alfadala H., Grootjans H.,(2007). Modeling and simulation of main cryogenic heat exchanger in a base-load liquefied natural gas plant. *Computer Aided Chemical Engineering*, **24**,219–224.

[25] Chang HM., Lim HS., Choe KH., (2012). Effect of multi-stream heat exchanger on performance of natural gas liquefaction with mixed refrigerant. *Cryogenics*, **52**(12), 642–647.

[26] Guizzi GL., Manno M.,Tolomei LM., Vitali RM. (2017). Thermodynamic analysis of a liquid air energy storage system. *Energy*, **93**,1639–1647.

[27] Marmolejo-Correa D., Gundersen T. (2012). A comparison of exergy efficiency definitions with focus on low temperature processes. *Energy*, **44**(1), 477–489.

[28] Krasae-in S., Stang JH., Neksa P.(2010). Development of large-scale hydrogen liquefaction processes from 1898 to 2009. *International. Journal of Hydrogen Energy*, **35**(10).4524–4533.

[29] Yilmaz C., Kanoglu M., Bolatturk A., Gadalla M. (2012). Economics of hydrogen production and liquefaction by geothermal energy. *International Journal of Hydrogen Energy*, **37**(2),2058–2069.

[30] Krasae-In S., Stang JH., Neksa P. (2010) Exergy analysis on the simulation of a small-scale hydrogen liquefaction test rig with a multi-component refrigerant refrigeration system. *International Journal of Hydrogen Energy*, **35**(15), 8030–8042.

[31] Ameel B.(2013) .Thermodynamic analysis of energy storage with a liquid air Rankine cycle *Applied Thermal Engineering*, **52**(1),130–140.

[32] Thomas, RJ., Ghosh, P., Chowdhury K., (2012). Application of exergy analysis in designing helium liquefiers. *Energy*, **37**(1), 207–219.

[33] Chang HM., (2015). A thermodynamic review of cryogenic refrigeration cycles for liquefaction of natural gas. *Cryogenics*, **72**, 127–147.

[34] Li Y., Wang X., Ding Y. (2012) An optimal design methodology for large-scale gas liquefaction. *Applied Energy*, **99**,484–490.

[35] Carnot S. (1986) , Reflexions on the motive power of fire : a critical edition with the surviving scientific manuscripts. New York : Lilian Barber Press.

[36] Kanoğlu M., Çengel YA., Dinçer I. (2012) Efficiency evaluation of energy systems. Springer Science & Business Media.

[37] Timmerhaus KD., Flynn TM., (2013) Cryogenic Process Engineering Springer Science & Business Media.

[38] Habets G., Kimmel H. (2013) Economics of cryogenic turbine expanders *gas* 1, 4-13, .

[39] Centre for Low Carbon Futures and Liquid Air Energy Network (2013) Liquid Air Technologies – a guide to the potential. 28.

[40] Morgan R.,Nelmes S., Gibson E., Brett G. (2015) Liquid air energy storage – Analysis and first results from a pilot scale demonstration plant. *Applied Energy*, **137**,845–853.

[41] Peters MS., Timmerhaus KD, West RD, (2003) Plant design and economics for chemical engineers. 5th edition New York : McGraw-Hill.

[42] Smith R. (2005), Chemical process: design and integration. John Wiley & Sons.

[43] ThomasNet® - Product Sourcing and Supplier Discovery Platform. (2018) https://www.thomasnet.com/

[44] Bejan A., Tsatsaronis G., Moran M. (1996). Thermal design and optimization New York : John Wiley.

[45] Seider WD., Seader JD., Lewin DR., (2003) Product & Process Design Principles - Synthesis, Analysis & Evaluation. John Wiley & Sons.

[46] Couper JR., (2012) Chemical process equipment selection and design. 3rd ed. Waltham, Mass. : Butterworth-Heinemann.

[47] Fisher M., (2017) Economic Indicators - CEPCI. *Chemical Engineering Online*.

[48] Kays W., London A. (1984) Compact heat exchangers *ESSOM CO., LTD*.

[49] Cayer E., Galanis N., Desilets M., Nesreddine H., Roy P.(2009) Analysis of a carbon dioxide transcritical power cycle using a low temperature source. *Applied Energy*, **86**(8) 1055–1063.

[50] Soyars WM. (1994). Fermi National Accelerator The Applicability Cryogenic of Constant Property Analyses Helium Heat Exchangers. Presented at. No. FERMILAB-CONF-94-427.

[51] Taal M., Bulatov I., Klemeš J., Stehlík P. (2003). Cost estimation and energy price forecasts for economic evaluation of retrofit projects *Applied Thermal Engineering*, **23**(14), 1819–1835.

APPENDIX

UNISIM MODELS OF CONSIDERED CYCLES

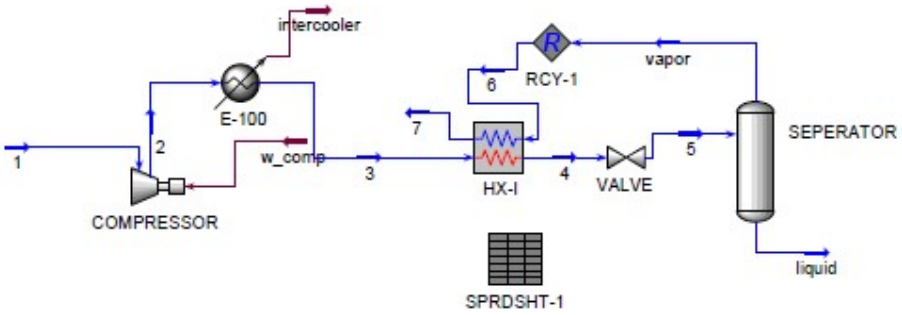

Figure A.1 Unisim model of Simple Linde-Hampson cycle

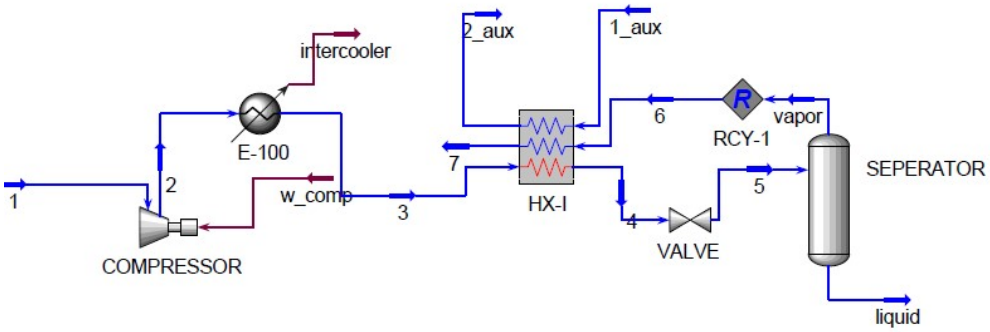

Figure A.2 Unisim model of Precooled Linde-Hampson cycle

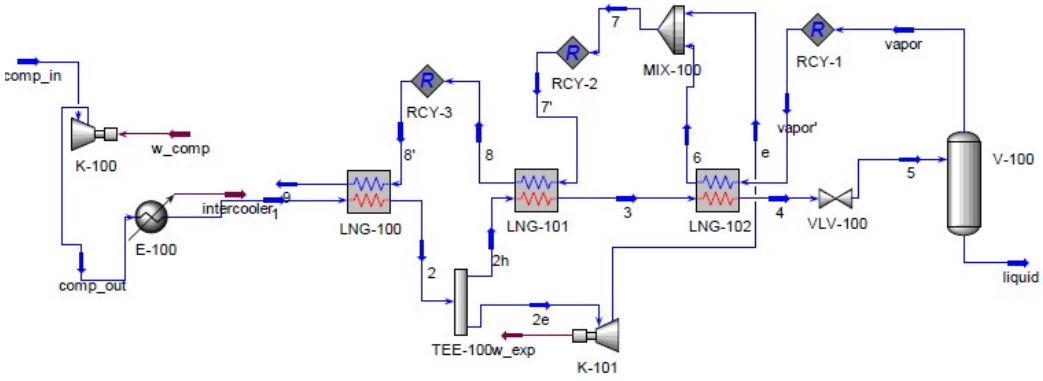

Figure A.3 Unisim model of Claude cycle

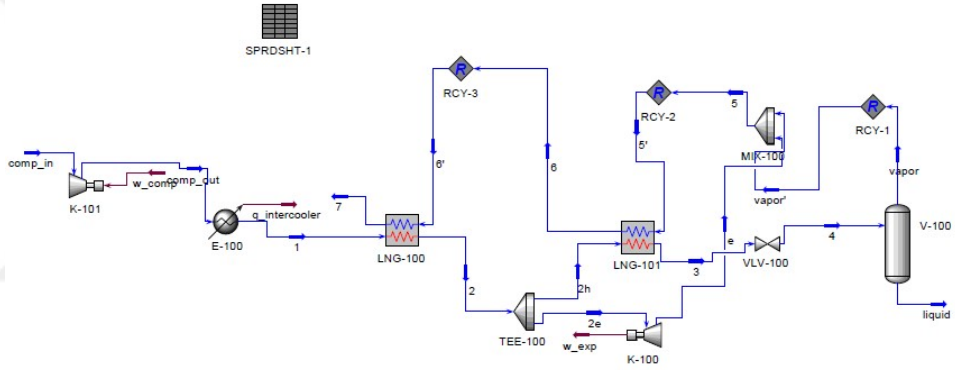

Figure A.4 Unisim model of Kapitza cycle